Master thesis title:

DRIFT and DRUV spectroscopy methods for studying the interaction of metal compounds with native cellulose

By

Jovana Visekruna

Thesis for the degree of European Master in Quality in Analytical Laboratories

Faro, Portugal

July 2015

Master thesis title:

DRIFT and DRUV spectroscopy methods for studying the interaction of metal compounds with native cellulose

By

Jovana Visekruna

Supervisors:

Ana Rosa Garcia, PhD

Isabel Cavaco, PhD

Thesis for the degree of European Master in Quality in Analytical Laboratories

Faro, Portugal

July 2015

Declaration of Authorship

I declare that I am the author of this work, which is original. The work cites other authors and works, which are adequately referred in the text and are listed in the bibliography.

The University of Algarve has the right to keep and publicize this work through printed copies in paper of digital form, or any other means of reproduction, to disseminate it in scientific repositories and to allow its copy and distribution with educational and/or research objectives, as long as they are non-commercial and give credit to the author.

Visekruna Jovana

Acknowledgements

This work was carried out at the University of Algarve in Faro under supervision of Prof. Isabel Cavaco and Prof. Ana Rosa Garcia, and supported by Erasmus Mundus Master in Quality in Analytical Laboratories (EMQAL).

Firstly, I would like to express my sincere gratitude to the European Commission who provided the scholarship and finances for the master. The last two years were valuable and amazing experience for me that would never be possible without this grant.

I would like to thank my supervisors, Prof. Isabel Cavaco and Prof. Ana Rosa Garcia for their support, guidance and constructive advices that enabled me to improve and successfully complete my work.

Also I would like to thank all personnel at University of Barcelona, University of Algarve and Instituto Superior Tecnico for their help and assistance. Big thanks to my family and all my friends, in and outside EMQAL, who always supported me and made my studies easier.

Table of Contents:

I - List of Abbreviations:

AA - Ascorbic acid

AGU - Anhydroglucose units

CMC - Carboxymethyl cellulose

CT - Charge transfer

Cys - L-cysteine

DP - Degree of polymerization

DR - dynamic range

DRIFTS - Diffuse Reflectance Infrared Fourier Transform Spectroscopy

DRUVS - Diffuse reflectance ultraviolet visible spectroscopy

FTIR - Fourier transform infrared

IR - Infrared

KM - Kubelka Munk

LD - limit of detection

LMCT - Ligand-to-metal charge transfers

LQ - limit of quantification

MCT - Mercury-cadmium-telluride detector

MID IR - Middle infrared

MIC - Microcrystalline cellulose

MLCT - Metal-to-ligand charge transfers

NMR – Nuclear magnetic resonance

R^2 - Coefficient of determination

UV/Vis - Ultraviolet/visible

II - List of Figures:

III - List of Tables

Abstract

Cellulose, the most abundant organic polymer on earth, has numerous applications including the application in pharmacy as excipient in different kinds of pharmaceutical formulations where it comes in contact with metal compounds used in therapeutic purposes. Chemically, is composed of hundreds to thousands of β 1→4 linked D glucopyranose units. It is insoluble in water and most organic solvents and its structure cannot be loosened by heat or with solvents without causing irreversible chemical decomposition. However it can be broken down chemically into glucose units by treatment with concentrated acids at high temperatures. Aqueous solutions of several metals are also known to dissolve cellulose by deprotonating and coordinative binding the hydroxyl groups in the C2 and C3 position of the anxydroglucose.

In this work, different metal complexes of copper, iron, vanadium and zinc, and native cellulose were used to a better understanding on the interactions established upon adsorption. Those metals are long used as components of dietary supplements, food additives and different kinds of drugs. It is also known from previous research that the metals complexes can react with cellulose, changing its structure or even cause its decomposition under certain conditions. In general, cellulose fibers have very few functional groups that are capable of bonding with metals and interaction between cellulose and metals and their compounds can occur in one of four ways: adsorption on the fibers, forming chemical bonds with the reactive groups of cellulose, incorporation into cellulose matrix, and formation of complexes with dissolved degradation products of cellulose.

The objective of this work was to study the interaction of cellulose fibers with these four metals complexes, evaluating the changes induced by the matrix on the metal complex, specially by the identification of different metal adsorbed species, and assessing the changes in the cellulose structure namely in its crystallinity degree, upon the metal complex adsorption. For the analysis two spectroscopic techniques were used: diffuse reflectance infrared spectroscopy (DRIFTS) and diffuse reflectance ultraviolet-visible spectroscopy (DRUVS).

One of the effects that the adsorption of the metal can have in cellulose is by altering its chain spatial arrangement changing its crystallinity degree. The cellulose crystallinity of the samples estimated by DRIFTS, using the region between 1300 and 1180 cm^{-1} and bands at 898 and 1430 cm^{-1}, showed that in the case of vanadium (V) and zinc (II) there has been increase in the degree of crystallinity while

for the other metals crystallinity was not influenced by the presence of metal complexes. However, quantification of this change was only possible in the case of vanadium (V) where it was clear that in the acidic environment at pH 3 and 5 and concentrations higher than 1mM / g cellulose, crystallinity increased from approximately 44 to 76% with the increase of vanadium complex concentration from 1 to 10 mM / g cellulose.

The influence of the matrix on the metal complex structure, in the case of vanadium (IV) was analyzed by the alterations observed in the infrared bands, in particular in the regions 1000 -1200 cm^{-1} and 600 – 670 cm^{-1}, showed that there has been a change in crystalline structure of the initial compound from water soluble α to insoluble β form. The shift of the bands at 1200 cm^{-1} in all three sets of samples (three different pH) indicated entrapment of the SO_4^{2-} ion into cellulose and shift in the band at approximately 980 cm^{-1} indicates entrapment of different vanadium species in the cellulose chains but only in the high range of concentrations. The ultraviolet-visible absorption spectra (DRUVS) shown low intensity of d-d transition bands in the region after 500 nm for the samples with pH 3 and non-adjusted pH, which can be related with the oxidation from V(IV) to V(V). However, considering the blue color of these samples, characteristic for V(IV), the low intensity of the d-d bands in diluted samples appear weak only because they are so in comparison with the stronger CT bands at ~240nm. On the other hand, the high intensity of the CT relative to the d-d bands in samples with cellulose compared to the control may be indicative of binding of cellulose groups to the metal. In the set of samples with pH 5 there are indications of the formation of a new complex and also partial oxidation of V(IV) to V(V).

For vanadium (V) adsorbed onto cellulose, the analysis of the new appearing bands present at wavenumbers 960, 971 and 965 cm^{-1}; 836, 829 and 829 cm^{-1} 703, 750 and 747 cm^{-1} for the non-adjusted pH set of samples, pH 3 and pH 5 sets of samples, respectively, revealed deposition of different polymeric vanadium species onto cellulose when vanadium is present in higher concentrations. Since the equilibrium of vanadium species greatly depends on the pH value it was expected that different species deposited onto cellulose will be observed in the sets of samples with different pH values. At low pH values such as pH 3 it is found that decavanadates are dominant species. At pH 5 dominant species seemed to be mixture of tri and decavanadates and at pH 6-7 we can expect to have mixture of tri and tetravanadates deposited on cellulose. These conclusions are also confirmed after analysis of the DRUV spectra which showed that there hasn’t been any reduction from V (V) to V (IV) and that only different polyoxovanadates are formed in the samples.

The DRIFT spectra of iron (II) indicated very weak interaction between the metal complex and the matrix, which means a deposition of the complex on the cellulose surface or on the amorphous phase. Analysis of DRUV spectra showed that it is possible that Fe (III) ions were formed in the samples during oxidation of Fe (II) under aerobic conditions.

A different behavior was proposed to iron (III), since in the DRIFT spectra of Fe(III) complex samples (at all preparation pH values) strong bands are appearing at 1384 cm^{-1} but they are probably just the result of the high complex concentration leading to deposition onto the cellulose exterior surface with low interaction. However, the shifted bands at 1360, 830 and 802 cm^{-1} indicate deposition of different species or more probably an adsorption onto the cellulose chains with stronger interactions.

In the case of zinc and copper metal complexes no significant effect is present in any of the spectra. In fact, neither the bands of the metal complex or those of cellulose are affected by the deposition of the metal complex onto cellulose. Moreover, no new bands are observed, pointing to a poor interaction between the complex and the matrix upon deposition. Since zinc has very low absorptivity in the UV/Vis region no additional information were obtained from the analysis of DRUV spectra. However, the absence of expected d-d bands at around 800 nm in the DRUV spectra of Cu (II) samples, confirmed that the deposition of octahedral copper species onto cellulose did not occurred.

Quantitative analysis is performed, for all the metals except zinc, using the Kubelka-Munk equation, or reemission function which gives the correlation between the intensity of the diffuse reflected radiation and concentration for solid samples, similarly to the lambert-Beer law for liquid samples. In all metal complex/cellulose pairs studied the increase of F(R) with increase of concentration was evident. In the full range of concentrations only regression models for V(V) set of samples with pH 5 and V(IV) set with pH 3 showed good fit for the data while in all the other cases only regression models in the lower range of the concentrations from 0.20 up to 1.00, 3.00 or 5.00 mM/g of cellulose (depending of the sample set) showed good fit. These results point to the necessity of optimizing the sample preparation, with a very low repeatability, reducing and replacing the steps involved that leads to a huge possibility of loss of analyte.

Resumo

A celulose, é o polímero orgânico mais abundante na crosta terrestre, de entre a suas inúmeras aplicações, é utilizado como excipiente em diferentes tipos de formulações farmacêuticas. Na qualidade de excipiente entra em contacto com compostos metálicos ou iões de metais utilizados para fins terapêuticos. Quimicamente, é composto por centenas de milhares de β 1 → 4 unidades de D-glucopiranose ligadas. É insolúvel em água e a maioria dos solventes orgânicos e a sua estrutura não alterada por acção calor ou por solventes, sem causar a sua decomposição química irreversível. No entanto, por acção química a celulose pode dividida em unidades de glicose, este efeito pode ser observado no tratamento com ácidos concentrados a temperaturas elevadas. Alguns metais em solução aquosa também têm capacidade para degradar a celulose, por desprotonação e coordenação aos grupos hidroxilo na posição C2 e C3.

Neste trabalho, diferentes complexos de metais de cobre, ferro, vanádio e zinco, foram usados para estudar as interações estabelecidas quando os metais se adsorvem em celulose nativ. Estes metais são muito utilizados em suplementos alimentares, aditivos alimentares e de diferentes tipos de medicamentos. É também conhecido, que os complexos de metálicos podem reagir com a celulose, alterando a sua estrutura, ou mesmo provocar a sua degradação em condições particulares. Em geral, as fibras de celulose têm poucos grupos funcionais com capacidade de ligação aos metais, assim a interacção entre a celulose e os metais e os seus complexos pode ocorrer de quatro modos: deposição, adsorção entre as cadeias, a formação de ligações químicas com os grupos reactivos de celulose, e formação de complexos com os produtos de degradação da celulose que se dissolvem.

O objectivo deste trabalho foi estudar a interacção de fibras de celulose com quatro complexos metálicos, avaliar as alterações induzidas pela matriz no complexo, especialmente por a identificação de diferentes espécies de metal adsorvido, e a avaliação das alterações na estrutura da celulose nomeadamente no seu grau de cristalinidade, após o complexo se adsorver. Para a análise foram utilizadas duas técnicas espectroscópicas: espectroscopia de reflectância difusa no infravermelho (DRIFTS) e espectroscopia de reflectância difusa no ultravioleta-visível (DRUVS).

Um dos efeitos que a adsorção do metal pode ter na celulose é, alterando a disposição espacial das cadeia, alterar o seu grau de cristalinidade. A cristalinidade de celulose das amostras estimadas por DRIFTS, na região entre 1300 e 1180 cm^{-1} e as bandas a 898 e 1430 cm^{-1}, indicam que, no caso de vanádio (V) e zinco (II), há aumento do grau de cristalinidade enquanto, para os outros metais esta

não foi influenciada pela presença dos complexos metálicos. No entanto, a quantificação desta mudança só foi possível no caso de vanádio (V), onde se mostrou que em meio ácido a pH 3 e 5 e concentrações superiores a 1 mM / g de celulose, a cristalinidade aumentou de cerca de 44 para 76% com o aumento da concentração de complexo de vanádio de 1 a 10 mM / g de celulose.

A influência da matriz no complexo metálico, no caso de vanádio (IV) foi analisado por as alterações observadas nas bandas de absorção no infravermelho, em particular nas regiões 1000 -1200 cm^{-1} e 600-670 cm^{-1}, mostraram que tem havido uma mudança na estrutura cristalina do composto inicial de solúvel em água (forma α) para a forma insolúvel (forma β). O desvio da banda a 1200 cm^{-1} em dos três conjuntos de amostras (aos três diferentes pH) indicou o aprisionamento do ião SO_4^{-2} (ligando do complexo metálico) entre as cadeias de celulose, por outro lado, para concentrações elevadas do complexo de V(IV) o deslocamento na banda a ~980 cm^{-1} indica adsorção de diferentes espécies de vanádio na celulose. Os espectros de absorção no ultravioleta-visível (DRUVS), têm baixa intensidade das transição d-d na região de 500 nm, nas amostras com pH 3 e pH não ajustado, o que pode estar ser explicado pela oxidação de V(IV) a V(V). No entanto, considerando a cor azul dessas amostras, característica de V (IV), a baixa intensidade das bandas d-d em amostras com baixa concentração de complexo pode apenas ser devida ao facto de as bandas CT a ~240 nm serem muito fortes. Comparando a relação de intensidades destas mesmas bandas quando o complexo está adsorvido em celulose, onde as bandas d-d parecem ser ainda mais fracas do que na amostra de controle (complexo depositado na ausência de celulose) , pode significar que existe ligação ou interacção forte entre alguns grupos da celulose e o metal. Nas amostras com um pH 5, existem indicações de formação de um novo complexo e também de oxidação parcial de V (IV) a V (V).

O vanádio (V) adsorvido em celulose, apresenta novas bandas a 960, 971 e 965 cm^{-1}, 836, 829 e 829 cm^{-1} e 703, 750 e 747 cm^{-1}, respectivamente para o conjunto de amostra de pH não-ajustado, amostras de pH 3 e amostras de pH 5. Estas novas bandas podem ser devidas à deposição na celulose de diferentes espécies de poli vanádio, em particular quando em concentrações mais elevadas. Uma vez que o equilíbrio das espécies de vanádio é dependente do valor de pH, seria de esperar que para cada conjunto de amostras, em que se varia o pH, diferentes espécies de metal adsorvido em celulose. As amostras a pH baixo, tal como o pH 3, verifica-se que são decavanadatos as espécies dominantes. A pH 5 nas amostras a espécie dominante parece ser uma mistura de tri e decavanadates, enquanto para as amostras a pH 6-7, podemos esperar ter mistura de tri e tetravanadatos depositados em celulose. Estas evidências são confirmadas na análise dos espectros

DRUV que mostrou não haver redução do V^{5+} nas amostras mas que apenas são formadas diferentes espécies de polyoxovanadates.

Os espectros DRIFT de ferro (II) indicam haver interacção muito fraca entre o complexo metálico e a celulose, o que significa uma deposição do complexo sobre a superfície da celulose ou na fase amorfa. No caso dos espectros DRUV mostraram que é possível existirem iões Fe^{3+} que se teriam formado nas amostras por oxidação do Fe^{2+}, em condições aeróbias.

No caso do ferro (III), dado que no espectro de DRIFT das amostras (a todos os valores de pH de preparação) é observada a banda forte de complexo de Fe^{3+} a 1384 cm^{-1}, provavelmente apenas como resultado da elevada concentração de complexo, por deposição sobre a superfície exterior da celulose e interação fraca. No entanto, os desvios das bandas a 1360, 830 e 802 cm^{-1} indicam a deposição de espécies diferentes ou, mais provavelmente, uma adsorção entre as cadeias de celulose com interacções mais fortes.

No caso dos complexos de zinco e cobre de nenhum efeito significativo é observado nos espectros. De facto, nem as bandas do complexo metálico nem as da celulose são afectadas pela deposição. Além disso, não são observadas bandas novas, apontando para uma interação fraca entre o complexo e a matriz. Uma vez que o zinco tem muito baixa capacidade de absorção na região de UV/Vis nenhuma informação complementar foi obtida por da análise dos espectros de DRUV. No entanto, a ausência de bandas d-d esperadas a cerca de 800 nm no espectro das amostras de Cu (II), confirmou que não ocorreu a deposição de espécies octaédricas de cobre na celulose.

A análise quantitativa é realizada, por todos os metais, com excepção do zinco, utilizando a equação de Kubelka-Munk, ou função de reemissão, que correlaciona a intensidade da radiação reflectida difusamente e concentração para amostras sólidas, de forma semelhante à lei de Lambert-Beer para amostras líquidas . Em todos os pares de metal complexo / celulose estudado o aumento de F(R) com o aumento de concentração foi evidente. No entanto, a linearidade entre F(R) e a concentração em toda a gama de concentrações somente se mostrou possível para as amostras de V(V) a pH 5 e V (IV) a pH 3. Em todos os outros casos apenas foi possível aplicar a regressão linear, com resultados aceitáveis, nas amostras com concentrações baixas, de 0,20 até 1,00, 3,00 ou 5,00 mM / g de celulose (dependendo do conjunto de amostras). Estes resultados apontam para a necessidade de optimizar a preparação das amostras, processo com repetibilidade muito baixa, reduzindo e substituindo os passos envolvidos com maior possibilidade de perda de analito.

1. Introduction

The objective of this project will be study the interaction of cellulose fibers with four different metals: vanadium, iron, copper and zinc.

Different compounds of all examined metals are used as components of various dietary supplements and food additives and also different kinds of drugs for treatment of conditions such as diabetes, cancer, anemia, as anti-parasitic agents etc.

Cellulose and its derivatives are one of the most commonly used pharmaceutical excipients.[1,2,3,4] Microcrystalline cellulose (MIC) and powdered cellulose are often used in pharmaceutical products as a diluent / filler but also as directly compressible excipient for tablets[1,2,3,5] due to its high compactibility which enables it to produce strong tablets at low forces.

One of the primary criterions for choosing excipients is compatibility with the active components and other excipients. Some metal compounds can interact with the cellulose fibers and change its structure and characteristics. Degree of crystallinity of cellulose can affect different properties of tablets such as crushing strength[6] and absorption of moisture from the air since in cellulose water is not taken up through the whole structure but only in the amorphous regions[4]. The amount of water absorbed into tablets changes with the different ratios of crystalline and amorphous regions in the cellulose so consequently the dissolution rate and the drug release from the tablets can be modified.[6,7] Interaction of metals with cellulose such as forming complexes can cause changes in chemical stability of administrated active components or decrease their bioavailability and therefore decrease the effect of the drug and therapy.

Besides these pharmaceutical uses interaction between cellulose and its derivatives and metals is also being used for other purposes such as preconcentration, separation and removal of heavy metals from water[8,9,10] or in the form of metal-containing fabrics with antimicrobial activity.[11]

1.1. Metals

1.1.1. Vanadium

Vanadium is found in over 100 different minerals, ores and in smaller amount in the form of organic complexes in some crude oils. In the marine environment it's the second most abundant transition element.[12] In biological systems vanadium is present in small amounts where it has different biochemical and physiological roles and among them is insulin mimetic or antidiabetic activity.[13] In human body vanadium is present in small amounts, in blood plasma, tissues and it can also be accumulated in bones, kidneys and liver.[12] Almost 90% of vanadium in human body is bonded to proteins and the rest is present in ionic form. The most common use of vanadium is industrial, the largest part being used as a steel additive in the production of ferrovanadium.[12] Other industrial applications are mostly in ceramics and electronics.[14] Apart from this uses vanadium is also used in chemical industry most often as a catalyst in the form of oxides, and in the pharmaceutical industry as a component of different kinds of drugs and food supplements. Due to its antidiabetic activity vanadium has long been used in the treatment of diabetes, and in the last years scientists have also been studied possible utilization of vanadium as anti-parasitic agent[14] and its role in prevention and treatment of cancer.[15] [16]

Vanadium can exist in four possible oxidation states: +2, +3, +4 and +5. However, since V (II) is very unstable and it is easy oxidized in V (III) only last three have importance in biological systems. In water solutions vanadium has very complex chemistry since it undergoes different chemical reactions which are highly dependent on the pH of the solution; depending of the prevalent oxidation state vanadium shows color pallet from violet (oxidation state 2+) to green (oxidation state 3+), blue (oxidation state 4+) and yellow (oxidation state 5+).[12] Range of existence of different oxidation states and species of vanadium is best reflected in Baes-Mesmer diagram (**Figure 1.1**) which shows speciation of V^{n+} according to the redox potential and pH of the media.

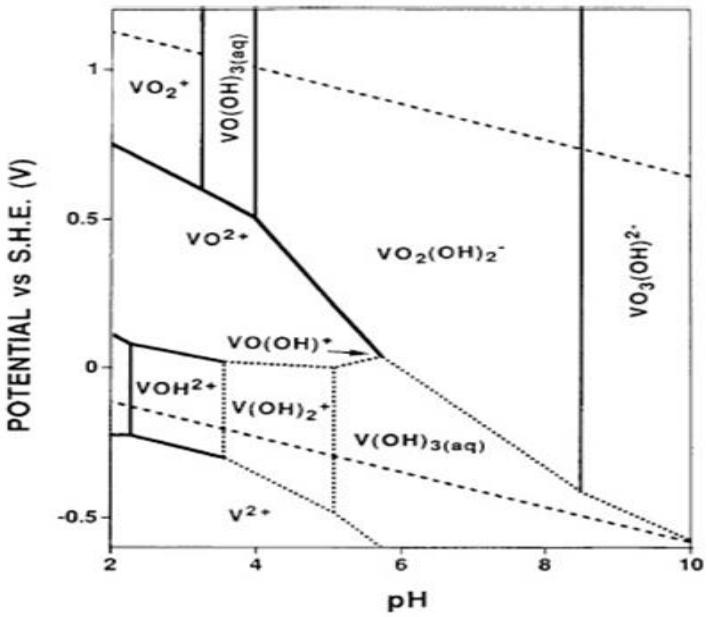

Figure 1.1. Baes–Messmer diagram for the aqueous vanadium system. Standard redox potentials (in V) vs the normal hydrogen electrode (NHE) are given. The two parallel dashed lines running from the upper left to the lower right indicate the range of stability of water.[12]

Stability of vanadium in aqueous solutions depends on pH, redox potential and ability to form complexes. V (II) is highly unstable in water solutions and it is quickly oxidized to V (III). Vanadium with oxidation state 3 and 4 are cationic in water solutions while vanadium 5 species are mostly anionic. Vanadium with oxidation state +4 is stabile in a form of hydrated vanaydil cation $VO(H_2O)_5^{2+}$ (or abbreviated just VO^{2+}) in acidic solutions, but it is unstable at higher pH values and easily oxidized to V(V).[17]

At neutral pH values dominant form of V (V) depends of concentration; at lower concentrations it is usually in the form of monomeric anion, $H_2VO_4^-$ or HVO_4^{2-} while in the high concentrations (above 1mM) dominant form is polymeric $V_4O_{12}^{4-}$.[12,18] Diagram showing speciation of V^{n+} as a function of pH and concentration is presented in Figure **1.2**.

Monomeric anion easily undergoes condensation reactions with different nucleophilic ligands including other vanadium species, and therefore dominant species in solution are different types of oligomers depending of the environmental pH. In pH values below 6 dominant oligomer is decavanadate $V_{10}O_{28}^{6-}$ (or just V_{10}). Decavanadates forms orange-yellow solutions and it is the only form of V (V) anion that is colored. Although V (V) is mostly anionic in aqueous solutions, in highly acidic environment (below pH 2) decavanadates became unstable and cationic vanadium (V) monomer VO_2^+ is formed in the form of octahedral complex $[VO_2(H_2O)_4]^+$.[12]

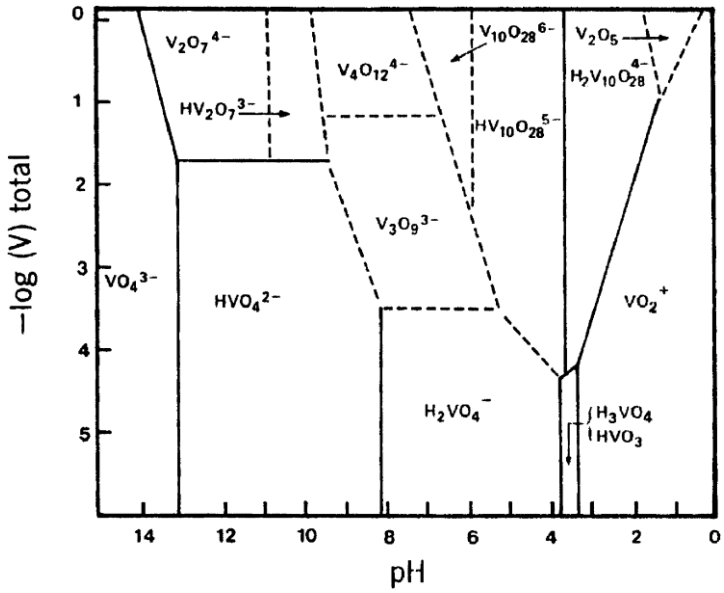

Figure 1.2 Predominance diagram, showing the regions in which the species indicated are those present in the highest concentration. Broken lines indicate less certain demarcations.[12]

1.1.2. Iron

Free iron is rare in nature, usually it is found in the form of oxides and different minerals. It exists in various oxidation states from -2 to +6 but two most common ones are +2 and +3.[19]

Pure iron is soft and usually it is mixed with different kind of impurities in order to achieve better properties. Most common form of iron is steal which is formed by adding carbon in different amounts. The most dominant usage of iron is industrial and mainly in construction. Iron is he most used of all the metals and about 95% of worlds metal production is accounted for iron. Besides this it is also used as catalyst in many chemical processes, in the process of water purification, dyeing of the textiles, coloring agent in paints, etc. It also used in medicine in treatment of different pathological conditions primarily anemia, iron deficiency[20,21] and coughs caused by ACE inhibitors[22]. There are also indications that in the future it can be used in treatment of conditions such as attention deficit-hyperactivity disorder (ADHD),[23,24] Crohn's disease, female infertility and others.

Regarding its biological role, iron is the essential element for almost all living organisms and it is vital for the processes in which cells generate energy. It is integral part of proteins and enzymes which are engaged in key metabolic roles in human body. The biggest part of iron in human body is found in a form of two proteins: hemoglobin and myoglobin, where it has crucial role in transportation of oxygen.

In aqueous media iron is found in two oxidation states, Fe (II) and Fe (III). Fe (II) is easily oxidized to Fe (III) under influence of environmental oxygen. This reaction occurs at all pH values but it is significantly faster in basic than in acidic solutions.[19]

Both ferrous (Fe^{2+}) and ferric (Fe^{3+}) compounds upon dissolution in water form strongly acidic solutions where predominant ion species are aqua complexes with octahedral geometry: ($[Fe(H_2O)_6]^{2+}$ and $[Fe(H_2O)_6]^{3+}$).[25] With an increase of pH value of aqueous solution of iron (III) or (II) insoluble hydroxides $Fe(OH)_3$ and $Fe(OH)_2$ are formed.

1.1.3. Copper

Properties of copper such as high occurrence in nature, good ability to form alloys, low corrosion, high thermal and electrical activity, has made it one of the most important and most utilized metals in the world. Free metal is found in small amounts in nature but it is usually found in the form of different compounds, most often minerals such as sulfides, carbonates or oxides. The most common oxidation states of copper are +1 and +2. Although it can form compounds with oxidation states +3 and +4, these are extremely rare and not very important.[26] Regarding its biological importance, copper is known to be essential microelement not only for humans but also for animals and plants. It has important role in functioning of several enzymes and proteins involved in wide range of different metabolic processes. Copper is needed for normal infant growth, normal functioning of organisms defense mechanisms, iron transport, blood cell maturation, formation of connective tissue, etc.[26]

Due to its good electrical conductivity it is extensively used for electrical purposes. It can be used as pure metal or in a form of alloys. It is also commonly used for water tanks and pipes, in construction, as fungicide and catalyst in different chemical processes[19] and in a form of copper containing fabrics as antimicrobial agent.[27]

The most important oxidation state of copper is +2 also known as cupric ion, and it is oxidation state generally found in water solutions. Most cupric compounds and complexes are blue or green and usually have high solubility in water[26] where they form aqua complexes $[Cu(H_2O)_6]^{2+}$ with distorted octahedral (tetrahedral) structure.[19] At low concentrations and pH values higher than 7.5 insoluble hydroxide $Cu(OH)_2$ is formed (**Figure 1.3**), however, at high concentrations it can also be formed even at lower pH values. $Cu(OH)_2$ stays dominant species in basic environment up to the pH 12.3 when forming of $Cu(OH)_3^-$ occurs.[28]

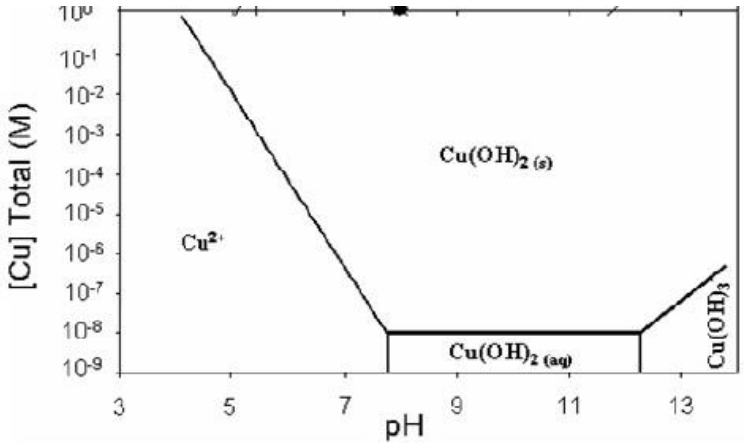

Figure 1.3. Speciation of copper as a function of pH and concentration at 25°C (only dominant copper species are shown).[28]

1.1.4. Zinc:

Zinc is most commonly found in association with other metals in the form of ores. It has low affinity for forming oxides and prefers to bond with sulfides so the most common form in which zinc is found is sphalerite (Zn,Fe(S)).

In human body zinc is vital for many biological functions and has an important role in functioning of large number of enzymes. It is also well known that zinc plays essential role in the normal functioning of immune system.[29] It is found in almost all parts of the human body but the largest part is located in muscles and bones.

It can be utilized as free metal or in a form of different compounds and alloys, especially brass. Due to its resistance to corrosion zinc is used as anti-corrosion agent for coating of iron (process known as galvanization). It is also used in production of batteries, white pigment in paints, as wood preservative, as catalysts, agricultural fungicide.[19] In pharmaceutical industry it is used as food supplement in treating zinc deficiency, diarrhea[29 30], Wilson's disease[31], acne, anemia, common cold etc.

Zinc can exist in two oxidation states, +1 and +2 but oxidation state +1 is extremely rare and doesn't have much significance. Zn (II) compounds are usually colorless and produce also colorless water solutions. In water it forms 4-coordinate, tetrahedral or (less commonly) 6-coordinate octahedral complexes. Therefore in aqua solutions it exists in the form of aquo- $[(Zn(H_2O)_6]^{2+}$ or hidroxo-

$[Zn(OH)_6]^{4-}$and $[Zn(OH)_4]^{2-}$ complexes. In aqueous solutions it has similar behavior as copper[28]; In basic conditions at pH higher than 8.7 (or lower depending on concentration) Zn (II) is precipitated in a form of hydroxide $Zn(OH)_2$. However in the higher pH values hydroxide is dissolved and zincates are formed $[Zn(OH)_4]^{2-}$.[19]

1.2. Cellulose:

Cellulose is the most abundant organic polymer on earth. In nature it can be found in pure form but most often it is combined with other polysaccharides such as lignin and hemicellulose in the cell wall of plants. Commercial cellulose is primarily produced from harvested sources such as wood or cotton.[32]

Chemically cellulose is linear homopolymer consisting of hundreds to thousands of β 1→4 linked D glucopyranose units (**Figure 1.4.)** where every other monomer is rotated by the angle of 180° with respect to its neighbors.[33] This chain conformation is the lowest possible free energy conformation of the molecule. In this case the hydroxyl groups are positioned in the ring plane and hydrogen atoms are in the vertical position. Free hydroxyl groups are contained at C-2, C-3 and C-6 atoms. Presence of numerous polar groups enables formation of hydrogen bonds within the molecule (intramolecular) and also between different molecules (intermolecular) making the cellulose structure more complex. It is assumed that intramolecular hydrogen bonds are formed between O-3-H and O-5' and between O-2-H and O-6' in the neighboring glucopiranose units and they play important role in the conformation and stiffness of single chain units. Intermolecular bonds are formed between OH groups at C-6 and C-3 positions at the neighboring chains and they are responsible for organization of linear polymers in the sheet-like structure of native cellulose. The order of the molecules in cellulose fiber is not uniform in the whole structure. There are regions with low or high crystalline order and low order regions are known as amorphous cellulose. Degree of crystallinity of cellulose depends of the origin and pretreatment of the sample but usually it is in the range between 40 and 60%.[32] When cellulose reacts with different substances reaction occurs in the amorphous region and on the surface of the crystalline region of the cellulose while intracrystalline region remains unaffected.[34]

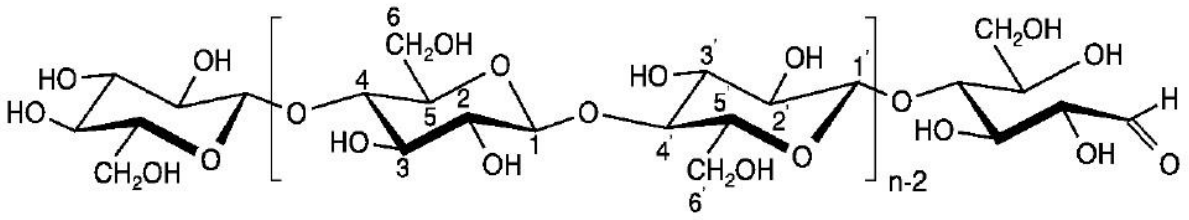

Figure 1.4. Molecular structure of cellulose

Glucose monomers are also called anhydroglucose units (AGU) due to the loss of water molecule in the process of polymerization. Number of AGU units determines degree of polymerization of cellulose (DP) and may significantly vary depending on the source.[33]

Cellulose can exist in 4 different crystalline modifications, the most important form being cellulose I, also known as native cellulose. Native cellulose consists of two different crystal structures Iα and Iβ where Iα has triclinic and Iβ has monoclinic cell structure.[32] Cellulose Iα is mainly contained in the cell wall of algae and Iβ in the cell wall of cotton, ramie and other wood fibers, and it is considered more stable form[35]. Small differences in the structure of these two forms also lead to different hydrogen bonding pattern.[32]

Cellulose II can be obtained from cellulose I by precipitating dissolved cellulose into an aqueous medium or in the so-called process of mercerization. The process of transforming cellulose I into cellulose II is irreversible. Cellulose III can be obtained by treating native cellulose with dry liquid ammonia at temperatures below 30 °C, and cellulose IV by treatment of other forms of cellulose with a suitable liquid at high temperature and under tension.[32]

Due to the strong dipolar attraction between the molecules, cellulose shows thermosetting behavior. Its structure cannot be loosened by heat or solvents without causing irreversible chemical decomposition.[35]

It is insoluble in water and most organic solvents but it can be broken down chemically into glucose units by treatment with concentrated acids at high temperatures. Aqueous solutions of several metals are also known to dissolve cellulose[36] by deprotonating and coordinative binding the hydroxyl groups in the C2 and C3 position of the anxydroglucose, as well as ionic liquids[37].

1.3 Spectroscopy:

Different spectroscopy techniques can be used for structure determination of the molecules. Although these techniques are versatile and operate over different frequency ranges within the wide range of electromagnetic spectra, they all work based on the same principle that under certain conditions materials absorb and/or emit energy. The condition for radiation absorption is that the energy difference between two energy levels of the molecule matches the energy of the radiation. In this case the absorption corresponds to a transition between two states and a spectrum is typically the set of all possible transitions in a spectral range of the electromagnetic spectrum. In the infrared (IR) and ultraviolet/visible (UV-Vis) regions two different transitions can be promoted, in IR the vibrational transitions are stimulated while in the UV-Vis are the electronic transitions.

A molecule can vibrate in many different ways and each of these vibrations is called a vibrational mode. The number of vibrational modes of a molecule depends on the number of atoms and each atom can be displaced in three directions corresponding to the three degrees of freedom. A nonlinear molecule with N number of atoms has 3 x N – 6 normal modes while in linear molecule 3 x N – 5 modes are possible.[38,39] There are two main types of vibrational modes: stretching mode characterized by movement along the bond axes where the distance between atoms is decreasing and increasing, and bending modes that are characterized by changes of the angle between bonds.[39] Molecular vibrations are not random motions but specific displacements of the atoms in given molecule and therefore characteristic of that molecule.[38]

Electronic transitions occur when the wavelength of the absorbed light has sufficient energy to move electron from a lower to a higher energy level. At room temperature all molecules are in the electronic ground state (lowest possible energy level) since the energy difference between the ground and excited states is relatively large.[40] The electrons that are situated in the outer shell of an atom can be found in one of three types of orbitals: single (σ) bonding orbitals with the lowest energy, double or triple (π) bonding orbitals and non-bonding (n) orbitals which have the highest energy. When the radiation is absorbed a transition occurs from one of these levels to an empty, anti-bonding orbital σ* or π*. Usually only π- π*, n- π* and n- σ* transitions are occurring.[41] The exceptions are d-d transitions that can happen in the complexes of transition metals that have partially filed d orbitals.[41,42]

When radiation with intensity I_o pass through the sample it is expressed as I intensity of the radiation that is transited. Transmittance is then defined as the ratio between I and I_o:

$$T = I/I_0 \qquad \textbf{(eq. 1)}$$

The absorbance is a quantification of the radiation that is absorbed by a molecule, and is defined as a logarithmic function of the inverse of the transmitted radiation:

$$A=\log_{10}(I_0/I) \qquad \textbf{(eq. 2)}$$

Transmittance and absorbance are connected through the relation:[43]

$$T = 10^{-A} \text{ (or } A = -\log_{10} T \text{)} \qquad \textbf{(eq.3)}$$

According to Lambert-Beer law the amount of radiation absorbed by the molecules (defined as absorbance, A) in the sample depends on the concentration and the length (or thickness) of the sample.

$$A = \varepsilon l c \qquad \textbf{(eq. 4)}$$

Where, ε is the molar absorption or extinction coefficient, l is the path length and c is the concentration of the absorbing species. The extinction coefficient for a given substance under constant conditions is characteristic and constant value. As it can be seen from the eq. 4, for the given path length, absorbance increases with the increase on concentration and in theory they should have linear behavior.[43] However in a lot of cases a plot of absorbance versus concentration shows a non-linear dependence which can be due to the chemical effects, stray radiation or low resolution, which is the most common case. Beer's law is only strictly valid for monochromatic radiation.[45]

The spectroscopic information in the reflectance mode is obtained based on the measurement of the reflected light. When radiation strikes liquid, solid or gas sample some of the photons are absorbed, some are transmitted and some of them are reflected of the surface of the sample or scattered by the sample. In powders or solid samples, no significant amount of radiation is transmitted; therefore, the radiation that does not interact with the sample is mainly reflected on the surface of the sample. This part of the radiation that is reflected of the surface of the sample is then studied as a function of a wavelength.[44]

Reflection in general can be specular or diffuse reflection. Specular or regular reflection is scattered with the same angle as the incident light angle and it is associated with the reflection from samples with smooth, polished, mirror-like surfaces, while the diffuse reflection is associated with the reflection from irregular, rough surfaces like powders as in case of our samples. In transmission spectroscopy the band intensity (its area in absorbance units) is directly proportional to concentration (see eq. 4), but no linear relation is obtained with transmittance. In diffuse reflectance spectroscopy also, there is no linear dependence between band intensity (or intensity of the reflected light) and concentration.[44]

Quantitative analysis is enabled by using Kubelka-Munk theory which deals with radiation transport in scattering media and gives the correlation between the intensity of the diffuse reflected radiation and concentration. The Kubelka-Munk equation is defined as:

$$f(R_\infty) = (1 - R_\infty)^2 / 2R_\infty = c/k = K/s \qquad \textbf{(eq. 5)}$$

where, where, $f(R_\infty)$ is the Kubelka-Munk function (or reemission function), R_∞ the absolute reflectance of the layer (the ratio of the sample diffuse reflectance spectrum and non-adsorbing reference, both measured at infinite depth), K is the absorption coefficient, s the diffusion (scattering) coefficient that is proportional to the fraction of diffused light, and c is the sample concentration. The more important condition is that the sample is thick enough that prevents radiation to reach the end of the sample (transmitted radiation is not possible) and it is known as infinite (∞) thickness.[44]

When we apply Kubelka-Munk function on the diffuse reflectance spectrum it is transformed to 'corrected' spectrum that resemblance the spectrum in absorption and demonstrates the linear relationship between the sample concentration and band intensity. In the y axis of this spectrum we have Kubelka-Munk units that relate concentration to reflectance using a scaling factor. In Kubelka-Munk theory it is assumed that 's' is constant and independent of wavelength, that sample layer is infinitely thick and that the sample has small absorbing power.[44]

Diffuse reflectance technique can be applied in the IR region (and then it is referred as Diffuse Reflectance Infrared Fourier Transform Spectroscopy or DRIFTS) or in UV-Vis region (and then it is referred as Diffuse reflectance ultraviolet visible spectroscopy or DRUVS).

In middle infrared region (MID IR, 4000-400 cm^{-1}) diffuse reflectance is very weak and can only be measured using Fourier transform infrared (FTIR) spectrometer.[44] Fourier transform is used to transform an interferogram of polychromatic light to its spectrum. The main part of FTIR spectrometers is an interferometer, most common is Michelson type. After the Fourier transform is applied using computer processing, interferogram of the polychromatic light is transformed into its spectrum and what we get is a new plot which represents signal intensity in correlation to wavenumber.[45]

Infrared is the portion of electromagnetic radiation that covers the region between 700 nm and 1 mm (or 14200 to 10 cm^{-1})[46,47] and can be divided into three regions:

- Near infrared 4000 – 13000 cm^{-1}
- Middle infrared 400 – 4000 cm^{-1}
- Far infrared 10 - 400 cm^{-1} [48]

Infrared spectroscopy is used for long time for determination of the structure of samples using characteristic absorption bands of each molecule. Today average modern instruments usually use spectra recordings at wavenumbers between 4000 and 400 cm^{-1}.[47]

Every molecule is composed of atoms tied together by chemical bands. These chemical bands have behavior that can be described as elastic springs between the atoms, so depending on the type of atoms (primarily its mass) and strength of the chemical bonds that connects them every molecule has a characteristic set of vibrational frequencies. Besides this, there are other factors that influence the vibrational frequencies of one molecule such as position and geometry of its chemical groups. Similar structural units will absorb infrared radiation at similar frequencies and intensities, the molecules with those groups will show similar bands in the spectra and these bands are called group frequencies.[46] These group frequencies may be viewed quantitatively as well as qualitatively since the absorption band assigned to a certain group increases proportionally to the number of times that group occurs within the molecule. The complete spectrum is basically a composed by the group frequencies, with band intensities in part related to the contribution of each functional group in the molecule.[47] When molecule absorbs infrared radiation it results in change in dipole moment of the molecule.

The spectra in the ultraviolet and visible region cover only a small portion of electromagnetic spectrum. Ultraviolet light is electromagnetic radiation with a wavelength from 10 to 400 nm, and visible light from 400 to 700 nm.[40] Photons of UV-Vis light have enough energy to cause transitions between electronic energy levels in atoms and molecules. In the case of molecules electronic level transitions are usually accompanied by a simultaneous change between numerous vibrational levels, which additionally has a number of rotational levels associated with it. Therefore the transition consists of electronic component, vibrational and rotational element. This causes superimposing of the vibrational and rotational energy levels and as a consequence the bands are broadened.[40] As opposed to IR spectroscopy, which gives us many narrow bands, in UV-Vis spectroscopy usually we obtain only a few broad absorption bands and it provides only a limited amount of qualitative information.[40] For that reason UV-Vis spectroscopy is in most cases used only for quantitative analysis.

Many inorganic molecules absorb UV-Vis light where absorption rises from charge transfer process when electrons are moved from one part of the system to another due to the energy provided by the light. Many metals also have the ability to form complexes with organic and inorganic molecules, and the basis for their spectroscopic determination is absorption due to movement of electrons between energy levels of ligand – metal complex.[49] Electronic transitions in transition metals complexes in general can occur in two ways: charge transfer (CT) transitions and d-d transitions. CT transitions can be ligand-to-metal (LMCT) or metal-to-ligand (MLCT) charge transfers. LMCT usually occurs when the metal is in high oxidation state and MLCT when the metal is in the low oxidation state. d-d transitions in complexes of transition metals happen because In this case d orbitals do not all have the same energy and therefore the transition of electrons from one to the other d orbital is possible. These transitions are forbidden in the most cases and can happen only if molecular vibration occurs together with the d-d transition.[42]

1.4. DRIFT and DR-UV/Vis spectroscopy methods for studying the interaction of metal compounds with cellulose

DRIFTS can be used to evaluate the crystallinity and structural changes of cellulose and of the metal complexes, while DRUVS can be used to analyze the metal compounds that are deposited over the cellulose surface.

Interaction between cellulose and metals and their compounds can occur in one of four main ways: adsorption on the fibers, forming chemical bonds with the reactive groups of cellulose, incorporation into cellulose matrix, and formation of complexes with dissolved degradation products of cellulose.[50,51] In general, cellulose fibers have very few functional groups that are capable of bonding with metals.[52]

Complexes between Cu and cellulose I can be formed but that process is very slow.[53] However, Cu can also interact with the cellulose by adsorption or by forming chemical bonds.[50] It is known from previous research that degree of complexation of Cu with the cellulose raises with the increase of pH value[50,52,54,55] probably due to the deprotonation of hydroxyl groups of cellulose.[50] In some cellulose derivatives such as carboxymethil cellulose COOH groups are also included in the formation of complexes with the Cu but the same behavior concerning pH has also been noted.[56,57]

When cellulose is treated with alkali in the process of mercerization its structure is changed (cellulose I is transformed to cellulose II) and formation of complexes is facilitated. Alkali causes swelling of the cellulose and rearrangement of its structure.[50,52,53] It is usually accompanied by a decrease in crystallinity and also a decrease in the degree of polymerization. The mercerization increases the separation between the cellulose chains and in that way facilitates the penetration of Cu into the structure.[52] Cellulose matrix that is changed in this way can easily bind copper and this process probably includes the formation of Cu (II) hydroxyl complexes.[50] Copper that interacted with cellulose can cause additional changes of cellulose structure by modifying it from twofold to trifold helix.[53] Concentrated aqueous solutions of cuprammonium hydroxide, or cuoxam, is known to dissolve cellulose through mechanism that also involves forming complexes between OH groups of cellulose and metal ions.[58,59]

Fe ions have similar behavior like Cu ions. Cellulose in general has low affinity for binding Fe (II) and Fe (III) ions. However in alkaline environment and in the presence of ligands such as D-gluconate and

hepta D-gluconate cellulose has distinct capacity to complex Fe (III) ions by ligand exchange reactions.[60,61,62] The mechanism of forming complexes involves first forming complexes between Fe (III) ions and ligands. In alkaline solutions competition for Fe (III) ions between ligands and cellulose occurs and leads to forming Fe-cellulose complexes.[61] Cellulose derivatives such as carboxymethyl cellulose (CMC) and hydroxyethil cellulose can form monoligand iron complexes with tetrahedral coordination.[63]

Fe (II) ions can form complexes with cellulose without involvement of the ligands through hydroxyl groups of cellulose. However, hydroxyl groups must be modified (oxidized) first in the high pH values and by presence of oxidizing agent such as hydrogen peroxide.[64] Coordination bonds are then formed between Fe (II) ions and modified OH groups at the 2^{nd}, 3^{rd} and 6^{th} carbon positions of cellulose.[64,62] However not all hydroxyl groups are oxidized and unreacted hydroxyl groups can also form complexes with iron involving cation exchange reactions.[62]

As opposed to iron and copper, zinc ions form complexes with cellulose at low pH values. In acidic conditions hydroxyl groups become protonated and as a result zinc ions can replace hydrogen and attach directly to oxygen atoms.[65,66] Depending on the reaction conditions such as concentration or temperature zinc can form complexes with different structure. When zinc chloride is used as a source of Zn (II) ions, at low concentrations loose complexes between C2 or C3 hydroxyl groups of cellulose and Zn (II) are formed. At higher concentrations of zinc chloride Zn ions form complexes involving C1, C3 and C5 atoms.[65] It is assumed that forming of Zn-cellulose complexes using Zinc chloride leads to decrease in cellulose crystallinity.[67] Dissolution of cellulose using concentrated solutions of zinc chloride is based on the same mechanism and depends on direct interaction of metal ions and OH groups. However, cellulose dissolving ability of zinc chloride also depends on amount of water present in the inner coordination sphere of the cation and while $ZnCl_2 \times 3H_2O$ can dissolve cellulose, $ZnCl_2 \times 2H_2O$ and $ZnCl_2 \times 4H_2O$ can only cause swelling but not the complete dissolution.[58]

In previous studies it has been demonstrated that vanadium in the form of polyoxometalates at aerobic conditions and low pH values has the ability to cause oxidative cleavage of C-C bonds in cellulose leading to formation of formic and acetic acid.[68,69,70,71] Good catalytic activity was also achieved using vanadylsulfate[71,72] although in this case different mechanism of reaction is proposed. It is assumed that VO^{2+} ion is the active species in isomerization of cellulose into fructose which is then fragmented into trioses by C-C cleavage and converted into lactic acid.[72]

In acidic environment V (V) ions are also known to form complexes with cellulose. In this process cellulose is serving as reducing agent and transformation of V (V) in V (IV) occurs.[73] Complexation of carboxyl methyl cellulose in acidic (pH 4) and neutral (pH 7) environment with both V (V) and V (IV) in the presence of ligands such as ascorbic acid (AA) or L-cysteine (Cys) was also described. In this case ligands react as reducing agents and depending on if the used ligand complexes with different structure are obtained. When AA was used five and six-coordinate V (IV) complexes are formed and when Cys was used five and six-coordinate V (V) complexes were dominant.[74] It is also noted that in the low pH values reduction from V (V) to V (IV) is generally more efficient but both species are equally able to form complexes.

2. Experimental:

2.1. Materials

All reagents used were of reagent grade. Native cellulose, iron (III) nitrate-9-hydrate and ammonium-meta-vanadate were purchased at Riedel -de-Haen, Germany. Iron (II) sulfate heptahydrate (Sigma – Aldrich, Germany), copper (II) sulfate pentahydrate (Scharlab S.L., Spain), zinc sulfate pentahydrate (Merck KGaA, Germany) and vanadyl sulfate hydrate (Aldrich Chemical Company Inc., USA). KBr and $BaSO_4$ (FITR grade from Aldrich).

2.2. Methods:

2.2.1. DRIFTS Measurements. The IR spectra were obtained using Mattson RS1 FTIR spectrometer with a wide-band mercury-cadmium-telluride (MCT) detector. All spectra were recorded in diffuse reflectance mode (with a Grasey/Specac accessory) and spectral range from 4000 to 450 cm^{-1} with a resolution of 4 cm^{-1}. The ratio of 500 single-beam scans to the same number of background scans was used. Before performing the measurement each sample was diluted with KBr in the ratio

approximately 1:5, placed in 8mm sample cup and manually pressed. The diffuse reflectance spectra were transformed to Kubelka-Munk units using the FIRST software. All fallowing spectra manipulation and data treatment was performed using OriginPro 7.0 software.

2.2.2. DRUVS Measurements. The UV-Vis spectra were performed on a double beam UV-Vis Shimadzu MPC-3100 Multi-purpose spectrophotometer using $BaSO_4$ as reference. Measurements were performed in diffuse reflectance mode at slow or very slow scan speed, sampling interval 2 and slid width 2. First scans were performed in the region from 200 to 800 nm but showed a lot of noise in the region from 200 to 214 nm so all fallowing scans were performed at the range from 214 – 600, 700 or 800 nm depending of the sample set. Powder samples were placed into a sample holder and compacted without the dilution with $BaSO_4$ except control samples for each metal that had to be diluted. All spectra were converted from the experimentally obtained reflectance (R) into remission function, F(R) in UVProbe software using the equation: $F(R)=[(1-R)2]/2\times R$. All DRUV spectra manipulation and data treatment was performed using OriginPro 7.0 software.

2.3. Sample preparation

Samples were prepared in two different ways. First group of samples was prepared by evaporation and second by filtration.

2.3.1. Evaporated samples:

In first group samples for 6 different compounds were prepared:

- copper (II) sulfate pentahydrate
- vanadyl sulfate hydrate
- ammonium-meta-vanadate
- Iron (II) sulfate heptahydrate
- iron (III) nitrate-9-hydrate
- zinc sulfate pentahydrate.

For each metal, three batches of samples were prepared: first batch with non-adjusted pH and second and third batch with pH values adjusted to 3 and 5, respectively. Each batch contained twelve samples including ten different concentrations and two blank samples, one blank containing only cellulose and water without the stock solution, and one control sample containing only and stock solution without cellulose). At the end we had 72 samples for each of the metals and therefore first group had 216 samples in total.

Samples for the each compound were prepared in the fallowing way: First, 1 g of native cellulose was weighed in 30 mL plastic beakers using the analytical balance. In each of the beakers we added 10 mL of distilled water and left for about 90 minutes for the cellulose to swell and allow uniform distribution of the metal. Then we added different amounts of previously prepared stock solution in each of the beakers: 0.0, 0.2, 0.25, 0.5, 0.75, 1.0, 3.0, 5.0, 6.0, 8.0, 10.0 and 10.0 mL.

Stock solution for each compound was prepared in concentration of 100 mM. Exception was ammonium-meta-vanadate solution where, due to the low solubility, stock solution had the concentration of 50 mM and therefore the amounts of the solution added in the beakers with the cellulose were doubled in order to achieve the same final concentration in each of the samples.

Finally, distilled water was added to each of the samples up to the volume of 20 mL, and initial pH vas measured and recorded. The final concentration of the metals was 0.2, 0.25, 0.5, 0.75, 1.0, 3.0, 5.0, 6.0, 8.0 and 10 mM /g of cellulose. Detailed tables for sample preparation are given in **Anex 5.1.**

Second and third batch of samples were prepared in the same way as the previous one. After measuring the initial pH values, pH was adjusted to the values of 3 and 5, respectively, using sodium hydrohyde and nitric acid solutions. All the samples were kept at room temperature in the fume chamber until complete evaporation of the liquid.

When the samples were evaporated sufficiently (to a soft paste consistency) we stirred them 2-3 times every day to achieve better homogeneity. This was repeated daily until a fine powder was obtained. Finally, the samples were put in the vacuum oven for 72 hours for removing the residual solvent and then sealed with plastic caps (**Picture 2.1**).

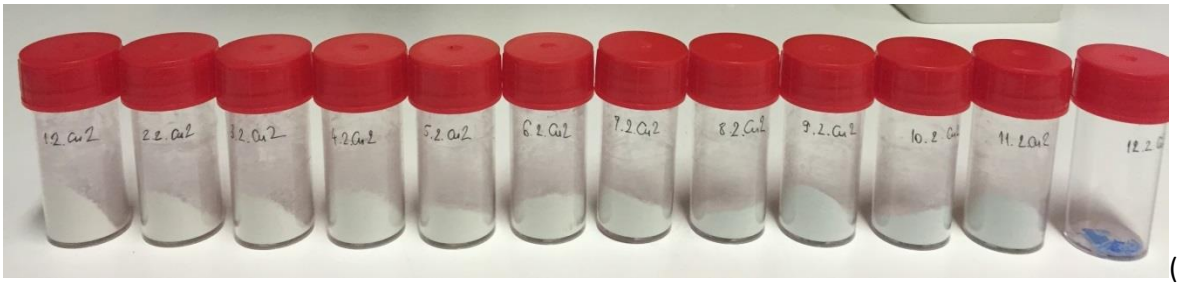
(a)

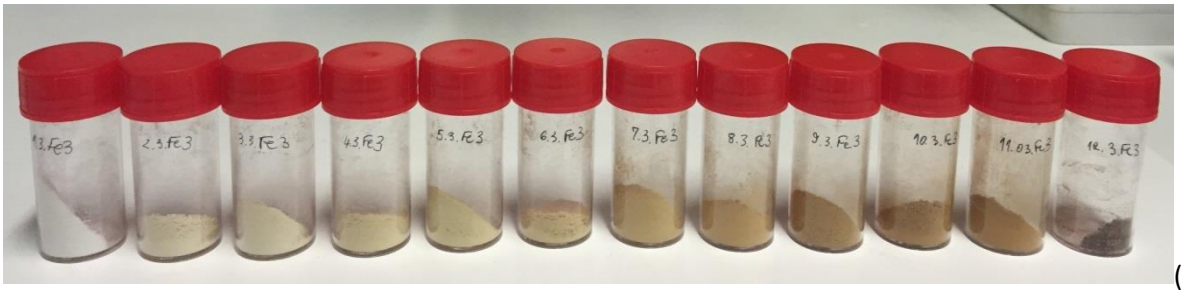
(b)

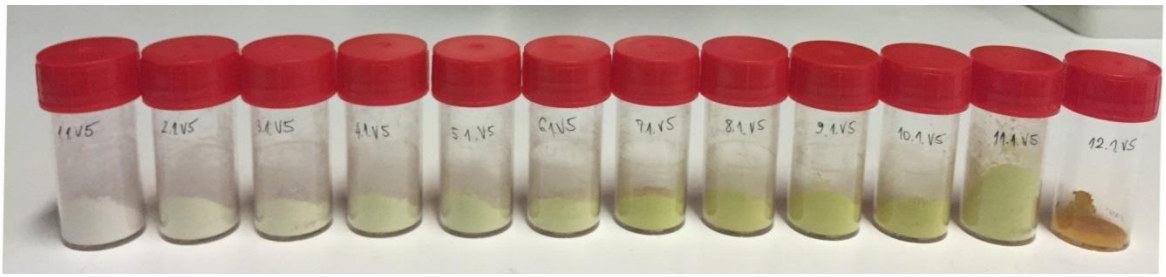
(c)

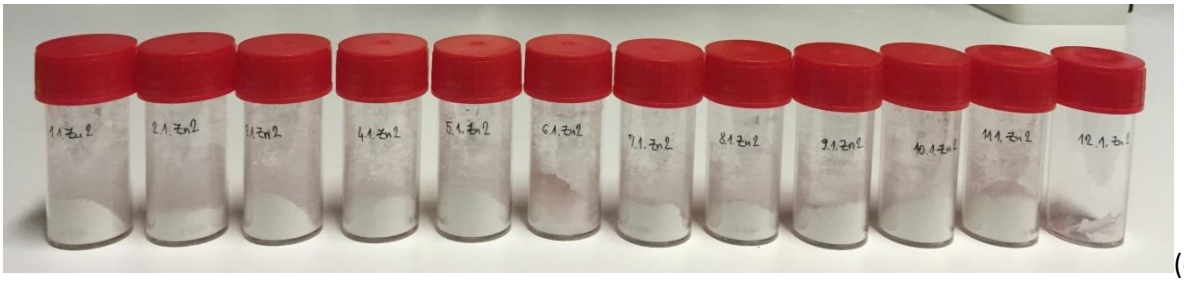
(d)

Picture 2.1. Prepared samples of (a) Cu(II) with pH 3, (b) Fe(III) with pH 5, (c) V(V) with non-adjusted pH and (d) Zn(II) with non-adjusted pH.

The only exception from this group of samples was batch of vanadium IV samples with non-adjusted pH. In this case the samples were prepared in glass beakers and supplemented with distilled water until total amount of 40 mL instead of 20 mL.

Samples were labeled with the five-character codes. The first number (1-12) is the serial number in each set of 12 samples, second number (1-3) represents pH value of sample set (1-non adjusted pH,

2-pH 3 and 3-pH 5), letter represents chemical symbol of each element and the last number is oxidation state of the metal in the initial compound.

The pH of all the samples was measured and recorded daily using portable pH meter. Time needed for the liquid phase to evaporate was usually between 7 and 10 days and during this time no significant changes in the pH were observed. In most of the cases changes in pH value were smaller than 0.4 pH units.

2.3.2. Filtrated samples:

For the second group of samples only three compounds were used:

- copper (II) sulfate pentahydrate
- vanadyl sulfate hydrate
- iron (III) nitrate-9-hydrate.

The samples for $VOSO_4$ and FeN_3O_9 were prepared in three batches. Each batch contained 6 samples including 4 different concentrations and two blank samples (one cellulose blank containing just water and cellulose and one control sample containing just stock solution without the cellulose). In total 18 samples were prepared for each compound. All three batches were prepared in the same way with the difference that pH value for the first batch is only measured and recorded after preparation and for batch two and three pH was adjusted to 3 and 5, respectively, using sodium hydrohide and nitric acid solutions.

First we measured 1 g of cellulose in 30 mL plastic beakers using analytical balance and 10 mL of water was added to each sample and left for about 90 min for cellulose to swell. After that, different amounts of stock solution were added to each sample: 0.0, 10.0, 5.0, 2.0, 1.0 and 1.0 mL. Finally, distilled water up to the volume of 20 mL was added in each sample. Detailed tables for sample preparation are given in **Anex 5.2.**

The stock solution concentration for both compounds was 0.1 M, and final concentrations of metal in samples were 0.0, 1.0, 2.0, 5.0 and 10.0 mM / g of cellulose.

Samples were held in sealed beakers for 10-15 days and then filtrated through grade 4 Sintered Glass Buchner Funnels using vacuum pump. pH for all the samples was measured again before filtration.

In the filtration process the samples were dried by keeping the pump on until apparently dry powder was obtained. The samples were collected from the funnels, transferred into plastic tubes and put into vacuum oven for 12 hours for final drying. After drying the samples were sealed with plastic caps.

Samples for copper were prepared without pH control. This set of samples contained 4 different concentrations of $CuSO_4$ and two blank samples (one with just cellulose and water and one with just $CuSO_4$ solution with the lowest concentration). For the samples 1 g of cellulose was measured in 150mL glass beakers using technical balance.

Aqueous solutions with following concentrations of $CuSO_4$ were prepared: 0.5, 0.25, 0.125 and 0.05 M. 75mL of each solution was added to cellulose and left for two weeks in fume chamber and then filtrated and dried using the same procedure described above.

Filtrated samples were labeled in a same way as evaporated ones with the addition of number 1 at the end of each code.

The samples pH was measured immediately after preparation and again just before the filtration. Significant changes were recorded only for V(IV) pH 5 set of samples where pH decreased in all the samples in the range from 1 – 1.7 pH units. In all the other samples pH also showed decrease but not significant and change in most cases was below 0.5 pH units.

3. Results and discussion:

3.1. DRIFT measurements – evaporated samples

3.1.1. Cellulose - Effect of pH adjustment and band assignment:

Effect of pH value on the cellulose was determined by comparing the IR spectra of blank cellulose samples with non-adjusted pH value and pH values 3 and 5. The pH value of the samples with non-adjusted pH was in the range from 5.25 to 6.05.

Blank cellulose samples were prepared in each different set of samples (6 blank cellulose samples for each pH value), however since the same conditions and procedure was used in the preparation of all the samples only cellulose samples prepared in the vanadium 4 and 5 sets are shown in **Figure 3.0.**

All samples contained bands characteristic for cellulose; OH stretching bands at 3342 cm^{-1} and OH bending mode between 1630 and 1640 cm^{-1}; IR spectra of cellulose should contain three bands in the OH stretching region but they can't be individually distinguished and usually appear as one wide OH stretching band.[75] However in all the samples a small shoulder at around 3280 cm^{-1} is present and together with the shoulder at around 710 cm^{-1} confirms the presence of cellulose Iβ as a dominant form.[35,76] Bands at 2900, 1318 and 1280 cm^{-1} are assigned to CH symmetrical stretching, CH_2 vibration and CH deformations, respectively.

All samples also have characteristic bands at 898 and 1430 cm^{-1} which are known as amorphous and crystallinity bands, respectively.[34, 75] Broadening or decrease / increase in the intensity of these bands may suggest changes in the degree of crystallinity in the samples. In the case of blank cellulose samples there were no significant changes.

Also there were no new bands in the spectra of any of the samples or any changes in position or shape of other characteristic cellulose bands so we can conclude that adjusting pH value of the samples had no effect on cellulose. Detailed band assignment for cellulose is given in **Table 3.1**.

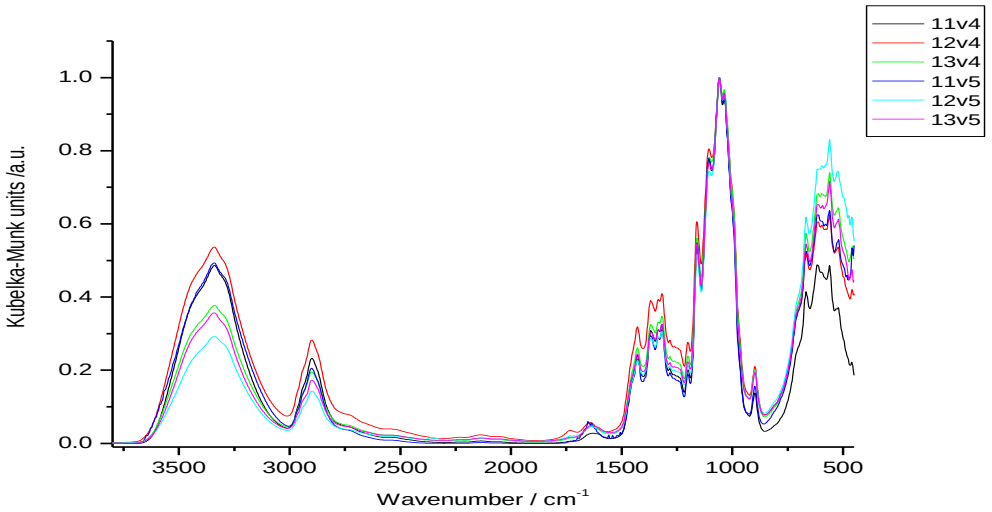

Figure 3.0. Compared DRIFT spectra of blank cellulose samples at different pH values

Table 3.1. Cellulose band assignment:

Vanadium 4			Vanadium 5			
pH 3	**pH 5**	**non adjusted pH (6)**	**pH 3**	**pH 5**	**non adjusted pH (6)**	**Band assignment**
13v4	**12v4**	**11v4**	**13v5**	**12v5**	**11v5**	
3341 (m)	3340 (m)	3340 (s)	3342 (m)	3340 (m)	3340 (s)	ν OH
2900 (m)	2900 (m)	2900 (m)	2899 (m)	2900 (m)	2901 (m)	ν_s CH
1633 (w)	1640 (w)	1631 (w)	1635 (w)	1635 (w)	1635 (w)	δOH adsorbed water
1429 (m)	1429 (m)	1429 (m)	1429 (m)	1429 (m)	1429 (m)	$\delta_s CH_2$, δOCH or δC-H
1368 (m)	1369 (m)	1369 (m)	1369 (m)	1369 (m)	1371 (m)	δCH
1334 (m)	1334 (m)	1335 (m)	1334 (m)	1334 (m)	1336 (m)	δOH and ν_{ring}
1318 (m)	1317 (m)	1318 (m)	1318 (m)	1317 (m)	1318 (m)	δ_{as}CH2
1282 (m)	1282 (m)	1283 (m)	1282 (m)	1282 (m)	1282 (m)	δCH
1200 (m)	1200 (m)	1201 (m)	1201 (m)	1200 (m)	1202 (m)	δOH
1160 (s)	1161 (s)	1161 (s)	1160 (s)	1160 (s)	1160 (s)	ν_{as}C-O-C
1105 (vs)	1105 (vs)	1106 (vs)	1105 (vs)	1105 (vs)	1106 (vs)	ν(ring)
1058 (vs)	1058 (vs)	1059 (vs)	1058 (vs)	1058 (vs)	1059 (vs)	νC-C, νC-OH, νC-H of ring and side group
1036 (vs)	1036 (vs)	1037 (vs)	1036 (vs)	1036 (vs)	1037 (vs)	νC-O
899 (m)	898 (m)	898 (m)	899 (m)	898 (m)	898 (m)	δCOC, δCOC or δCH
667 (s)	667 (s)	667 (s)	667 (s)	667 (s)	667 (s)	δC-OH (out of plane)

*vs - very strong, s - strong, m - medium, w - weak, vw - very weak, sh - shoulder, br -broad

Next to the blank cellulose samples prepared by evaporation blank cellulose samples were also prepared in the set of samples prepared by filtration and analyzed in the same conditions. Spectra of filtrated samples did not show any significant differences compared to evaporated samples and contained the same characteristic bands. Therefore, it is possible to conclude that different treatment of cellulose samples during the preparation did not influence its structure.

3.1.2. Effect of dissolution on IR spectra of M^{n+} compounds

In order to determine how or if the dissolution of compounds effected their structure we compared the IR spectra of the control samples prepared at different pH values with the spectra of corresponding solids used to prepare the stock sol. obtained under the same conditions (**Figure 3.1.**)

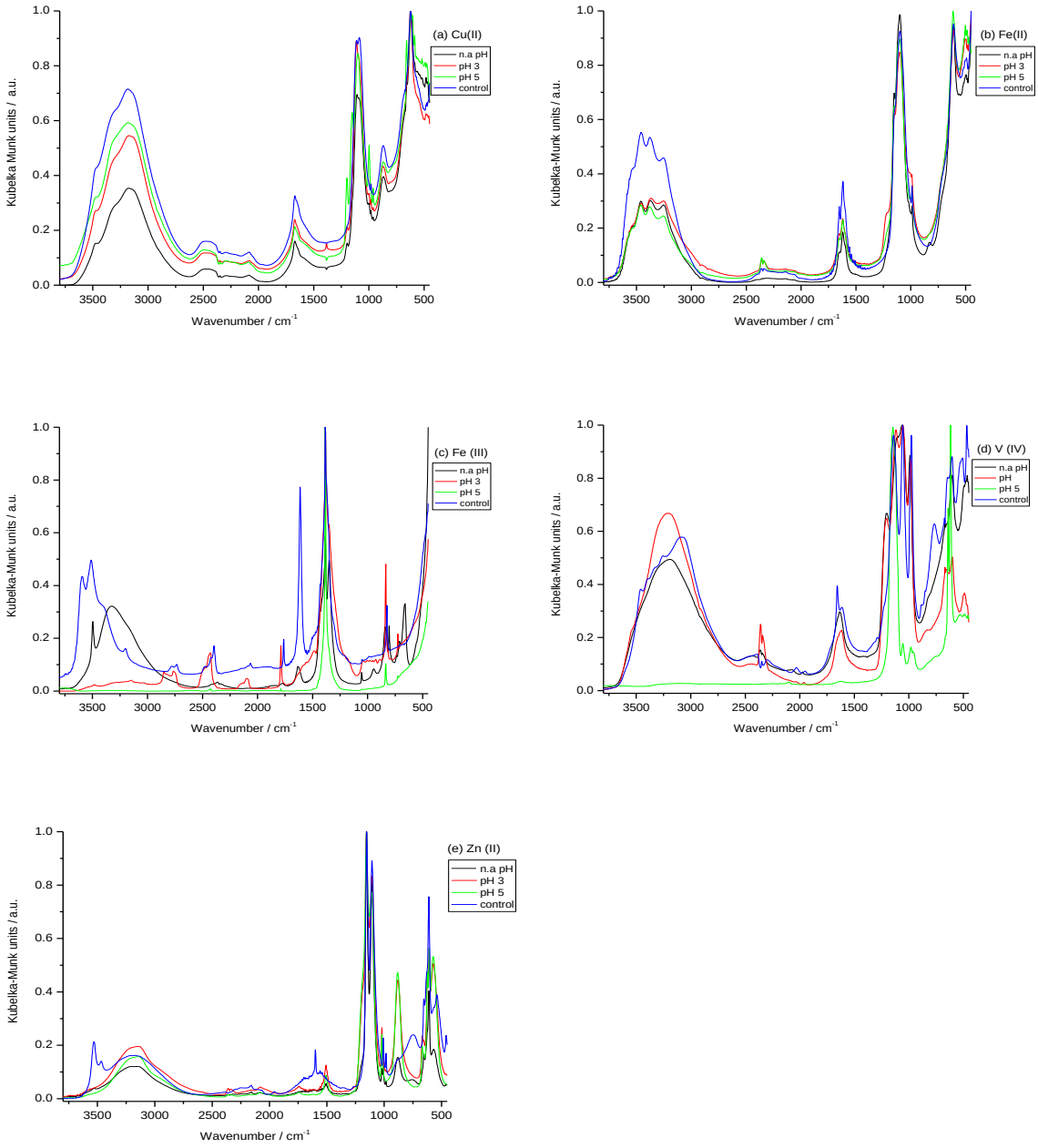

Figure 3.1. Compared spectra of control samples for Cu(II) - (a), Fe(II) - (b), Fe(III) - (c), V(IV) - (d) and Zn(II) – (e), and corresponding solids used to prepare the stock solutions

Some differences are present in IR spectra of $ZnSO_4$ and $Fe(NO_3)_3$ but mostly in the regions of the spectra assigned to the water bands and probably result of the high degree of hydration of initial compound. In the case of $ZnSO_4$ additional bands are present in the OH stretching region at 3530 and 3465 cm^{-1}; also peak assigned to water HOH bending mode was shifted to the 1599 cm^{-1}.

In the spectra of pure $Fe(NO_3)_3$, the OH stretching bands in the 3300-3400 cm^{-1} region are shifted to lower wavenumbers and the HOH bending mode at around 1620 cm^{-1} is more intense when compared to non-adjusted pH set sample. Also in the spectra of pure compound band at 661 cm^{-1} present in set sample is missing which is expected since this band is assigned to Fe-O stretching mode of αFe-OOH that is formed in diluted water solutions of $Fe(NO_3)_3$ as a result of slow hydrolysis during longer time at room temperature.

In the region between 900 and 1300 cm^{-1} in spectra of pure vanadyl sulfate bands assigned to sulfate modes are sharper and better separated compared to spectra of diluted samples which can be due to the crystalline structure of the solid, and also additional peak is present at 770 cm^{-1}.

Spectra of pure compounds in almost all the cases showed no or not significant differences compared to the spectra of corresponding sample with non-adjusted pH value. Therefore it is safe to assume that any differences in the spectra of three control samples for each metal are due to the pH adjustment and not to the dissolution in distilled water.

3.1.3. Vanadium IV

3.1.3.1. Effect of pH on vanadyl sulfate and band assignment

Effect of pH to vanadyl sulfate was determined by examining control vanadium samples – solutions of vanadyl sulfate in distilled water without addition of cellulose. After evaporation of the water the residuals were mixed with KBr and IR spectrum was obtained in the same manner as for the all other samples.

In the case of sample with adjusted pH 3 (122V4) and sample with non-adjusted pH (121V4, pH value was around 2.6) we couldn't achieve complete evaporation of the liquid. The samples contained

some crystals but mixed with the part of the sample which had consistency of oil. For that reason spectra of these samples contained a lot of water bands (3800-2500 cm^{-1}, and ~1640 cm^{-1}, the stretching and the deformation modes region of water, respectively) and in the low frequency region from 1300 to 4500 cm^{-1} showed big differences compared to the completely dry sample with pH 5 (123V4) which had no significant bands in that region (**Figure 3.2**).

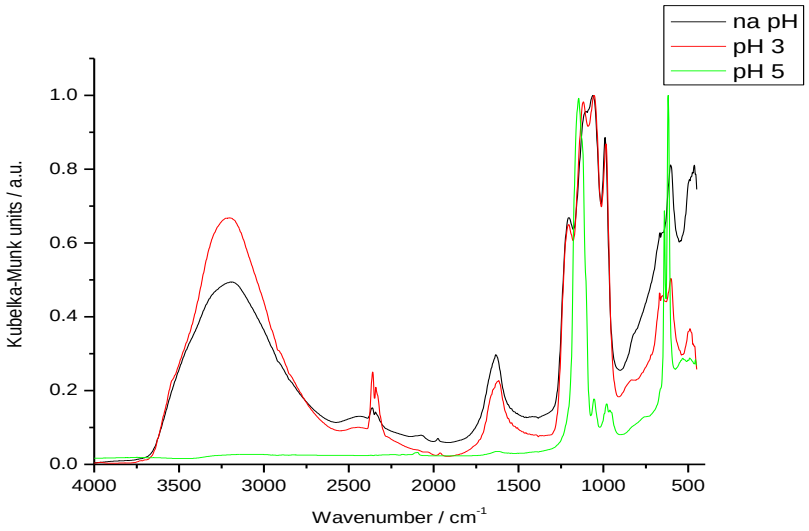

Figure 3.2 Compared DRIFT spectra of control V (IV) samples at different pH values

Considering that the $VOSO_4$ crystal is composed of SO_4^{2-} and $VO^{2+,}$ we should expect to see free group vibrations of V=O at 985 cm^{-1} and bands that can correspond to one of the four possible sulfate modes v1**,** v2, v3 and v4 at 980, 450, 1100 and 615 cm^{-1}, respectively [77].

Vanadium (IV) in aqueous media forms monooxido complexes based on the oxidovanadium (IV) anion VO^{2+} which stays in the solution under acidic condition (precipitation of insoluble hydrate and forming of oligonuclear hydroxo species begins at pH values higher than 5). In aqueous solution, vanadyl sulfate can only exist in the acidic region.[12]

$VOSO_4$ is a hydroscopic substance and there are several possible hydration possibilities ($VOSO_4$ x n H_2O), typically from 3 - 5. It can also occur in three modifications; one water soluble, known as α-$VOSO_4$ with tetragonal crystal structure, water insoluble β- $VOSO_4$ with orthorhombic structure and γ- $VOSO_4$.[77,78] Beta modification contains distorted VO_6 octahedra linked together in a zigzag course parallel to the a-axis by sharing opposite corners in infinite chains along which adjacent VO_6 octahedra are also connected by a bridging sulfate group. The remaining two oxygen atoms of the

sulfate groups link by corner sharing to upper and lower lying VO_6 octahedra along the b-axis, thus forming a three-dimensional network.

The crystal structure of α- $VOSO_4$ is characterized by continuous chains of corner shared VO_6 octahedra running parallel to the c-axis where each chain is connected to four other chains by corner sharing with sulfate tetrahedra.[79]

All three samples showed bands characteristic for the presence of $SO_4^{2+.}$ Dry sample with pH 5 had very sharp peaks at 1146/1054 cm^{-1} and 640/617 cm^{-1}, characteristic for v3 (SO_4^{2-}) and v4 (SO_4^{2-}) modes, respectively. Less intense peaks were at 962 and 994 cm^{-1} indicated the presence of V=O bonds.[77]

Other two samples have very similar spectra and both also showed clear presence of SO_4^{2-} - strong peaks at region around 1200, 1110 and 1055 cm^{-1} characteristic for v3 (SO_4^{2-}), 669 and 602 cm^{-1}, characteristic for v4 (SO_4^{2-}).

It is known from previous research that α- and β- modifications have infrared bands at slightly different wavenumbers. In particular, the characteristic V=O stretching band has been reported at lower wavelengths (938-945 cm^{-1}) in β-$VOSO_4$ compared to α -$VOSO_4$ (970-983 cm^{-1}).[77]

The spectra of pure compound used for the preparation of stock solution shows V=O bands from 964 to 994 cm^{-1} (Table 3.2) which can be assigned to both modifications. We might therefore assume that it was a mixture of water soluble α-$VOSO_4$ form and insoluble β form. However, compared to the pure compound, the IR spectra of our samples showed majority of the bands characteristic for β modification (**Table 3.2**)**,** therefore it appears that there has been a change in crystalline structure of $VOSO_4$ from α to β modification.

On the other hand, published data applies to pure crystalline forms of $VOSO_4$. The present results were obtained from evaporation of solutions, some of which with adjusted pH 3 and non-adjusted pH are forming oils so they are most probably amorphous forms of hydrated $VOSO_4$. Detailed band assignment for vanadyl sulfate is presented in **Table 3.2**.

Table 3.2.band assignment for V (IV) samples

Pure $VOSO_4.5H_20$	pH 3	pH 5	non adjusted pH (2,6)	Band assignment
	122v4	**123v4**	**121v4**	
3464 (m)				νOH (water)
3070 (s)				νOH (water)
	3199 (s)		3189 (s)	νOH (water)
1656 (m)			1634 (m)	δOH (water)
1612 (m)	1617 (m)			δOH (water)
	1203 (s)		1202 (s)	ν3 (SO_4^{2-}) of β-$VOSO_4$
1141 (vs)		1146 (vs)		ν3 (SO_4^{2-}) of β-$VOSO_4$
		1126 (sh)		ν3 (SO_4^{2-}) of β-$VOSO_4$
	1118 (vs)		1104 (vs)	ν3 (SO_4^{2-}) of α-$VOSO_4$
1055 (vs)	1055 (vs)	1054 (w)	1061 (vs)	ν3 (SO_4^{2-}) of β-$VOSO_4$
	985 (vs)	994 (sh)	990 (vs)	ν(V=O)
976 (vs)		980 (w)		ν1 (SO_4^{2-})
		962 (w)		ν(V=O)
	825 (sh)		822 (sh)	ν(VO_2)
766 (s)				νV-O-V
	669 (s)		667 (s)	ν4 (SO_4^{2-}) of β-$VOSO_4$
	650 (s)	640 (vs)		ν4 (SO_4^{2-}) of β-$VOSO_4$
		617 (vs)		ν4 (SO_4^{2-}) of α -$VOSO_4$
603 (s)	602 (s)		603 (vs)	ν4 (SO_4^{2-}) of α-$VOSO_4$
	490 (s)		494 (sh)	ν(V-O)
470 (s)			474 (sh)	ν(V-O) of V_2O_5

*vs - very strong, s - strong, m - medium, w - weak, vw - very weak, sh - shoulder, br -broad

3.1.3.2. Effect of vanadium (IV) deposition on native cellulose

Effect of vanadium (IV) deposition on native cellulose is determined by comparing spectra of native cellulose deposited at pH values 3, 5 and in the range from 2 -4 for set of samples with non-adjusted pH. The concentration of vanadium was in the range from 0,2 – 10 mM per gram of cellulose. Compared DRIFT spectra for all three pH values and different vanadium concentrations are shown in **Figure 3.3**.

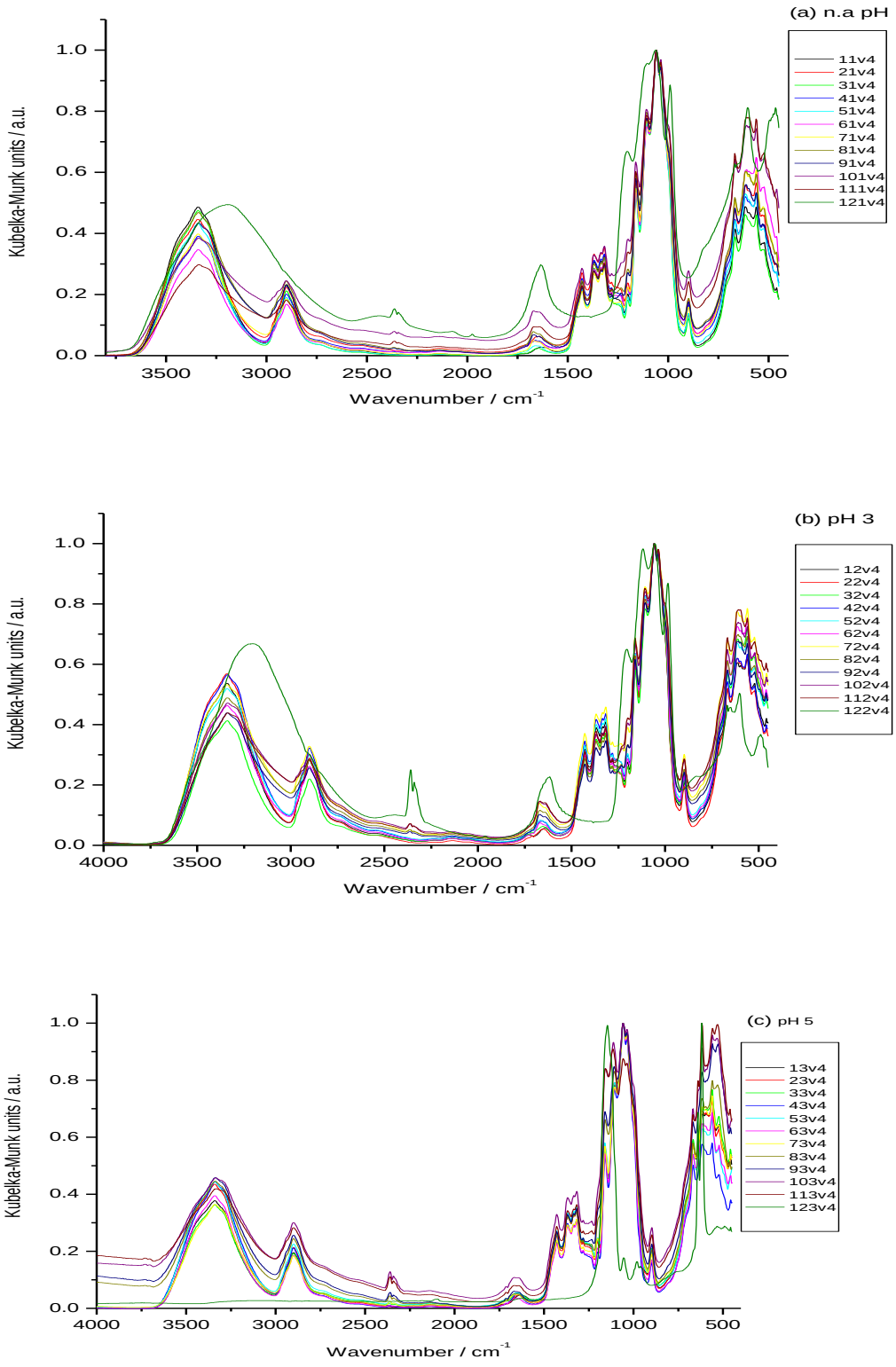

Figure 3.3. Effect of vanadium (IV) deposition on native cellulose at non-adjusted pH (a), pH 3 (b) and pH 5 (c) at different concentrations of vanadium

In the spectra of all three sets of samples there are some similar changes. In the regions from 3200 to 2945 cm^{-1} and from 1700 to 1550 cm^{-1}, bands for samples with the highest range of concentrations are shifted and there seems to be some changes in the spectra. Initially, samples with non-adjusted pH and pH 3 have peaks in these regions but in the dry vanadium (IV) sample there are no bands at all in this region. Therefore, the bands were assigned to adsorbed water and the observed changes in the spectra in these regions most probably are not the result of vanadium presence. Being so, those shifts can be due to water presence. Nevertheless, the presence of some kind of vanadium aqua complexes, not present in the dry samples (pH 5) cannot be excluded.

In the region from 1100 to 900 cm^{-1} a small shift in the bands is noticeable particularly in the band at 985 cm^{-1}, assigned to V=O **(Figure 3.4).** As the concentration of V increases so does the intensity of the V=O band, as expected. The shift to lower wavelengths may be due to the decreasing influence of the cellulose bands at 1030cm^{-1}. This change is present in the pH 3 samples (**Figure 3.4a**) and samples with non-adjusted pH, but again also present in the samples with pH 5 **(Figure 3.4b)**. Any interaction with a ligand, such as cellulose OH groups, involving weak axial binding to V=O would result in an increase of the V=O band wavelength. In this case, the observer shift in the V=O band could be explained by a predominance of the "free" $VOSO_4$ at higher concentrations, relative to the "bound" $VOSO_4$ at lower metal concentrations. Hence, it is not possible to ascertain whether the shift of the V=O is due to a spectroscopic artifact (overlapping with stronger cellulose bands at lower metal concentration) or to axial binding to vanadium.

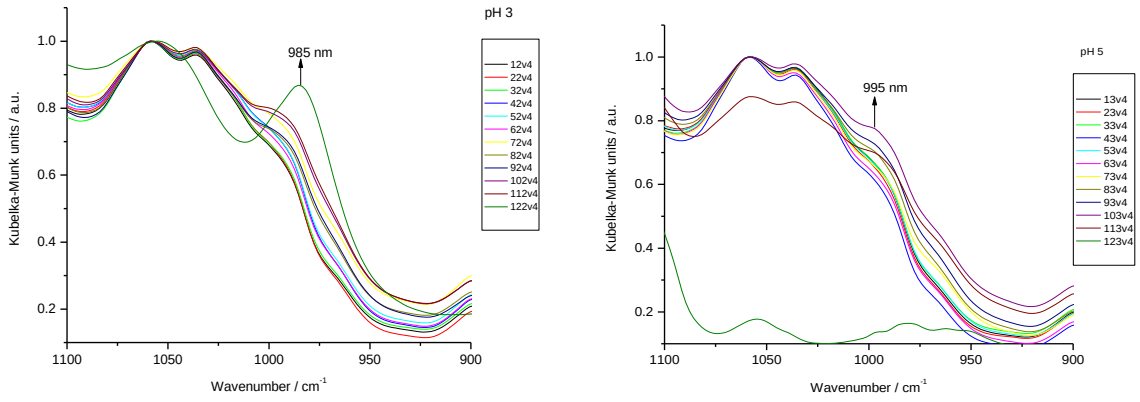

Figure 3.4 Changes in the spectra in the region from 1000 cm^{-1} and spectra of pH 3 (a) and pH 5 (b) sets of samples

In all three sets of samples, the spectra of the ones with high concentration present a shift of the bands at 1200 cm^{-1} assigned to v3(SO_4^{2-}). These peaks are clear in the samples with pH 3 and non-adjusted pH samples and may indicate entrapment of the SO_4^{2-} ion into cellulose. Also related with the ligand, in the set of samples with pH 5 there is a shift of the bands in the higher range of concentrations at 1160 and 1115 cm^{-1}, corresponding to the peak at 1146 cm^{-1} in vanadium blank sample assigned to v3(SO_4^{2-}) of β-$VOSO_4$. In other two sets of samples there is no change in the position or intensity of the band and no vanadium peaks also. This may be due to the formation of β-$VOSO_4$ and its' bonding to cellulose at pH 5.

3.1.4. Vanadium (V)

3.1.4.1. Effect of pH on ammonium metavanadate and band assignment

The effect of pH to ammonium metavanadate is determined by examining control vanadium samples – solutions of ammonium metavanadate in distilled water without addition of cellulose. After evaporation of the water the residuals were mixed with KBr and spectrum was obtained as described in experimental section.

The spectrum of three control samples is shown in **Figure 3.5** Very small differences are observed between samples 122V5 (pH 3), 123V5 (pH 5) and sample 121V5 (for which pH was measured after preparation and the value was approximately 7). The most distinct difference is in the band at 900 nm, which is only present in the sample without pH adjustment. Besides that the differences are still negligible and the influence of pH on the samples is not considered to be significant.

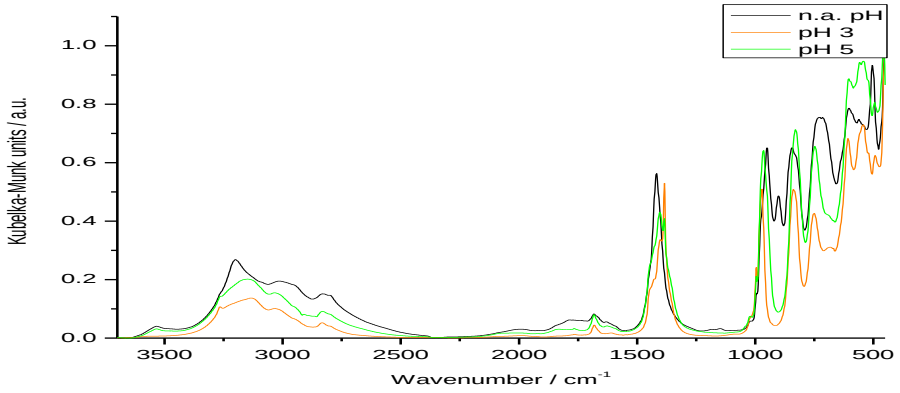

Figure 3.5 Compared DRIFT spectra of control V(V) samples at different pH values

The NH^{4+} ligand should have four characteristic vibrational modes in the region between 1400 and 3500 cm^{-1}: totally symmetric stretching mode v1, doubly degenerate bending mode v2, triply degenerate asymmetrical stretching mode and triply degenerate bending mode v 4.[80,81] Existence of the bands in these regions in our samples clearly indicates the presence of NH_4^+ ion.

In the region between 2500 and 3500 cm^{-1} at the room temperature IR spectra of NH_4VO_3 provides usually three broad bands; however, some of these modes (except for v 1) are expected to split in more than one band; this behavior is usually noticed when spectra are recorded in low temperatures.[80] In the case of all three samples there are 2-3 more expressed bands in this region: at 3201, 3134 and 3150 cm^{-1} assigned to v3 mode and at 3016, 3034 and 3034 cm^{-1} assigned to v1 mode for samples 121V5, 122V5 and 123V5, respectively. And also band at 2830 cm^{-1} assigned for v4 mode for all three samples. Next to these, there are also a few less intense bands and shoulders in this region assigned to v3 and v4 modes. Detailed band assignment is presented in the **Table 3.3**.

Mode v4 has characteristic intense band in the region around 1400 cm^{-1} that is usually composed of at least three bands.[80] Intense bands are present at 1418, 1401 and 1404 cm^{-1} in the samples 121V5, 122V5 and 123V5, respectively, and also strong bands at 1385 cm^{-1} for both 122V5 and 123V5 samples. Besides that there are also number of less strong bands and shoulders of the bands in the region from 1420 and 1450 cm^{-1} for all three samples which can indicate presence of NH_4^+ ion.[80, 81]

Bands at the region from 1610 to 1630 cm^{-1} in all the samples are assigned to OH symmetric deformation of adsorbed water.[82,85]

Characteristic vibration bands of the ammonium metavanadate are also located at 935 (strong, v_sVO_2), ~890 (weak, v_sVO_2), 840-850 (strong, $v_{as}VO_2$) and 690 cm^{-1} (strong, v_{as}V-O-V).[81]

Strong peaks assigned to v(VO_2) asymmetric modes of ammonium metavanadate are present at 838 and 845 cm^{-1} in the 123V5 and 121V5 sample, respectively. The rest of the characteristic bands are not present in the samples, or are present only as small shoulders masked under the other stronger bands. Therefore, by looking to the spectra we can conclude that only small amount of the initial compound is present in our samples.

Other vanadium species that most probably can be present in the samples are V_2O_5, different polymeric vanadate species (hexavanadates, decavanadates..) metavanadate ions with cyclic form and tetrahedral coordination and vanadium linear tetrameric species.

The V_2O_5 species are identified by its very strong V-O stretching bands observed near 1020 and 825 cm^{-1} [83,84,85]. The V-O bonds in V_2O_5 have different lengths and the band at 1020 cm^{-1} is assigned to the bond that is significantly shorter than the other bonds in the structure.[83] In our samples there is no clear evidence of presence of V_2O_5 except for the very strong peak at 829 in 123V5 sample (but also can be the sign of the presence of decavanadates). Other characteristic bands are missing or they are present only as shoulders (at 1020 cm^{-1} for all samples and shoulder at 829 cm^{-1} for 121V5 sample).

The presence of bands characteristic for V-O-V bridging vibrations confirms that there polymeric vanadates are present in our samples.[86] These bands are present in all the samples in the region between 830 and 520 cm^{-1}.

The spectra of hexavanadates have characteristic VO stretching modes in two regions, 950 to 1000 and 720 to 760 cm^{-1}.[83] Decavanadates are identified based on a presence of characteristic bands at 960, 825/750 and 590 cm^{-1}, assigned to νV=O (terminal groups), ν_{as}V-O-V and ν_sV-O-V (bridging groups), respectively[83,86,87,88].Differentiation between hexa and decavanadates is enabled since decavanadates have one strong band in the region around 960 cm^{-1} while hexavanadates have two bands[83].

In the spectra of each of our three samples there is only one band in this region; at 950, 972 and 950 cm^{-1} for 121V5, 122V5 and 123V5 samples, respectively. Therefore in this case decavanadates are dominating species in our samples. Apart of this, there are several more bands characteristic for decavanadates such as strong peaks at 750 and 747 cm^{-1} for samples 122V5 and 123V5 and also at 732 cm^{-1} for the sample 121V5. However, the sample 121V5 has pH around 7 and at this pH value decavanadates are not usually formed, so in the case of this sample these bands can be probably assigned to other polyoxovanadate species.

Strong peaks at 829 cm^{-1} are present in 123V5 and 121V5 samples. However, bands at this wavenumber are also characteristic for V_2O_5 so at these wavenumber we can't be sure which compound is responsible for the bands.

Metavanadate ions with cyclic form and tetrahedral coordination have characteristic bands at around 900 cm^{-1} ($\nu_{as}VO_2$) and 953 (ν_sVO_2) [81,89]. Only in the sample 121V5 there is evidence of the presence of this vanadium species: strong bands at 900 and at 950 cm^{-1}. The band at 950 cm^{-1} can also be assigned to decavanadates. Decavanadates are not thermodynamically stable at pH 7 but are

sometimes observed in these conditions because they are kinetically quite stable. During the evaporation the solution is not perfectly homogeneous, and the media close to glass surface may be more acidic than the bulk solution. In these conditions, decavanadates may be formed locally, and, because they are kinetically stable, may not decompose in contact with the solution at higher pH. Nevertheless, it is more likely that these bands are the sign of the presence of metavanadates, such as $H_nV_2O_7^{n-4}$, $H_nV_3O_9^{n-3}$, $H_nV_4O_{12}^{n-4}$, $H_nV_5O_{14}^{n-3}$.

The vanadium linear chain tetrameric species (monoprotonated monomer $[HVO_4]^{2-}$ and the dimer $[V_2O_7]^{4-}$) present characteristic bands at around 930 cm^{-1} (νVO_2), and also very strong bands at around 640 and 520 cm^{-1} that can be related with protonated species[90] (νV-O mode of VOH groups). In the region around 930 cm^{-1} there are no characteristic bands and also the strong band at 640 cm^{-1} characteristic for all metavanadates with polymeric chain structure[90] is missing. The only band suggestions that can be related to the protonated species are shoulders at 520 cm^{-1} in the spectra of 122V5 and 123V5 samples.

Table 3.3. Band assignment for vanadium (V) samples

n.a. pH (7)	**pH 3**	**pH 5**	**band assignment**
121v5	**122v5**	**123v5**	
3534 (w)		3531 (w)	ν(V-)OH or νNH_4^+
	3265 (w)	3265 (sh)	$\nu3(\nu NH_4^+)$
3201 (m)			$\nu3(\nu NH_4^+)$
		3150 (m)	$\nu3(\nu NH_4^+)$
	3134 (m)		$\nu3(\nu NH_4^+)$
	3034 (m)	3034 (m)	$\nu1+\nu3\ (\nu NH_4^+)$
3016 (m)			$\nu1+\nu3\ (\nu NH_4^+)$
2950 (sh)			$\nu1(\nu NH_4^+)$
2830 (w)	2830 (m)	2830 (m)	$\nu4(\nu NH_4^+)$
2800 (sh)	2800 (sh)	2800 (sh)	$\nu4(\nu NH_4^+)$
1683 (w)	1681 (w)	1681 (w)	$\nu2(\delta NH_4^+)$
1610 (w)	1630 (w)	1626 (w)	δOH (water)
1447 (sh)	1447 (sh)	1447 (sh)	$\nu4(\delta NH_4^+)$
	1426 (sh)	1426 (sh)	$\nu4(\delta NH_4^+)$
1418 (s)			$\nu4(\delta NH_4^+)$

n.a. pH (7)	pH 3	pH 5	band assignment
121v5	**122v5**	**123v5**	
	1401 (w)	1404 (s)	v4(δNH_4^+)
	1385 (s)	1385 (s)	v2(δNH_4^+)
1020 (sh)	1020 (sh)	1020 (sh)	ν_sV=O in V_2O_4
995 (w)	995 (m)	995 (w)	vs(V=O)
	972 (s)		ν_sV=O of terminal groups in decavanadates
		965 (vs)	ν_sV=O of terminal groups in decavanadates
950 (vs)			ν_s (VO2) (cyclic metavanadates or decavanadates)
900 (s)			ν_s (VO_2) (cyclic form)
845 (vs)			ν_{as} (VO_2) linear metavanadates
	838 (s)		ν_{as}(VO_2) linear metavanadates
829 (sh)		829 (vs)	ν_{as}(V-O-V)
732 (vs)	750 (s)	747 (vs)	vV-O-V bridging
714 (vs)			ν_{as}(V-O-V)
	682 (sh)		ν_{as}(V-O-V)
604 (vs)	607 (vs)	604 (vs)	ν_{as}(V-O-V)
560 (vs)	558 (sh)	558 (vs)	vV-O-V bridging
	542 (vs)	542 (vs)	vV-O-V bridging
	520 (sh)	520 (sh)	vV-O-V bridging

*vs - very strong, s - strong, m - medium, w - weak, vw - very weak, sh - shoulder, br -broad

These results show that upon evaporation, a mixture of different metavanadates and possibly decavanadates are formed, as expected from the aqueous chemistry of V(V). The IR spectra shows that different species form at different pH.

3.1.4.2. Effect of vanadium (V) deposition on native cellulose:

Effect of vanadium deposition on native cellulose is determined by comparing spectra of native cellulose deposited at pH values 3, 5 and approximately 6 - 7 for set of samples with non-adjusted pH. The concentration of vanadium was in the range from 0,2 – 10 mM per gram of cellulose. Compared DRIFT spectra for all three pH values and different vanadium concentrations are shown in

Figure 3.6. The evolution of the cellulose bands in the region around 3000 and 2700cm^{-1} and between 1500 and 1000cm^{-1} seems to be random and not dependent on vanadium concentration.

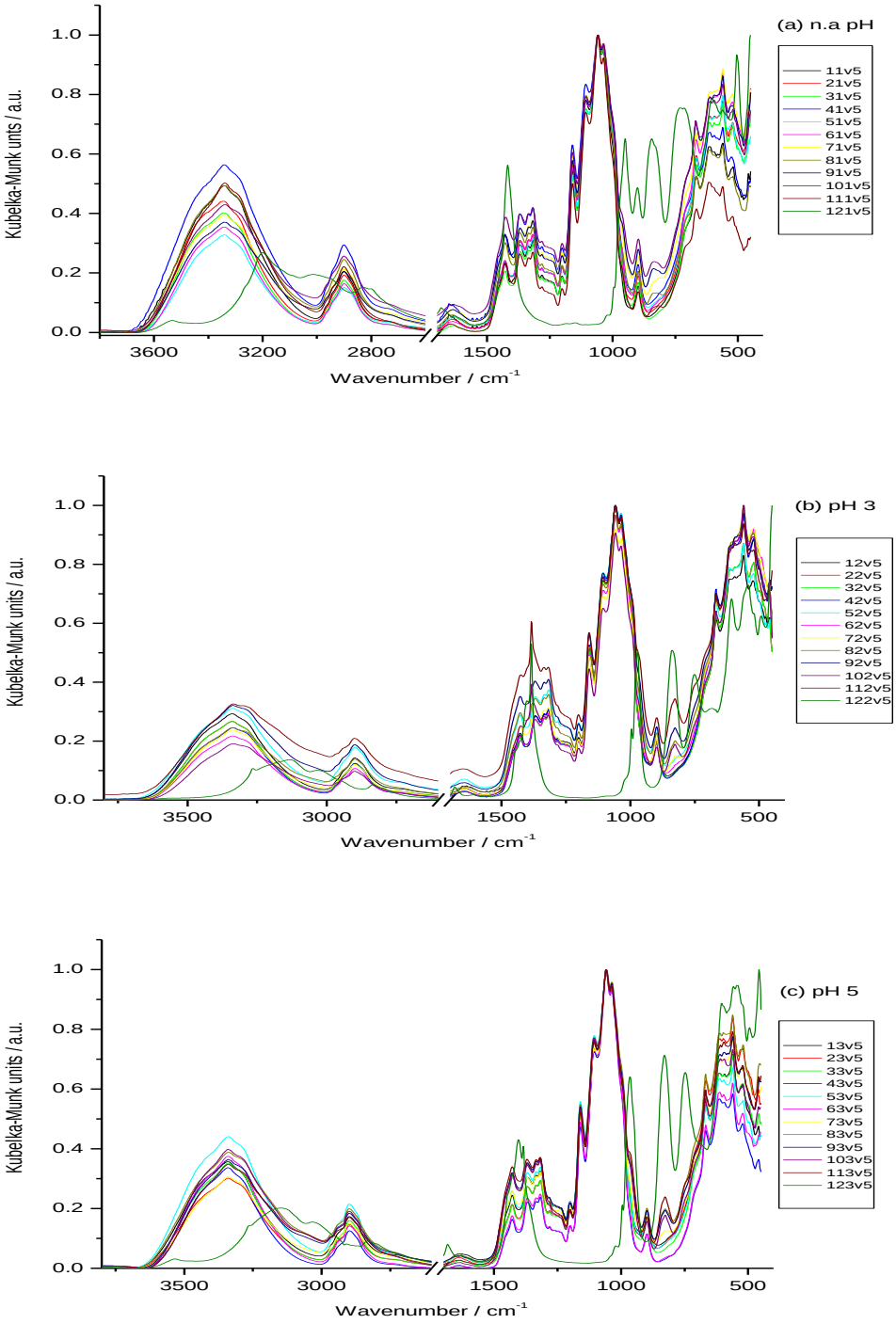

Figure3.6 Effect of vanadium (V) deposition on native cellulose at non-adjusted pH (a), pH 3 (b) and pH 5 (c) at different concentrations of vanadium

However, in the spectra of all the three sets of samples there are some similar changes; new bands are present at wavenumbers 960, 971 and 965 cm^{-1}; 836, 829 and 829 cm^{-1} 703, 750 and 747 cm^{-1} for the non-adjusted pH set of samples, pH 3 and pH 5 sets of samples, respectively. New bands are present only in the spectra of samples in the higher range of concentrations (**Figure 3.7**). In the pH 3 and 5 samples these shifts correspond to the bands assigned to decavanadates and V-O-V bridging vibrations of other polymeric species. This can be an indication of the deposition of polymeric vanadate species on cellulose when vanadium is present in higher concentrations. At low pH values such as pH 3 decavanadates can form even at low concentrations, however in the samples with pH 5 we probably have a mixture of tri and decavanadates deposited on cellulose.

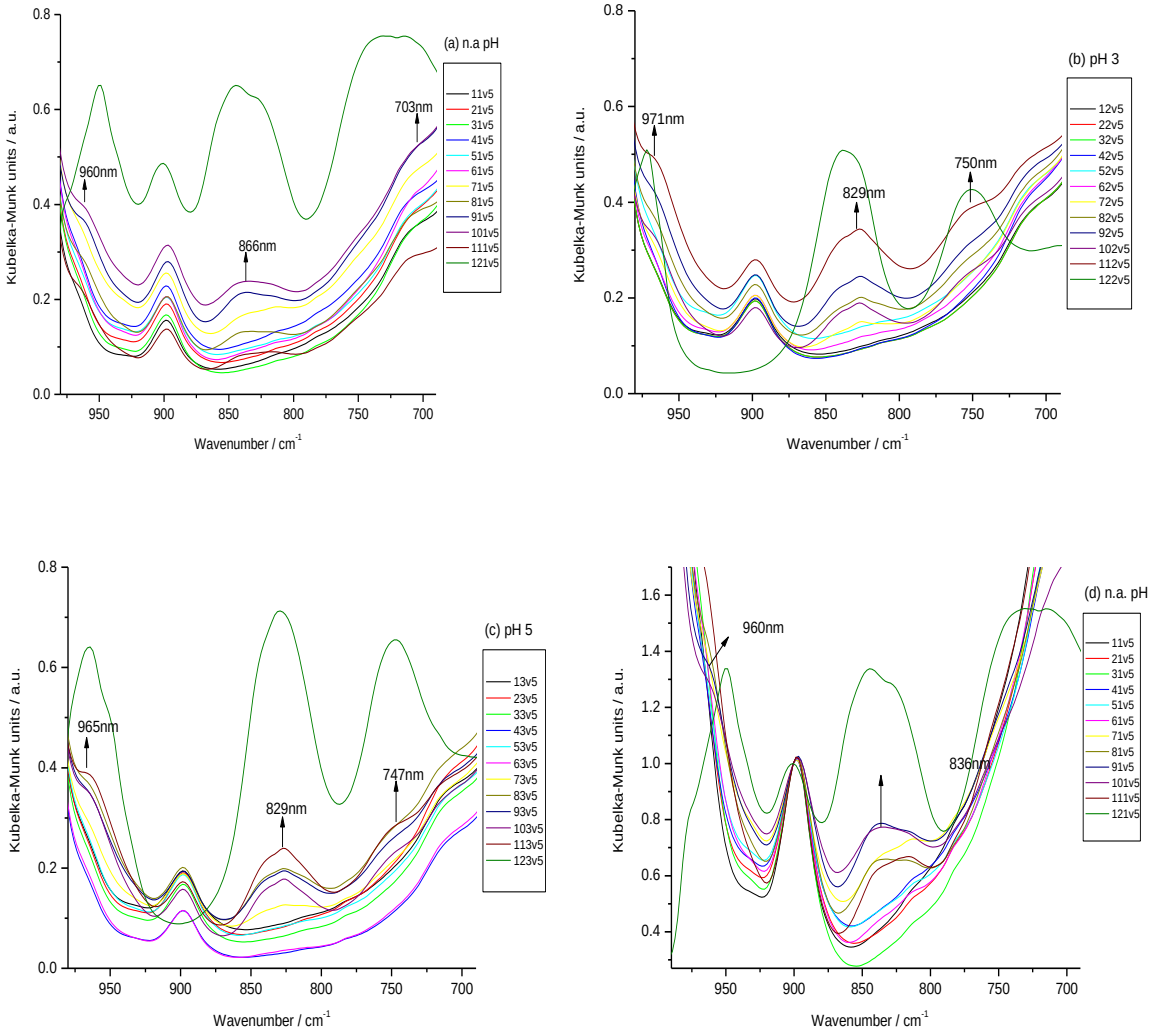

Figure 3.7 Changes in the region from 980 to 700 cm^{-1} in the spectra of non-adjusted (a), samples with pH 3 (b), samples with pH 5 (c) and spectra of non-adjusted pH set normalized at 900 (d).

For the samples with non-adjusted pH value (pH in the range from 5.50-7.20) bands at 950 and 845 cm^{-1} are both assigned to metavanadates. Small changes in the spectra are also present at 703 cm^{-1} possibly due to the band at 714 cm^{-1} assigned to V-O-V bridging vibrations of polymeric vanadate species. After normalization of the spectra at 900 nm **(Figure 3.7d)** we can better see the evolution of the bands at 960 and 836 nm. In both cases new bands are present only in the 5 samples with the high concentration of vanadium. These new bands are probably due to the presence of the mixture of different polyoxovanadates and at these pH values (in the range from 6.40 to 6.75 for the most concentrated samples) we can expect to have mixture of tri and tetravanadates deposited on cellulose.

3.1.5. Iron (II) and iron (III)

3.1.5.1. Effect of pH on iron (II) sulfate and iron (III) nitrate and band assignment:

Effect of pH for both iron (II) and iron (III) was examined by comparing infrared spectra of residuals obtained after evaporation of water from control iron samples that contained no cellulose. Spectra are shown in **Figure 3.8** and **3.9**. In the case of Fe (II) samples there is no significant difference between spectra of three solid residues (**Figure 3.8**); they all show characteristic sulfate bands in the region below 1300 cm^{-1}. These bands generally appear in regions ~1050-1250, ~1000, ~500-700, and ~400-500 cm^{-1}, corresponding to the asymmetric stretch (v3); symmetric stretch (v1); asymmetric bend (v4) and symmetric bend (v2), respectively.[91]

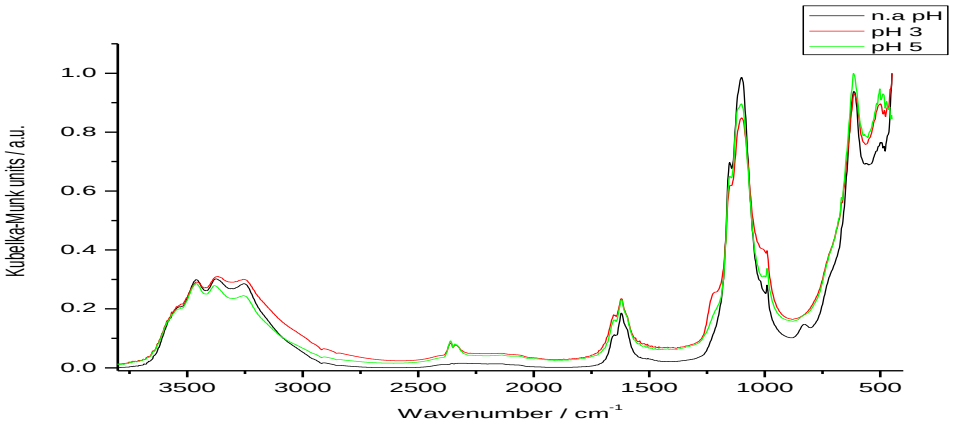

Figure 3.8 Compared DRIFT spectra of control Fe (II) samples at different pH values

It is found in previous research that all four characteristic sulfate bands are expected to be found in $FeSO_4$ x nH_2O compounds due to the low sulfur site symmetry.[92] All three sets of samples have bands with maximum at 1151, 1100, 614 and 500 cm^{-1}, assigned to v3, v3, v1, v4 and v2 modes, respectively. Additionally, samples with pH 3 and 5 have bands at 1216 cm^{-1} assigned to v3 mode. Since all four fundamental sulfate vibrations are present in the sample we can conclude that sulfate is present in a form of coordinated rather than free pyramidal sulfate ions.[93]

The position and maximum of the fundamental bands depends on the sulfate symmetry as well as the degree of deformation of the anion, but also on the presence of OH and H_2O in the molecular structure.

The amount of hydration will mostly affect the high-frequency position of the v3 fundamental bands in a way that v3 band occurs at a lower-frequency (lower wavenumber) position if the state of hydration is higher.[91]

Spectra of all three samples contained characteristic water bands in the region around 3200 – 3500 and 1620 – 1650 cm^{-1}, assigned to stretching and bending modes of water, respectively. Detailed band assignment is given in **Table 3.4a**

Table 3.4a. Band assignment for Fe (II) samples:

Pure $FeSO_4$.7H2O	**121Fe2 n.a. pH (3.4)**	**122Fe2 pH 3**	**123Fe2 pH 5**	**assignment**
3455 (m)	3460 (m)	3460 (m)	3460 (m)	νOH (water)
3377 (m)	3374 (m)	3368 (m)	3381 (m)	νOH (water)
3254 (m)	3255 (m)	3255 (m)	3255 (m)	νOH (water)
1651 (w)	1650 (w)	1652 (w)	1650 (w)	δOH (water)
1619 (m)	1620 (m)	1620 (m)	1620 (m)	δOH (water)
		1216 (sh)	1216 (sh)	v_3 ($v_{as}SO_4^{2-}$)
	1151 (vs)	1151 (vs)	1151 (vs)	v_3 ($v_{as}SO_4^{2-}$)
1100 (vs)	1100 (vs)	1100 (vs)	1100 (vs)	v_3 ($v_{as}SO_4^{2-}$)
989 (m)	989 (s)	989 (s)	989 (s)	v_1 ($v_sSO_4^{2-}$)
	828 (w)			δFe-OH (α-FeOOH)
613 (vs)	614 (vs)	614 (vs)	614 (vs)	v_4 ($\delta_{as}SO_4^{2-}$)
	498 (vs)	500 (vs)	500 (vs)	v_2 ($\delta_sSO_4^{2-}$)

*vs - very strong, s - strong, m - medium, w - weak, vw - very weak, sh - shoulder, br -broad

In the case of Fe(III) samples there are big differences in spectra of the three samples with different pH values (**Figure 3.9**). Common features for all three samples are found in the region of the spectra highly characteristic for bands of nitrates at frequencies between 815 – 840 and 1350 – 1380 cm^{-1}.[94] All samples have very strong peaks with maximum at 1384 cm^{-1} and bands at 842 (121Fe3) and 836 cm^{-1} (122Fe3 and 123Fe3) assigned to nitrate modes. Detailed band assignment is presented in **Table 3.4b**.

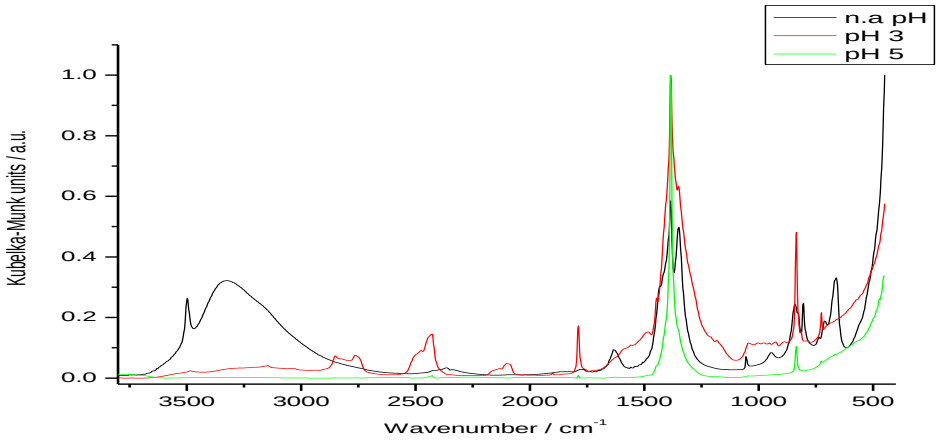

Figure 3.9 Compared DRIFT spectra of control Fe (III) samples at different pH values

Table 3.4b: Band assignment for Fe(III) samples:

Pure $Fe(NO_3)_3.9H_2O$	**121Fe3**	**122Fe3**	**123Fe3**	**assignment**
3596 (s)				vOH (water)
3510 (s)				vOH (water)
	3479 (m)			vOH (water)
	3326 (s)			vOH (water)
		2830 - 2080(w)		Overtones and combination bands
2395 (w)				Overtones and combination bands
		1789 (m)		vN=O (NO_3^-, bidentate)
1612 (s)				vN=O (NO_3^-, monodentate)
	1633 (w)			δOH (water)
1384 (vs)	1384 (vs)	1384 (vs)	1384 (vs)	$v_s(NO_2)$ of NO_3^-
	1350 (s)	1350 (s)		$v_s(NO_2)$ of NO_3^-
825 (w)	842 (m)	836 (s)	836 (w)	$\delta(NO_2)$ of NO_3^-
	804 (m)			δOH of FeOOH
	661 (s)			vFe-O

*vs - very strong, s - strong, m - medium, w - weak, vw - very weak, sh - shoulder, br -broad

In the spectra of the sample 123Fe3 (pH 5) besides these two bands at 836 and 1384 cm^{-1}, no additional bands are present. However, in other two samples more bands characteristic for nitrates are present; strong bands at 1350 cm^{-1} in spectra of both samples and also peaks at 1789 cm^{-1} (122Fe3) and 1633 cm^{-1} (121Fe3).

In the spectra of the sample 121Fe3 (non-adjusted pH) the bands at 3479 and 3326 cm^{-1} are consistent with the presence of water and assigned to its OH stretching modes. The bands at 661 and 804 cm^{-1} which can be assigned to the Fe-O stretching and Fe-O-H bending modes of α-FeOOH, respectively. In fact, this is consistent with the formation of α-FeOOH that is usually formed in diluted aqueous solutions of $Fe(NO)_3$ as a result of slow hydrolysis (during long time) at room temperature.[95]

The sample 122Fe3 has a lot of bands in the region from 2000 – 2800 cm^{-1} that are assigned to overtones and combination bands of the fundamental modes.

3.1.5.2. Effect of iron deposition on cellulose:

Effect of iron deposition on cellulose is studied by comparing the spectra of cellulose samples treated with different iron concentrations and at different pH values.

For analysis of iron samples, Fe(II) and Fe(III), from each of the three sets of samples (with three different pH values) analyzed by DRIFTS we only discuss the highest concentration (10.00 mM/g cellulose), one in the middle range (3.00 mM/g cellulose), one in the low range of concentrations (0.25 mM/g cellulose) and control iron samples. Since after comparing the obtained infrared spectra for Fe (II) there was no significant difference. However in the spectra of Fe (III) samples there was some difference so two more samples from each set were discussed. The spectra are shown in **Figure 3.10** and **Figure 3.11.**

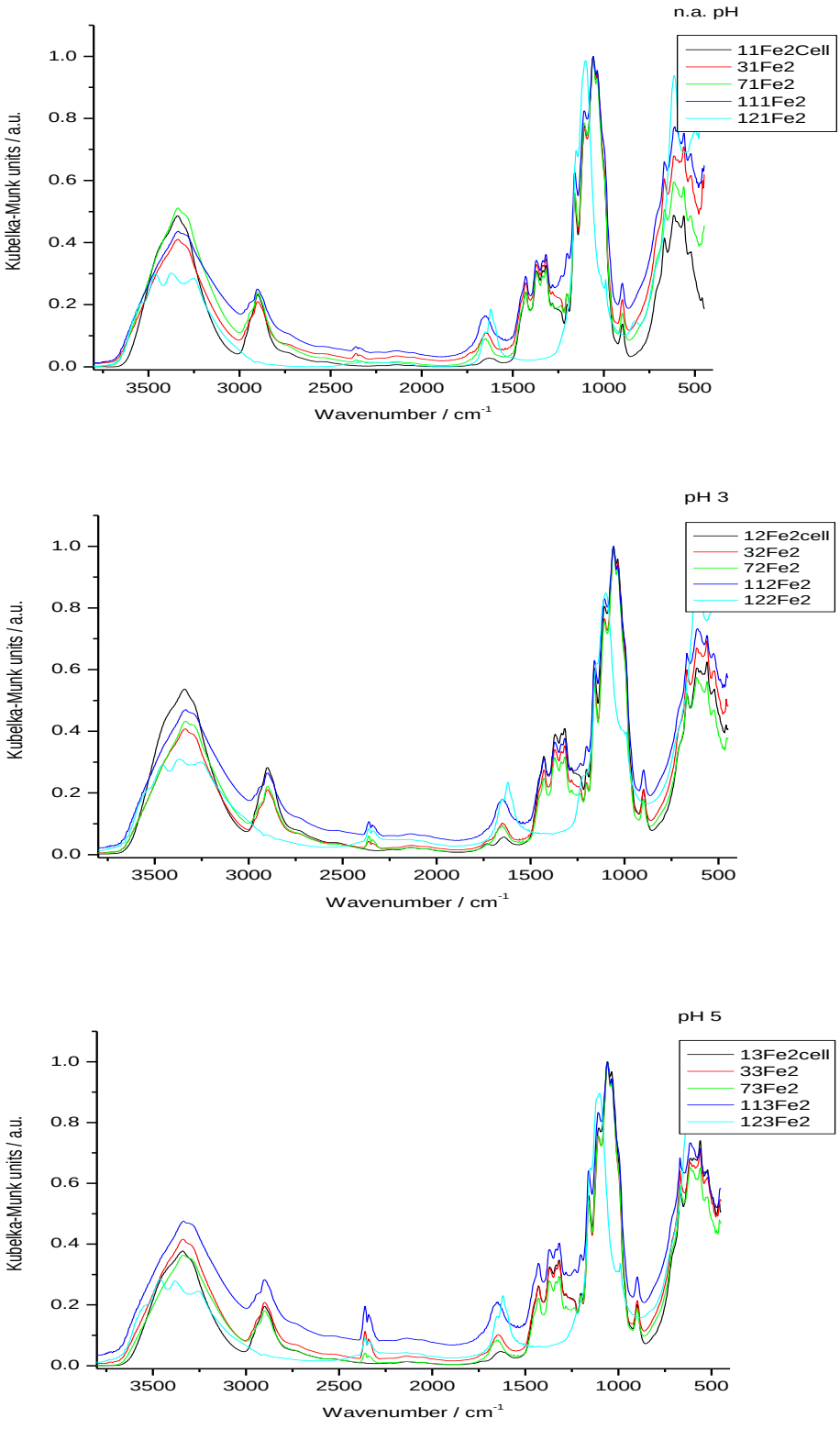

Figure 3.10 Effect of Fe (II) deposition on native cellulose at non-adjusted pH (a), pH 3 (b) and pH 5 (c) at different concentrations of iron

Compared spectra of Fe(II) samples at three different pH values is shown in **Figure 3.10**. The relative intensity of some cellulose related increases with the increase of metal complex concentration, but there is no change in the band shape and no additional bands. Pointing to a very weak interaction between the metal complex and the matrix, which means a deposition of the complex on the cellulose surface or on the amorphous phase.

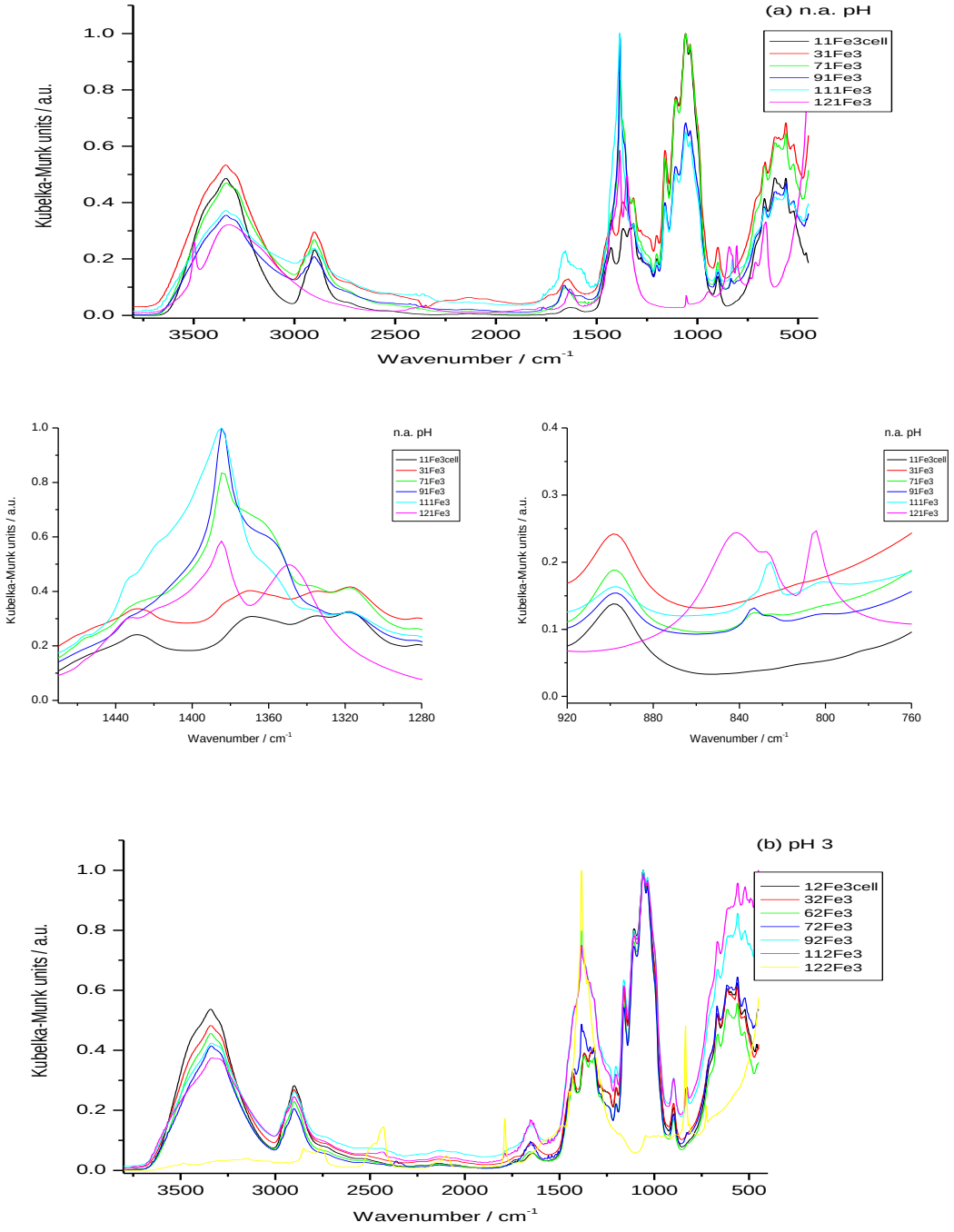

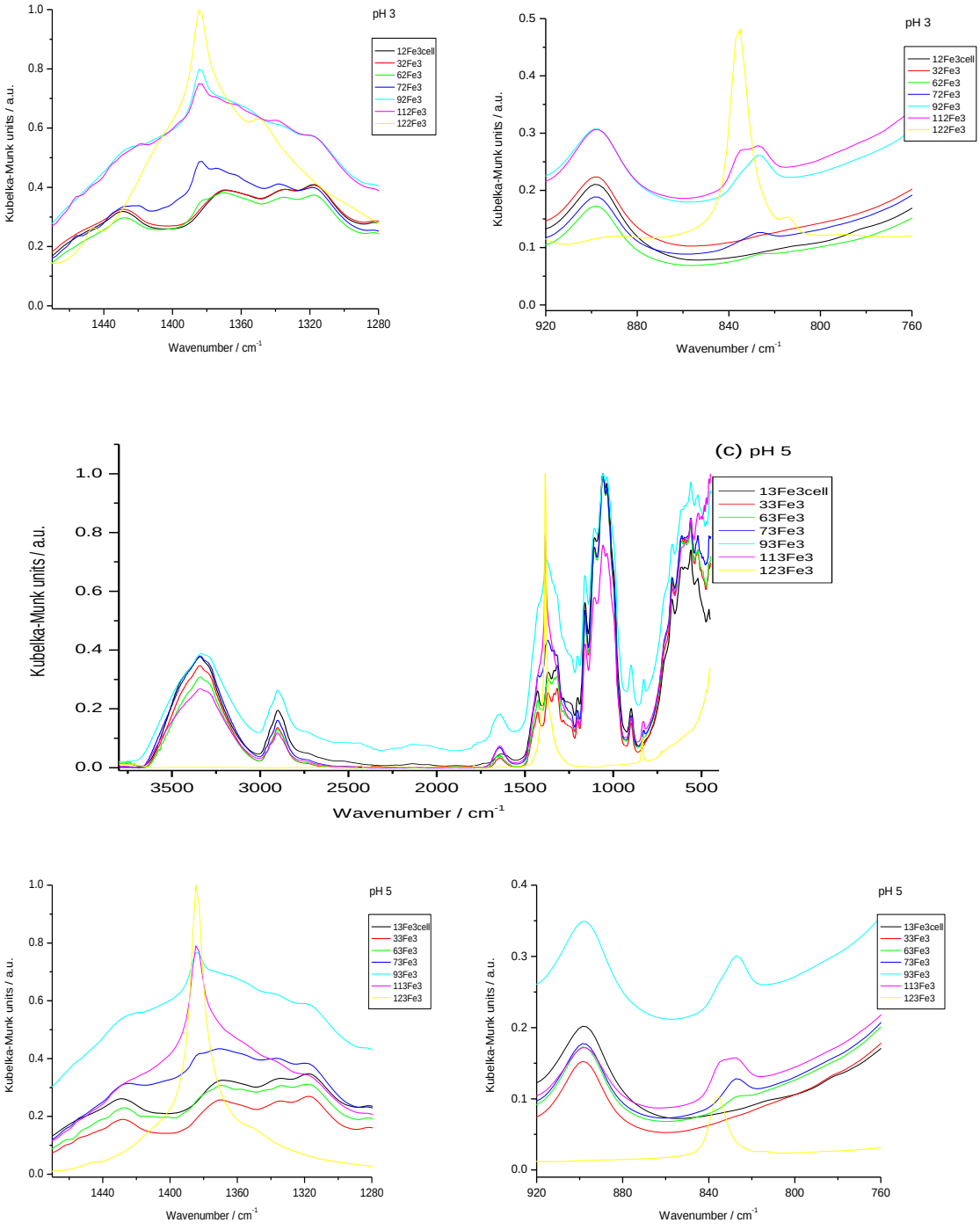

Figure 3.11. Effect of Fe(III) deposition on native cellulose at non-adjusted pH (a), pH 3 (b) and pH 5 (c) at different concentrations of iron

The spectra of samples prepared with the complex of Fe(III), in **Figure 3.11**, with non-adjusted pH (pH value was in the range from 3.58 for lowest concentration to 1.92 for the most concentrated sample) no clear changes in the cellulose bands for low metal complex concentration, but for the higher concentrations some changes are present in the spectra region characteristic for nitrates. Additional bands at 1384 cm^{-1}, shoulders of the bands at 1360 cm^{-1} and new bands in the samples with high concentrations at ~830 cm^{-1}. All this changes are related with nitrate bands, at 1384, 1350 and 840 cm^{-1}, respectively, that became visible with increasing complex concentration on cellulose matrix. In the sample with the highest metal complex concentration there is a small band at 802 cm^{-1} corresponding to the peak at 804 cm^{-1} assigned to Fe-OH bending vibrations of Fe-OOH.

These differences enable to conclude that the peaks appearing at 1384 cm^{-1} are probably just the result of the high Fe complex concentration leading to deposition onto the cellulose exterior surface with low interaction, while the shifted bands at 1360, 830 and 802 cm^{-1} indicate deposition of different species or more probably an adsorption onto the cellulose chains with stronger interactions.

The same spectral changes can be observed for the samples with pH 3 and pH 5, however the changes in the region around 1380 cm^{-1} seem to be more pronounced in the lower pH values. In fact, for the samples prepared with pH 5, besides the cellulose bands, the complex band at this wavenumber is present only in the two samples with the highest concentrations, while for the samples with lower pH values the-band is also present in lower concentrations, being visible already at the concentration of 3 mM/g cellulose.

3.1.6. Copper (II) and Zinc (II)

3.1.6.1. Effect of pH on Cu (II) and Zn (II) sulfate and band assignment:

Effect of pH for both Cu (II) and Zn (II) was examined by comparing infrared spectra of residuals obtained after evaporation of water from control samples that contained no cellulose. Spectra are shown in **Figure 3.12** and **3.13**.

The DRIFT spectra of all three $CuSO_4$ set of samples show that there are no meaningful differences in the spectra of samples with pH 3, pH 5 and non-adjusted pH (pH value around 4.20). All samples contain absorbed water molecules and therefore have stretching OH bands in the region between

2500 and 3200 cm^{-1} and water bending modes at 1670 cm^{-1}.[96,97] Also fundamental vibrations of SO_4^{2-} ion are present at 685 cm^{-1} and region between 960 and 1200 cm^{-1}.[94,96,97] The band assignment is given in **Table 3.5a**.

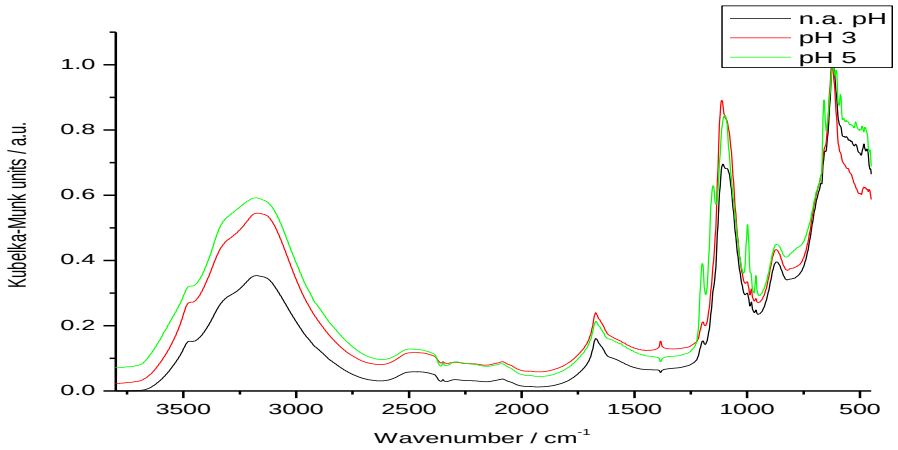

Figure 3.12 Compared DRIFT spectra of control Cu (II) samples at different pH values

Table 3.5a. Band assignment for Cu (II) samples.

Pure $CuSO_4$	**121Cu2**	**122Cu2**	**123Cu2**	**assignment**
	pH 4	**pH 3**	**pH 5**	
3477 (sh)				νOH (water)
	3468 (sh)	3468 (sh)	3468 (sh)	νOH (water)
	3318 (sh)	3322 (sh)	3322 (sh)	νOH (water)
3177 (m)	3170 (m)	3167 (s)	3174 (s)	νOH (water)
2476 (w)	2478 (w)	2478 (w)	2478 (w)	overtones and combination bands
1673 (m)	1670 (m)	1670 (m)	1670 (m)	δOH (water)
	1197 (s)	1197 (s)	1199 (s)	ν_3 ($\nu_{as}SO_4^{2-}$)
	/	/	1150 (s)	ν_3 ($\nu_{as}SO_4^{2-}$)
1112 (vs)	1106 (vs)	1112 (vs)	1098 (vs)	ν_3 ($\nu_{as}SO_4^{2-}$)
1088 (vs)				ν_1 ($\nu_sSO_4^{2-}$)
	1000 (sh)	1000 (sh)	1000 (s)	ν_1 ($\nu_sSO_4^{2-}$)
	962 (m)	962 (m)	962 (m)	ν_1 ($\nu_sSO_4^{2-}$)
870 (s)	870 (s)	870 (s)	870 (s)	ρOH (water)
	658 (sh)	658 (sh)	658 (s)	ν_4 ($\delta_sSO_4^{2-}$)
622 (vs)	622 (s)	622 (s)	622 (s)	νCu-O
	587 (sh)	587 (sh)	587 (s)	νCu-O

*vs - very strong, s - strong, m - medium, w - weak, vw - very weak, sh - shoulder, br -broad

In water solution the cupric ion typically forms aqua complexes $[Cu(H_2O)_6]^{2+}$ with distorted octahedral structure. Insoluble hydroxides are formed at higher pH values, usually higher than pH 4 at high Cu (II) concentrations (above 10 M), and for low Cu (II) concentrations at higher pH values. Since the concentration of copper in our samples was between 10^{-2} to 10^{-4} M and pH value around and below 5 is not expected that formation of hydroxides to occur.[98] In low pH values from 3-7 small amount of $Cu(OH)^+$ is also formed.[98] Peaks at low frequencies below 700 cm^{-1} are due to the Cu-O vibrations.[99,100]

The behavior in aqueous solutions of Zn (II) is similar to copper, but in the case of zinc the formation of hydroxides was detected at a concentration range from 10^{-2} to 10^{-4} M and starts at even higher pH values (higher than 7)[98]. Bands characteristic for $Zn(OH)_2$ should be located at 1080, 830, 750 and 715 cm^{-1}. In the spectra of our samples there are no bands at these wavenumbers which confirms that there was no forming of Zn(OH).[101] The band assignment is given in **Table 3.5b.**

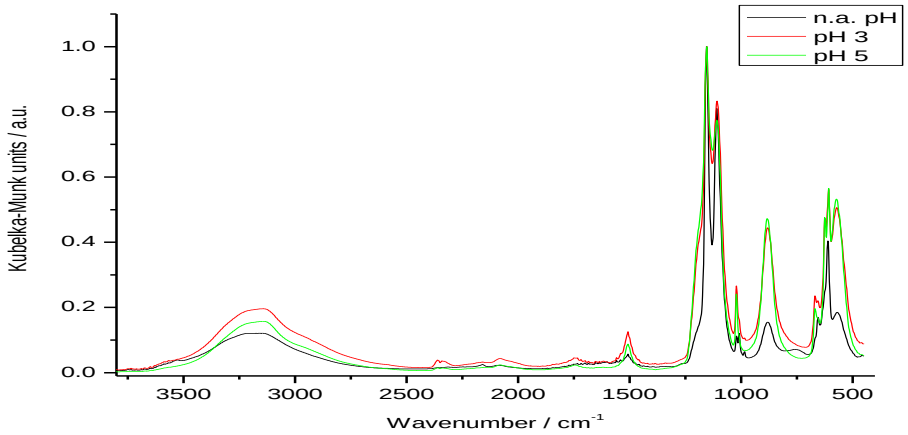

Figure 3.13 Compared DRIFT spectra of control Zn (II) samples at different pH values

Table 3.5b. Band assignment for Zn (II) samples

Pure $ZnSO_4$	**121Zn2 n.a. pH (5)**	**122Zn2 pH 3**	**123Zn2 pH 5**	**assignment**
3531 (m)				vOH (water)
3464 (m)				vOH (water)
3176 (m)	3174 (m)	3142 (m)	3139 (m)	vOH (water)
1598 (w)				combination band
	1506 (w)	1506 (m)	1506 (m)	combination band
		1190 (sh)	1190 (sh)	v_3 ($v_{as}SO_4^{2-}$)

Pure $ZnSO_4$	121Zn2 n.a. pH (5)	122Zn2 pH 3	123Zn2 pH 5	assignment
1153 (vs)	1153 (vs)	1153 (vs)	1153 (vs)	v_3 ($v_{as}SO_4^{2-}$)
1106 (vs)	1108 (vs)	1108 (vs)	1108 (vs)	v_3 ($v_{as}SO_4^{2-}$)
	1020 (w)	1020 (m)	1020 (m)	v_1 ($v_sSO_4^{2-}$)
1004 (w)	1009 (w)	1009 (sh)		v_1 ($v_sSO_4^{2-}$)
	882 (m)	882 (s)	882 (s)	ρOH (water)
655 (m)	657 (m)	668 (m)	668 (m)	v_4 ($\delta_sSO_4^{2-}$)
		642 (s)	624 (s)	v_4 ($\delta_sSO_4^{2-}$)
611 (s)	610 (s)	607 (s)	607 (s)	v_4 ($\delta_sSO_4^{2-}$)
	570 (m)	572 (s)	572 (s)	vZn-O

*vs - very strong, s - strong, m - medium, w - weak, vw - very weak, sh - shoulder, br -broad

Compared DRIFT spectra of Zn control samples (Figure 3.13) shows bands at around 3150, 880 and 570 cm^{-1} assigned to stretching and bending water modes[102,103] and also characteristic vibrations of SO_4^{2-} ion in the regions around 1100, 1020 and 600-700 cm^{-1} assigned to v3 stretching, v1 stretching and v4 bending SO_4^{2-} modes, respectively.[102,103,104] The band at 570 cm^{-1} is assigned to Zn-O band probably of an aqua complexes.[105]

Other Zn-OH vibrational modes as a frustrated translation (bending) and a deformation should be found at around 445 and 1462 cm^{-1} respectively[106]. However in the spectra of our samples there are no characteristic bands in those regions.

The DRIFT analysis showed that the species formed upon dissolution and pH control are very similar to the pure reagent although some bands can be associated to the presence of aqua complexes of the corresponding metals.

3.1.6.2. Effect of copper and zinc deposition on cellulose:

The deposition of Cu and Zn onto cellulose is analyzed by comparing DRIFT spectra of cellulose with different concentrations of initial metal complex at different pH values. From each set of samples only three samples will be used in the discussion, one with high (10.00 mM/g cellulose), one with medium (3.00 mM/g cellulose) and one with low concentration (0.25 mM/g cellulose). Compared spectra at different pH values and different concentrations are presented in **Figures 3.14a** and **3.14b**.

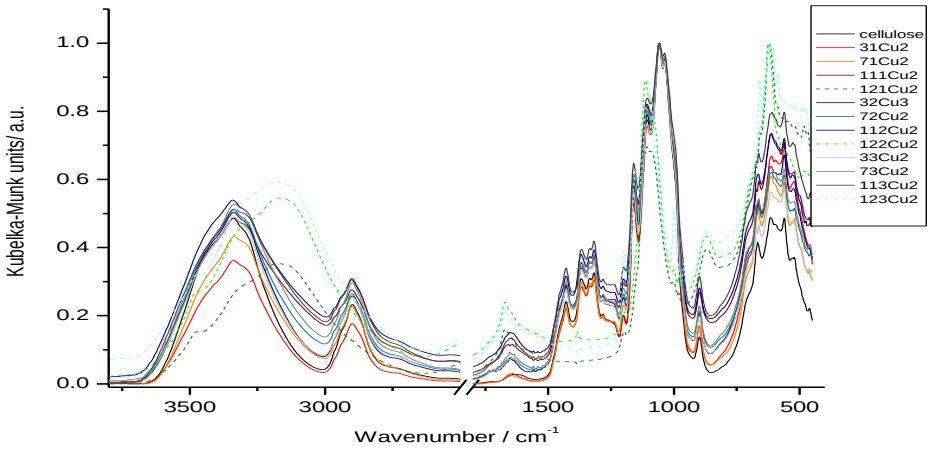

Figure 3.14a

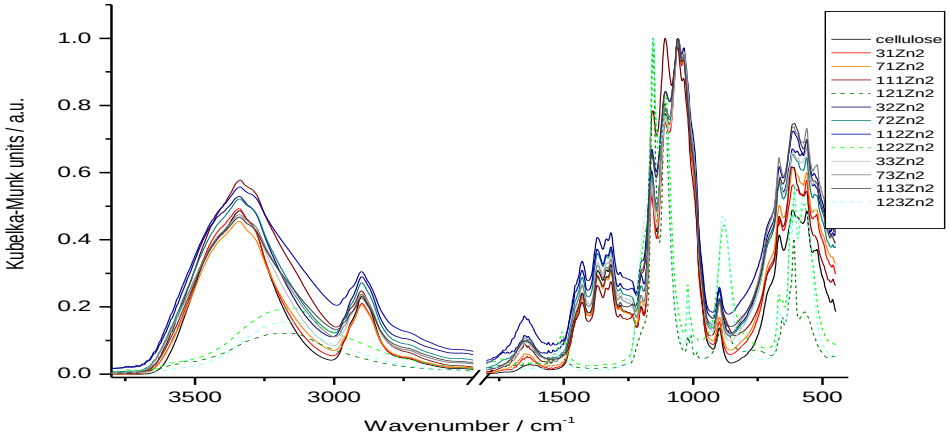

Figure 3.14b

Figure 3.14 Effect of Cu (II) (3.14a) and Zn(II) (3.14b) deposition on native cellulose at different pH values and different concentrations

In the case of both zinc and copper metal complexes no significant effect is present in any of the spectra. In fact, neither the bands of the metal complex or those of cellulose are affected by the deposition of the metal complex onto cellulose. Moreover, no new bands are observed, pointing to a poor interaction between the complex and the matrix upon deposition.

3.2. Filtrated samples - DRIFT analysis

The filtrated samples are prepared only for three compounds ($VO(SO)_4$, $Cu(SO)_4$ and $Fe(NO_3)_3$) and in higher concentrations (10, 5, 2 and 1mM/g of cellulose), then DRIFT spectra was collected fallowing

the same procedure as for the evaporated samples and for comparison used spectra of control samples obtained by evaporation with corresponding pH values.

In the case of V(IV) all samples form the set were analyzed but for Cu(II) and Fe(III) we only analyzed the samples with the highest concentrations from each pH set. Effect of metals deposition on the structure of native cellulose was determined by comparing the spectra of native cellulose deposited at pH values 3, 5 and for set of samples with non-adjusted pH. For Cu and Fe, there was no significant difference in the spectra compared to blank cellulose samples, the collected spectra of Cu and Fe samples are shown in **Figure 3.15a**. Only was observed that the intensity of cellulose bands is higher in the samples with higher pH values, in fact no shift of bands maxima or additional bands was identified in spectra. In the spectra the bands related to the metal complex were not clear. Therefore, it is possible to conclude that copper and iron probably didn't have any effect on cellulose, but about the metal complex no deductions can be inferred.

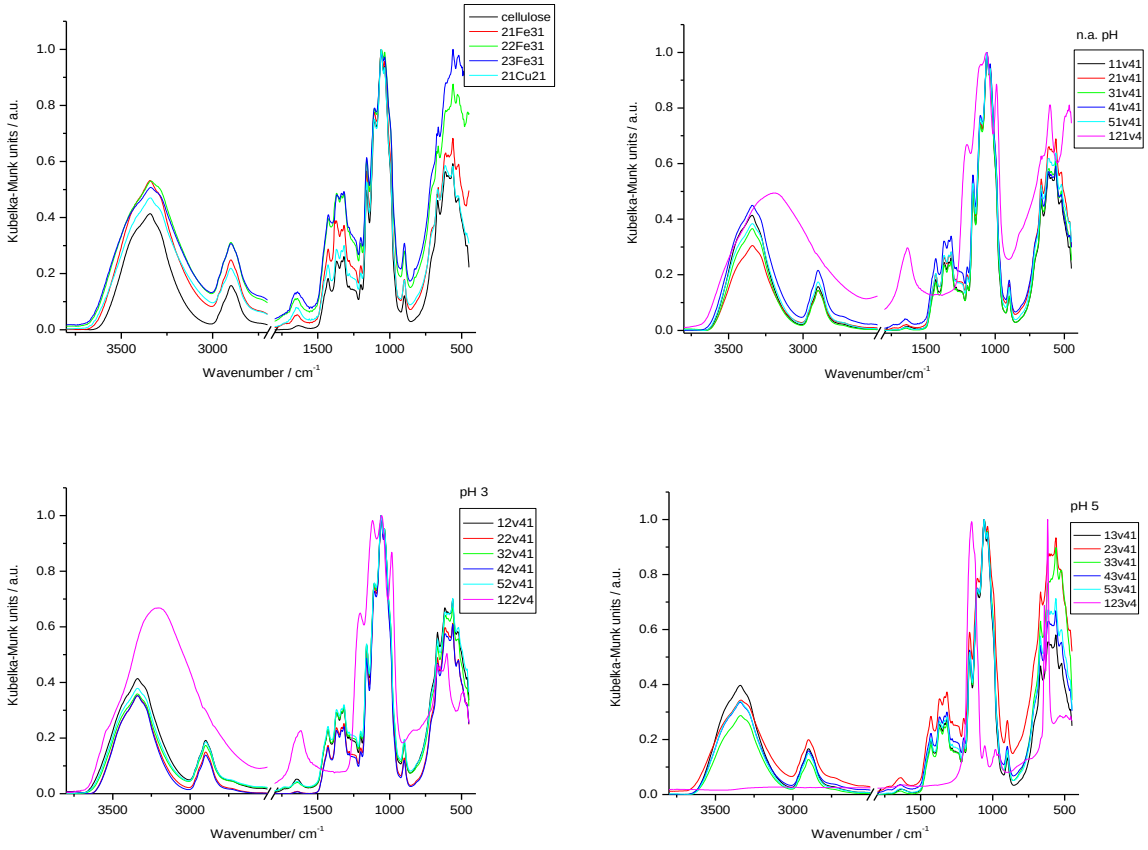

Figure 3.15. Effect of vanadium (IV) deposition on native cellulose at different pH values and different concentrations of vanadium

In the case of vanadium all the samples were analyzed from all three sets of samples (Figure 3.15b, c and d) but there are also no significant changes in the intensity or position of the cellulose bands. As for the other metal complexes there are no clear vanadium complex bands. Based of those spectra there is no evidence for deposition of vanadium species or any changes in the cellulose structure.

Therefore, conditions used in preparation of evaporated samples were not suitable for FTIR analysis since we can't get any significant information in the spectra about the metal complex depositing species using the samples prepared in this manner. Probably this is due to a poor affinity of the metal complex species in solution to adsorb onto the cellulose chains.

3.3. Effect of metal complexes on the degree of crystallinity of cellulose

The cellulose crystallinity is defined as the ratio of the amount of crystalline cellulose to the total amount of material. It is expressed as degree of crystallinity and, as said before, usually is in the range from 40 to 60 %[32]. It can be measured by different methods such as X-ray diffraction[107,108,109], RAMAN spectroscopy[76,110], NMR[111,112] and FTIR spectroscopy[76,113,114]. The crystallinity of our samples was estimated by DRIFT following two approaches: using the region between 1300 and 1180 cm^{-1}, and by the relation of the bands at 898 and 1430 cm^{-1} (amorphous and crystalline bands, respectively). In the case of the region 1300 and 1180 cm^{-1} it is the ratio between intensities of the bands at 1200 and 1280 cm^{-1} (I_{1280}/I_{1200}) that are related with the crystallinity degree of cellulose. The band at 1280 cm^{-1}, assigned to the C-H bending mode should increase with the increase of crystallinity while the band at 1200 cm^{-1} assigned to the C-O-C stretching mode should not be sensitive to changes in crystallinity.[115,116] After obtaining I_{1280}/I_{1200} ratio ($R_{c,h}$), the degree of crystallinity was calculated using the equation[116]:

$$\mathbf{x_c = 1.06\ R_{c,h} + 0.19} \qquad \textbf{(eq. 6)}$$

For vanadium (V) samples it is possible to calculate crystallinity in this way since V^{5+} shows no bands in the targeted region. However in the case of all other metals it was not possible to use this method for calculation of crystallinity because control samples of all the metals had bands in this region and therefore influence the ratio between the cellulose bands.

Calculated crystallinity for the blank cellulose samples is in the range from 42 – 44% and it is in the agreement with the specifications for native cellulose. The variation is obviously related with the experimental error of the measurements and with the fact that we only have one cellulose sample for each set of samples. The results are in **Table 3.6** and **Figure 3.16a**

Table 3.6. Changes in degree of crystallinity of cellulose with concentration.

sample (non adj)	cryst % (non adj)	sample (pH 3)	cryst % (pH3)	sample (pH 5)	cryst % (pH 5)	conc V (V) / g cell
1.1.V5	44.60	**1.2.V5**	42.42	**1.3.V5**	43.30	/
2.1.V5	41.02	**2.2.V5**	45.92	**2.3.V5**	41.08	0.20
3.1.V5	42.30	**3.2.V5**	42.40	**3.3.V5**	43.53	0.25
4.1.V5	46.70	**4.2.V5**	44.49	**4.3.V5**	42.79	0.50
5.1.V5	41.85	**5.2.V5**	47.43	**5.3.V5**	45.45	0.75
6.1.V5	44.72	**6.2.V5**	44.62	**6.3.V5**	44.16	1.00
7.1.V5	44.91	**7.2.V5**	52.92	**7.3.V5**	51.29	3.00
8.1.V5	48.18	**8.2.V5**	59.48	**8.3.V5**	60.41	4.99
9.1.V5	44.86	**9.2.V5**	66.29	**9.3.V5**	64.62	6.00
10.1.V5	51.01	**10.2.V5**	62.93	**10.3.V5**	70.37	7.99
11.1.V5	48.91	**11.2.V5**	73.77	**11.3.V5**	76.08	10.01

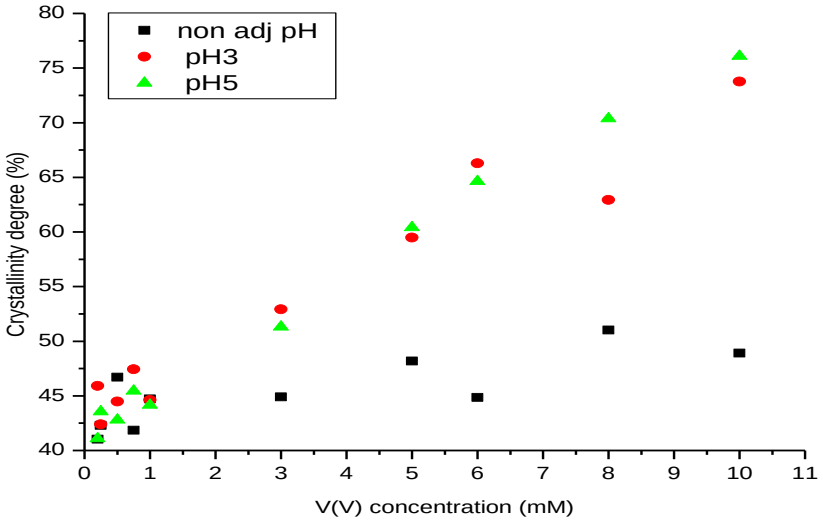

Figure 3.16a. Changes in degree of crystallinity of cellulose with vanadium concentration.

In the V(V) set of samples with non-adjusted pH calculated crystallinity was in the range from 41 to 51% but the changes seemed to be random with no noticeable connection between the crystallinity variation and vanadium complex concentration. However, in the samples with acidic pH values the degree of crystallinity increased with the increase of vanadium complex concentration from 42.4 to 73.8 % and from 41.1 to 76.1 % for samples with pH 3 and 5, respectively (**Figure 3.16**). This increase in crystallinity is more pronounced in the higher concentration levels, in the samples with vanadium concentrations from 1.00 – 10.00 mM/g of cellulose, while in the lower concentration range, from 0.20 – 1.00 mM/g of cellulose, changes are random and concentration seems to have no influence on the degree of crystallinity (**Table 3.6**).

In an attempt to overcome the overlapping between the complex bands and those of cellulose used to quantify its crystallinity, other cellulose bands can be used, although only in a qualitative form, to attest the influence of the metal in the cellulose structure. This analysis is based on the bands at 890 and 1430 cm^{-1}. In the case of iron (III) there is a big overlap of the metal complex bands and therefore this method can't be used to estimate if there has been changes in crystallinity or not. The ratio between the intensity of the bands at 1430 and 898 nm for all the other metals are presented in the **Tables 3.7** (for vanadium) and **3.8** (for iron, copper and zinc).

Table 3.7. Ratio between intensities of the bands at 1430 and 898 nm for Vanadium (IV) samples

	Ratio 1430 / 898		
mM / g cell	**n.a. pH**	**pH 3**	**pH 5**
0.00	2.09	2.13	1.80
0.20	2.11	2.13	1.85
0.25	2.13	2.00	1.76
0.50	2.13	2.27	2.09
0.75	2.17	2.07	2.20
1.00	2.00	1.95	1.88
3.00	2.08	2.21	2.09
5.00	2.13	2.24	2.10
6.00	2.11	2.20	2.27
8.00	2.29	2.21	2.10
10.00	2.29	2.50	2.20

Table 3.8. Ratio between intensities of the bands at 1430 and 898 nm for Iron (IV), Copper (II) and Zinc (II) samples

	Iron (II)			Zinc (II)			Copper (II)		
	Ratio 1430 / 898								
mM / g cell	n.a. pH	pH 3	pH 5	n.a. pH	pH 3	pH 5	n.a. pH	pH 3	pH 5
0.25	2.20	2.30	2.27	2.18	2.12	2.08	1.80	2.23	2.08
3.00	2.36	2.43	2.00	2.14	2.44	2.21	1.88	2.31	2.22
10.00	2.56	2.47	2.64	1.79	2.91	2.40	2.43	2.47	2.23

Small increase in crystallinity is present only in the zinc samples with pH values 3 and 5. In the case of all the other samples the ratio of the bands is more or less constant and random, so there seems to be no influence on the degree of crystallinity (**Figure 3.16b).**

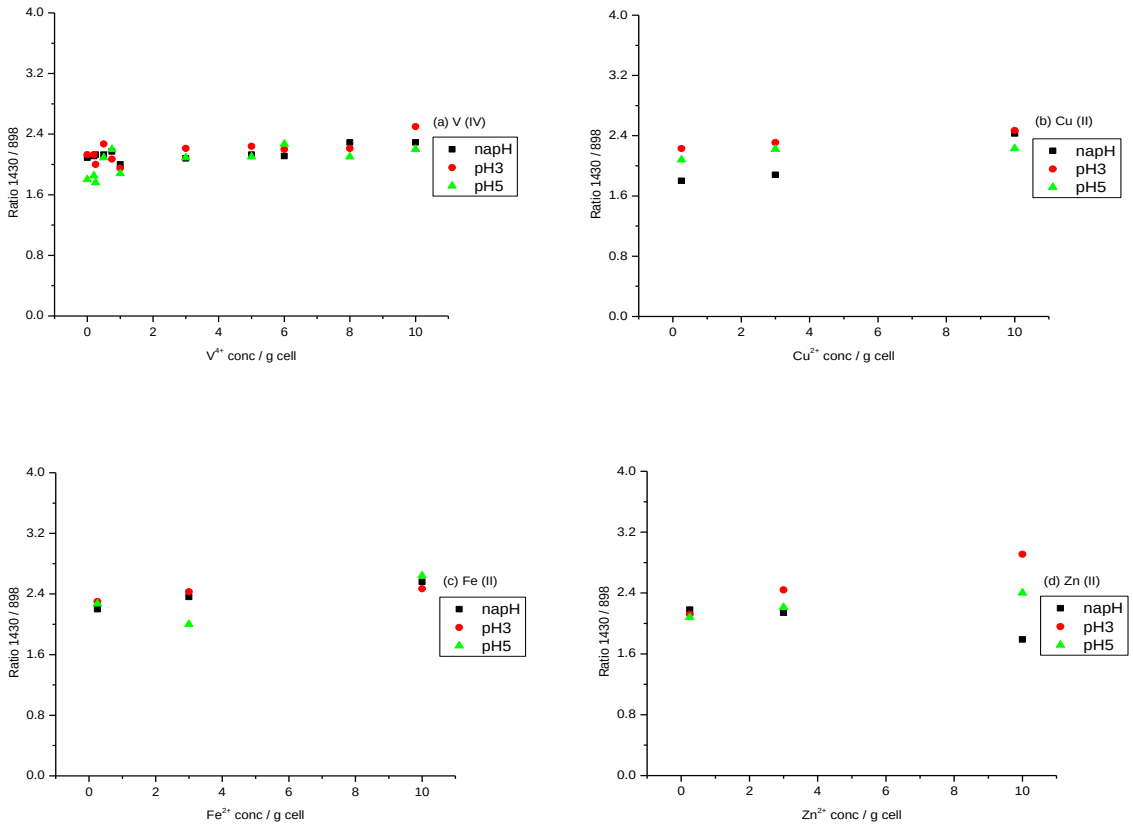

Figure 3.16b. Changes in degree of crystallinity of cellulose with concentration of: (a) vanadium (IV), (b) copper (II), (c) iron (II) and (d) zinc (II).

The increase of cellulose crystallinity on the samples with V(V) and Zn(II) complexes can be explained by the hydrolysis of the amorphous regions of cellulose, catalyzed by the metal ions in acid medium.

3.4. Absorption in the ultra-violet/visible analysis

3.4.1. Vanadium metal complexes in cellulose

The vanadium UV-Vis spectra, depending on the oxidation state, we can expect to see CT transitions and d-d transitions.[117] In the case of V^{5+} it has $3d^0$ electronic configuration and therefore it does not show d-d transitions.[118] UV-Vis spectra of V (V) are characterized by charge transfer (CT) transitions between central vanadium atoms and oxygen ligands in the region below 400-500 nm.[118,119,120,121] The energy of these transitions is influenced by the number and nature of ligands that are surrounding central vanadium ion. In general, isolated species shows bands at higher energy (lower wavenumbers) compared to polymeric species.[122]

Bands characteristic for pseudo-tetrahedral coordinated V (V) species are in the range from 285 to 330 nm[117,122,123] and octahedrally coordinated species have CT transition bands at lower frequencies, usually around 400nm.[118,122] A band at around 470 - 487 nm is characteristic for crystalline V_2O_5.[121,122]

In the UV-Vis spectra of V (IV) we should expect to see bands corresponding both CT and d-d transitions. CT transitions of V (IV) are appearing the range from 250 to 285 nm.[122] The d-d transitions are usually characterized by three bands. The first one is usually superimposed with a CT band; other is located at around 300 nm[120] and the third one in the region 600 – 800nm.[117,121] These d-d transitions typically have much lower intensity than the very broad CT transitions.[120] Therefore, if both transitions are occurring sometimes it can be difficult to distinguish d-d transitions from the CT transition bands that are easy to identify due to its high intensity.

3.4.1.1. Vanadium (V)

The DRUV spectra for V (V) samples were scanned in the range between 214 and 600 nm since it does not show any absorption in the higher wavenumbers spectral region, the spectra are shown in **Figure 3.17**. However, additional spectra at full wavelength from 214 to 800 nm were done for two samples with the highest concentration from each pH set and control V^{5+} sample to prove that there

was no reduction of V (V) and that no V (IV) species is present in these samples. Since no additional information is obtained the spectra are not shown.

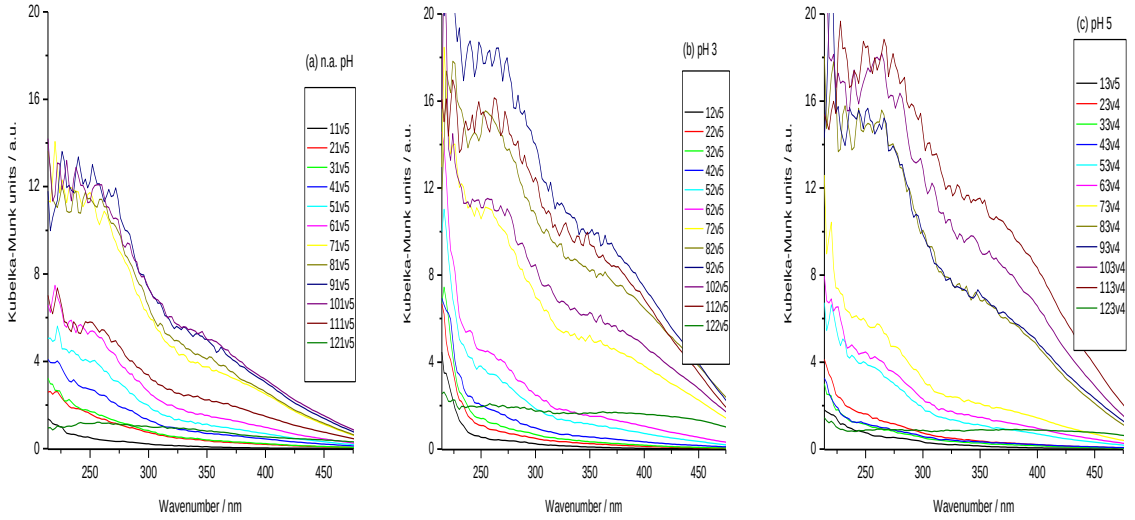

Figure 3.17 DRUV spectra of V (V) samples with non-adjusted pH (a), pH 3 (b) and pH 5 (c).

In all three sets, in the samples with low metal concentration the CT band is observed around 250 nm (**Figure 3.17**), while for the samples with higher metal concentration the CT transitions have two relative maxima. These two CT transition maxima are located at 244, 254 or 258 nm and at 352, 370 or 356 nm for samples with non-adjusted pH pH 3 and 5, respectively. It should be noted that in the samples without pH adjustment it ranges from 5.51 for the least concentrated sample to 6.95 for the sample with the highest concentration.

The position of the CT band can give indication of the geometry if the vanadium adsorbed species. CT bands at around 250 nm indicate presence of tetrahedraly coordinated VO_x species, and the region between 350 -370 nm to 2D-square pyramidal or 3D-octahedrally coordinated VO_x species. The spectra normalized at 244, 256 and 258 nm for non-adjusted pH, pH 3 and pH 5, respectively, are shown in **Figure 3.18.**

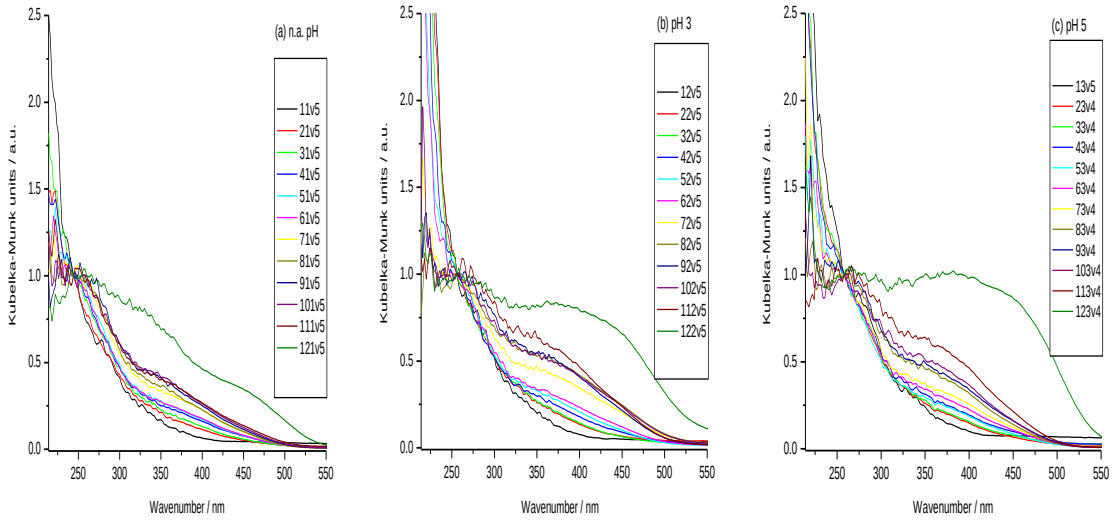

Figure 3.18 Normalized DRUV spectra of V (V) samples with non-adjusted pH (a), pH 3 (b) and pH 5 (c)

After the DRUV spectra normalization becomes clearer that in the samples with higher metal complex concentrations a new band in the visible region of the spectra is appearing. Since in the spectra which cover the whole range up to 800 nm there are no absorption bands above 600 nm we can safely say that there was no reduction of V (V) to V (IV) and therefore only different polyoxovanadates are formed. This conclusion also agrees with the results obtained with DRIFT scans.

3.4.1.2. Vanadium (IV)

The DRUV spectra for the vanadium (IV) complex adsorbed on cellulose, scanned in different spectral regions, are shown in **Figure 3.19.** In the region above 600 nm only in the evaporated vanadium (IV) samples with pH 5 have a small absorption, and its spectra were scanned from 214 to 800 nm. In the other samples no significant bands after the wavelengths of 600 nm were observed, therefore all the corresponding spectra were done at the wavelength range from 600 to 214 nm. However additional scans at full range from were done for the non-adjusted and pH 3 sets but only for the higher concentrated samples.

The spectra of the samples with pH 3 and non-adjusted pH (pH in the range from 2.5 to 4.2) were very similar; in the range from 214 and 300 nm with bands of very low intensity especially in the lower concentration range (**Figure 3.19a**). The bands due to the d-d transitions that are expected in

the region from 600 – 800 are present but, due to the low intensity, only in samples with high concentrations are observed (**Figure 3.19b**).

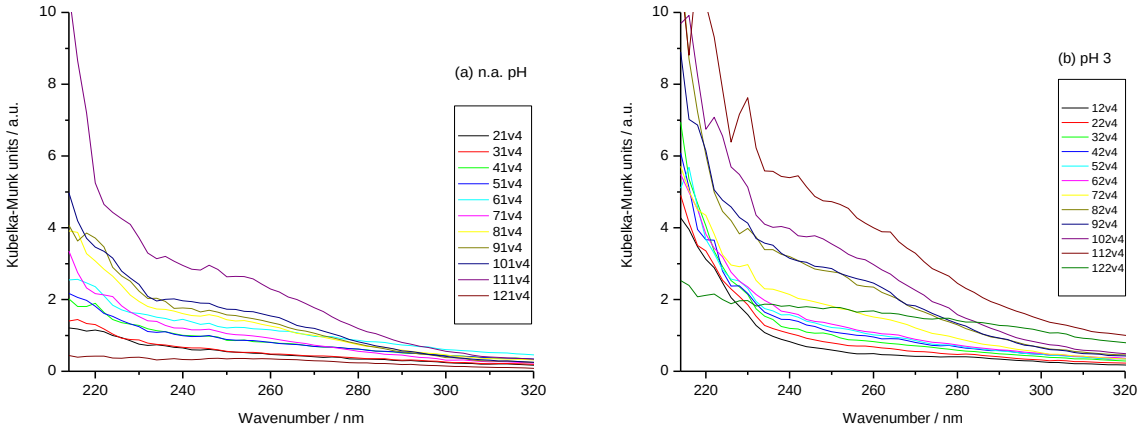

Figure 3.19a DRUV spectra of V (IV) non-adjusted (a) and pH 3 samples (b) - range 214 – 320 nm.

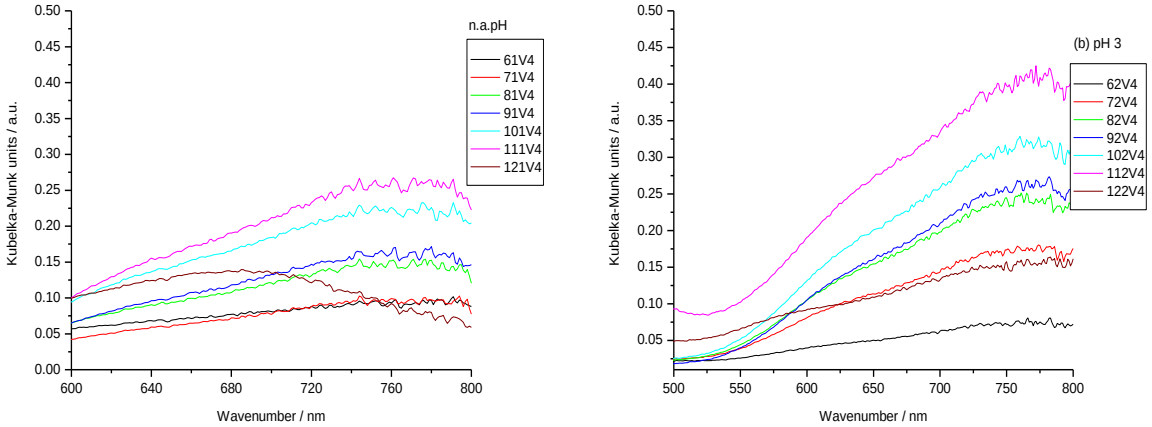

Figure3.19b DRUV spectra of V (IV) non-adjusted (a) and pH 3 samples (b) - range 600 – 800 nm.

In **Figure 3.20** are shown the spectra after normalization at 250 nm, being clear that only control vanadium samples showed significant absorption beyond 500 nm. This band is assigned to a d-d transition, in the samples with low metal complex concentration the band is also present but with very low intensity. Since water has neutral or slightly oxidizing redox potential we would infer that in these samples oxidation from V (IV) to V (V) occurred. . Nevertheless, the samples have a blue color, which is characteristic of V (IV). A partial oxidation to V (V) would render the samples green, and a

complete oxidation would make them yellow or colorless. Hence, the d-d bands in diluted samples appear weak only because they are so in comparison with the stronger CT bands at ~240nm. On the other hand, the high intensity of the CT relative to the d-d bands in samples with cellulose compared to the control may be indicative of binding of cellulose groups to the metal.

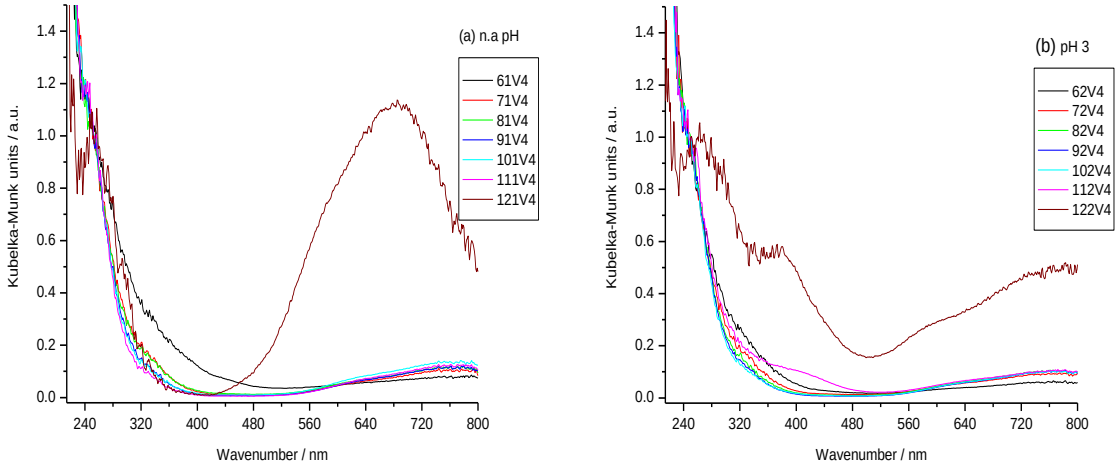

Figure 3.20 Normalized DRUV spectra of V (IV) samples with non-adjusted pH (a) and pH 3 (b)

The set of samples with pH 5 (**Figure 3.21**) had intense bands corresponding to CT and V (IV) d-d transitions. When the metal complex is in higher concentrations we can see three distinct bands at 244, 346 and 700 nm. The band at 244 nm is a CT band and at 700 nm a V(IV) d-d band (band I, according to the model of Balhausen and Gray[12]). The absorption at 346 nm could be caused by a charge transfer or a d-d transition (band II of V(IV)). As the intensity ratio of this band with band I is not constant, we assume this must be another CT band. This is quite interesting, because the appearance of a new ligand-to-metal CT band shows the formation of a new complex. This could be simply the result of hydrolysis and formation of V hydroxides, but it could also result from binding to cellulose groups.

In the samples with low metal complex concentrations only the CT bands, with very low intensity, are present and the d-d band either disappeared or is very weak. These samples had green color, which shows there has been some level of oxidation of V(IV) (blue) to V(V) (typically yellow), resulting in the green as a mixture of the two colors.

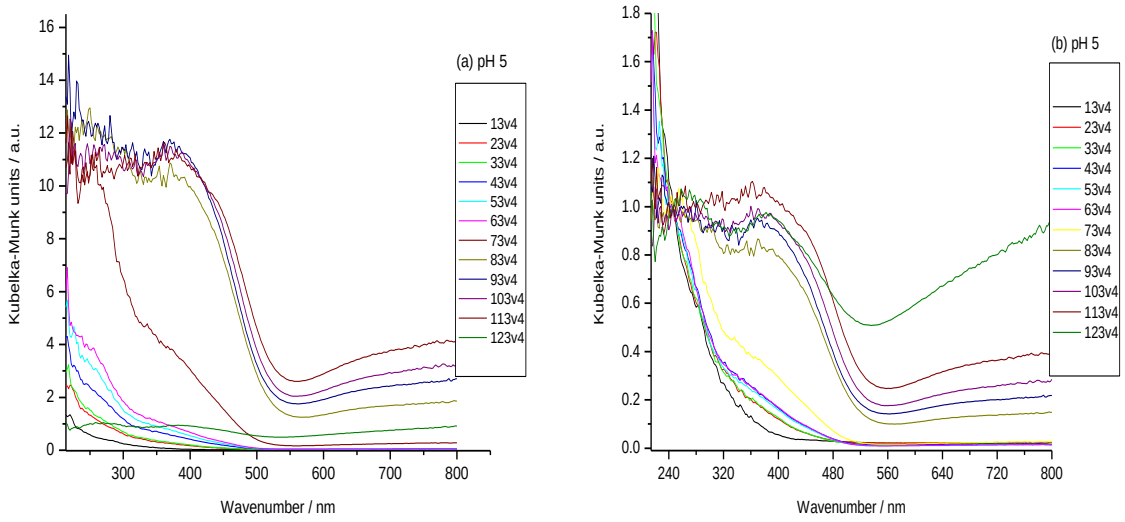

Figure 3.21 DRUV spectra of V (IV) pH 5 samples: (a) spectra without treatment and (b) spectra normalized at 246 nm

3.4.1.3. The Vanadium (IV) filtrated samples

The DRUV spectra of filtrated V (IV) are shown in **Figure 3.22**, for the samples with adjusted pH 5.

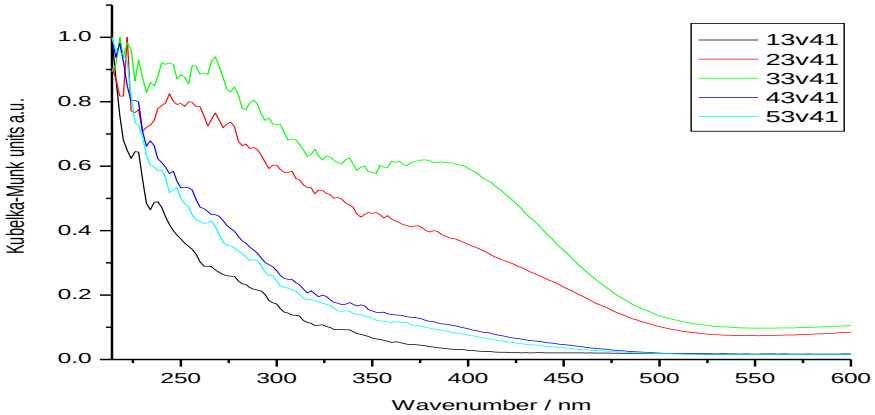

Figure 3.22 Normalized DRUV spectra of filtrated V(IV) samples with pH 5

In the DRUV spectra of the samples with non-adjusted pH and pH 3 showed no clear bands can be detected. Nevertheless, the two highest concentrations samples with pH 5 two bands at 252 and 402 nm, corresponding to CT and d-d transitions, respectively are observed in the spectra. However, full scans of these samples were not clear of the third d-d transition band at around 700 nm. If this is the

case, and only two bands are present in the spectra, then this could mean that at this pH value the metal V (IV) is oxidized to V (V) and these bands point to the presence of the polymeric V (V) species.

3.4.2. Iron metal complex in cellulose

3.4.2.1. Iron (III) samples:

The Fe (III) ion is expected to show two bands in DRUV spectra, usually below 300 nm, due to the CT transfer. The exact position of these bands depends on the number of ligands; it is expected that the bands will be shifted to higher wavenumbers with the increase of coordinating oxygen ligands.[124]

The spectra of the samples of the Fe (III) adsorbed onto cellulose are shown in **Figure 3.23**. For the samples with non-adjusted pH (pH around 2 for the samples with higher metal complex concentration) the spectra present two bands: one at 253 and the other at 338 nm that can be assigned to CT transitions of tetrahedral and octahedral Fe (III) species, respectively.[124,125,126]

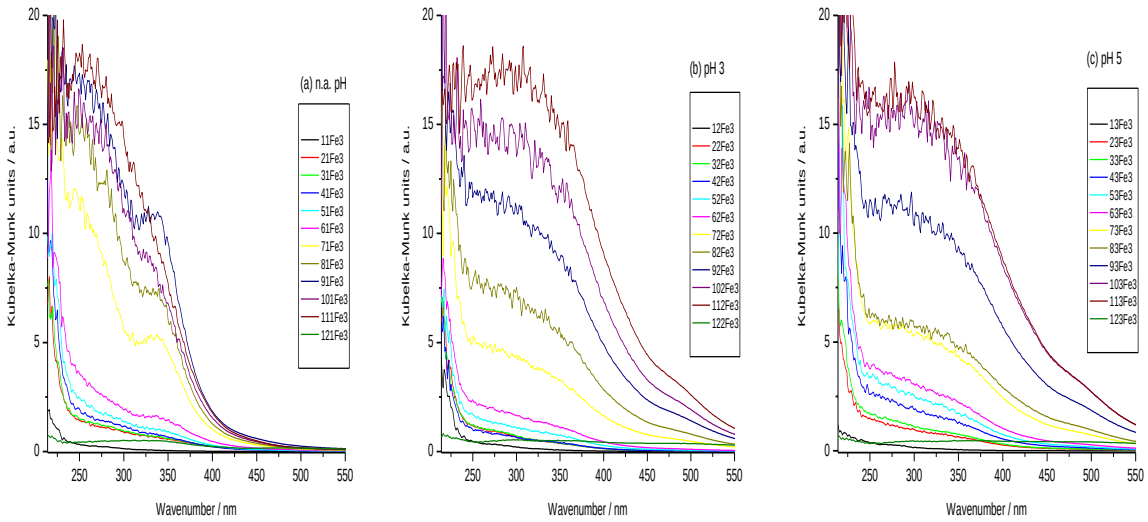

Figure 3.23 DRUV spectra of Fe(III) samples with non-adjusted pH (a), pH 3 (b) and pH 5 (c).

The DRUV spectra of Fe(III) samples with pH 3 and pH 5 are very similar with two bands one at around 300 nm and the other with weak intensity around 470 nm. The band at 300 nm can be an indication of the presence of Fe (III) ions in octahedral symmetry.[124] This band can also be assigned to $FeOH^{2+}$ which has two characteristic bands in ultraviolet spectra, one around 300 nm and the other with maximum at around 205 nm.[127,128] Since the band at 205 nm is not possible to identify in the spectra due to the high spectral noise level in this region, this hypotheses cannot be confirmed.

In order to detect more changes in the absorption bands of the samples prepared with Fe(III) the spectra were normalized at 253, 297 and 300 nm for the samples with non-adjusted pH, pH 3 and 5, respectively (**Figure 3.24**).

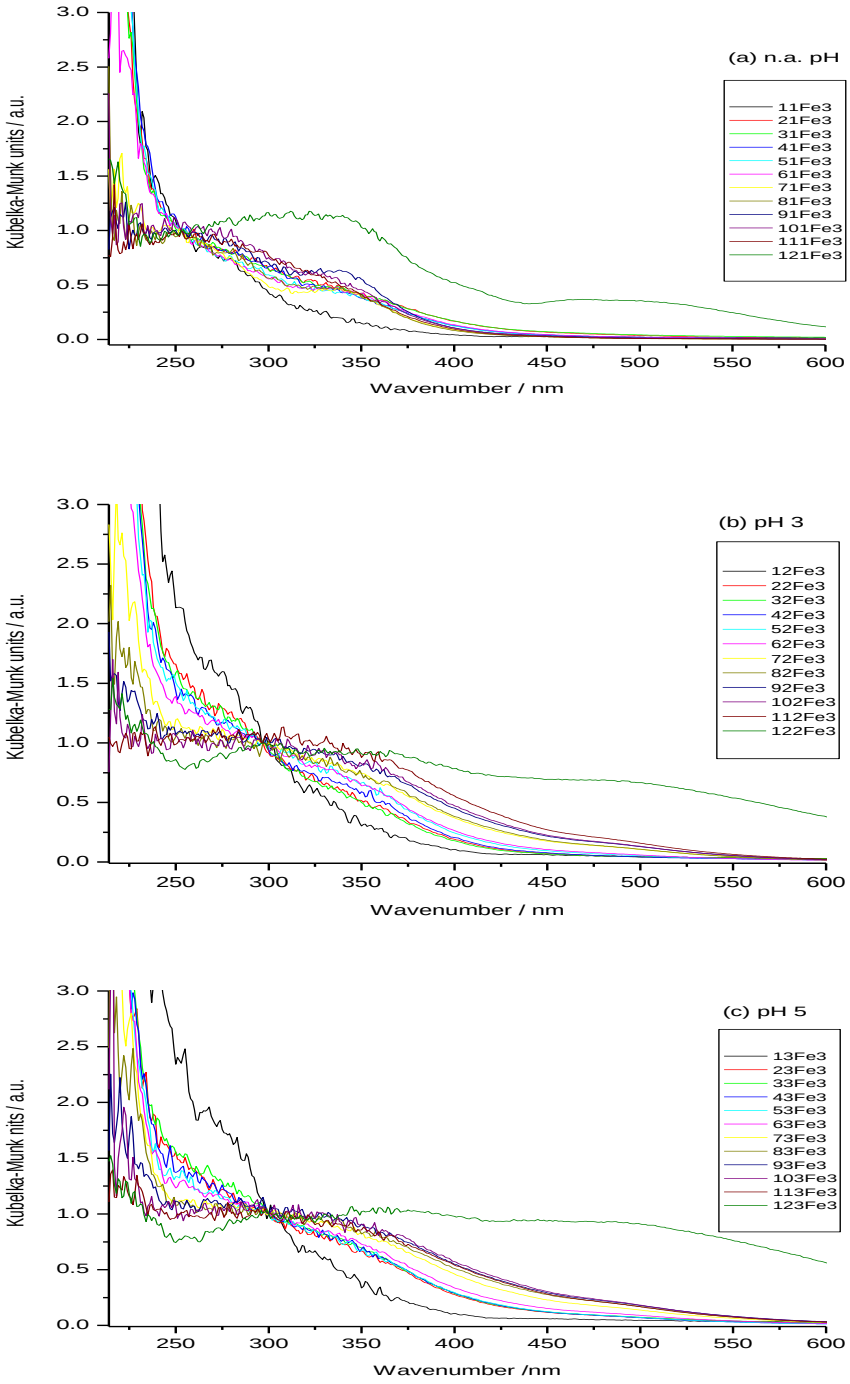

Figure 3.24. DRUV spectra of Fe (III) samples with (a) non-adjusted pH, (b) pH 3 and (c) pH 5, normalized at 253, 297 and 300 nm, respectively.

Two bands are visible in the spectra of the samples prepared at pH 3 and 5 as can be observed in **Figures 3.24a** and **3.24b**, respectively. The first band at around 350 nm, which increases in intensity with the metal complex concentration increasing, and the other very weak band around 470 nm which is present only in the samples with high Fe(III) concentration and in the control Fe(III) sample. In the normalized spectra of samples prepared without pH adjustment the band at 340 nm is present in all the samples while the band at 470 nm is visible only in the residual (control) Fe sample.

These CT bands above 450 nm can be indicators of the presence of octahedral Fe (III) in larger Fe_2O_3 particles[124] or FeO_x oligomers, which have characteristic band at around 500 nm.[129]

3.4.2.2. Iron (II) samples:

The DRUV spectra of the Fe(II) complex adsorbed onto cellulose are in **Figure 3.25**, and according to the literature UV-Vis spectra of Fe (II) ion should show absorption bands at the region between 220 to 250 nm and no or little absorption at 300 nm[130,131]

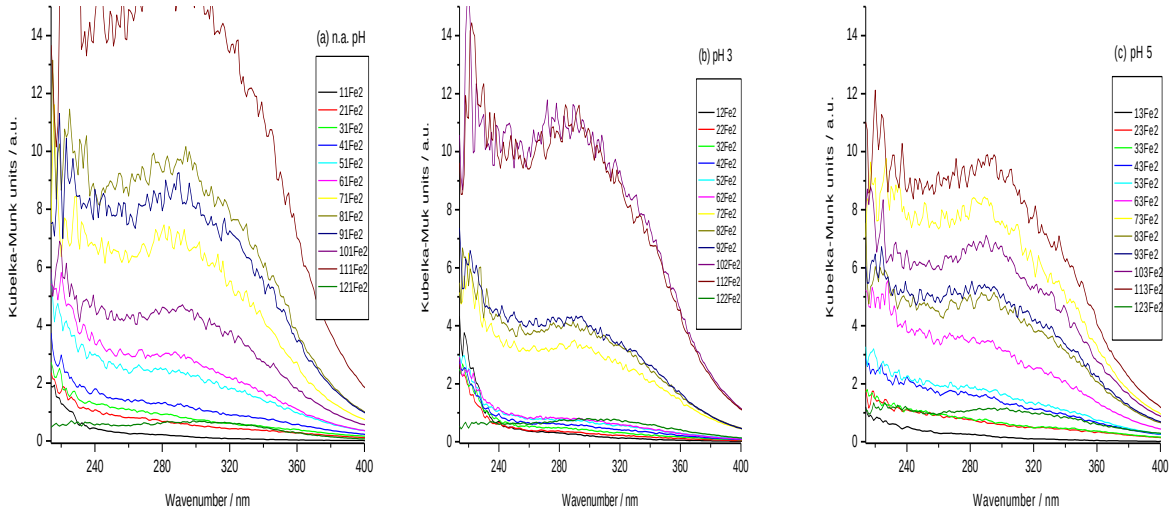

Figure 3.25 DRUV spectra of Fe(II) samples with (a) non-adjusted pH, (b) pH 3 and (c) pH 5

The spectra of all three Fe (II) sets of samples are very similar, with one broad band with the maximum around 280 nm and no significant absorption above 400 nm. Since Fe (II) can be oxidized in Fe (III) under aerobic conditions and the bands are shifted to higher wavelengths that expected, this band is can be related to the CT transitions of Fe (III) ions formed in the samples. In the samples prepared with non-adjusted pH and pH 5 the intensity of bands increases gradually with the metal complex concentration but surprisingly in the set of samples prepared with pH 3 the bands intensity

are in three groups not directly depending on concentration, pointing to the possibility of different species formation, which equilibrium is dependent on the metal concentration.

After normalization at 286 nm only one weak band at 320 nm is present in all the samples (**Figure 3.26**):

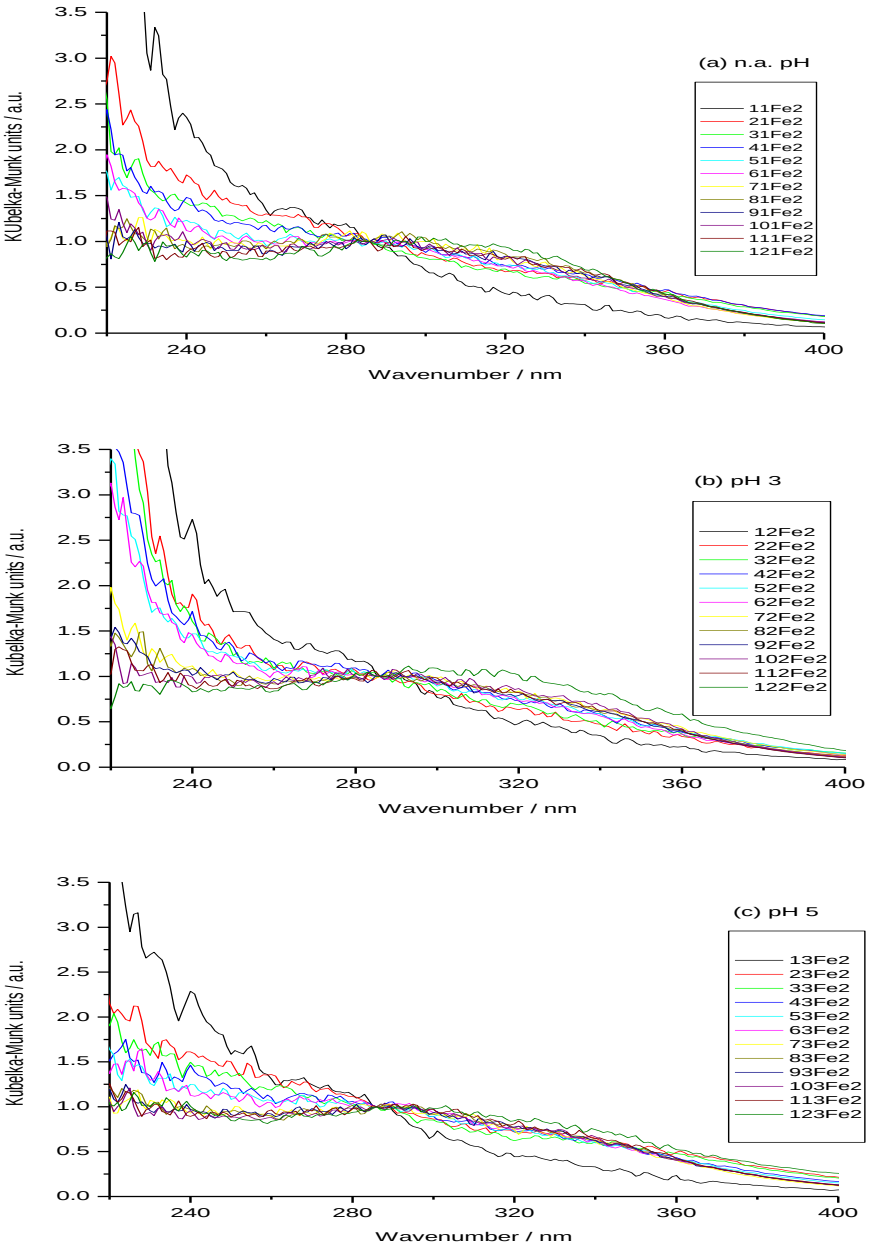

Figure 3.26 DRUV spectra of Fe(II) samples with (a) non-adjusted pH, (b) pH 3 and (c) pH 5, normalized at 286 nm

This band can be indication of the presence of Fe(III) ions formed in the samples during oxidation of Fe(II) under aerobic conditions.

3.4.2.3. Iron (III) filtrated samples:

In the case of Fe (III) filtrated samples only the most concentrated samples were analyzed from each pH set, the DRUV spectra normalized at 256 nm are in **Figure 3.27**.

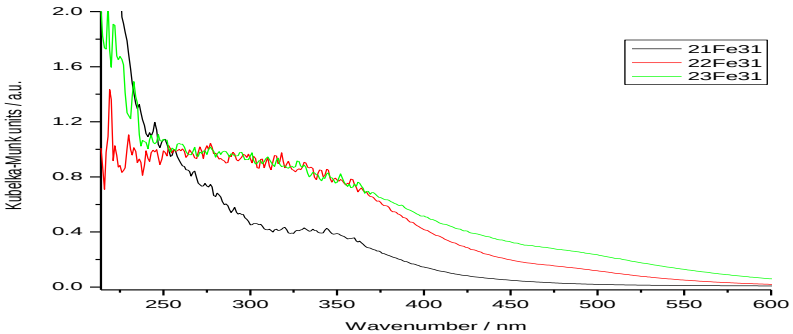

Figure 3.27 Normalized DRUV spectra of Fe(III) filtrated samples

After normalization at 256 nm one band was noticeable in the sample with non-adjusted pH at 337 nm which can be assigned to octahedral Fe(III) or $FeOH^{2+}$; in the pH 3 and 5 samples two bands are present, one at 315 nm and other very weak one at 490 nm. The band at 315 can be assigned to $FeOH^{2+}$ while the band at 490 nm corresponds to the oxygen to metal CT transition involving octahedral Fe^{3+}. Compared to the evaporated, filtrated samples provided us very limited amount of information due to the low affinity of me metal complex to adsorb onto cellulose that leads to a low concentration of metal on cellulose after filtration of the samples.

3.4.3. Copper and zinc metal complexes in cellulose

3.4.3.1. Copper (II) samples:

Typically the UV-Vis spectra of $CuSO_4$ usually contains two maxima, one between 700-800 nm due to the d-d transitions of Cu (II) ions and the other one around 240 nm that is assigned to Cu-O CT transition[132,133,134]. Moreover, a band around 700 nm is assigned to d-d transitions originating from Cu (II) linearly coordinated[135,136] while when the band is shifted to higher wavelengths (around 800 nm) can indicate presence of Cu (II) in a distorted octahedral symmetry.[133,137] The DRUV spectra of

Cu(II) adsorbed onto cellulose is in **Figure 3.28**, for an easy discussion the spectra were normalized at 240, 244 and 242 nm for samples with non-adjusted pH, pH 3 and pH 5 respectively.

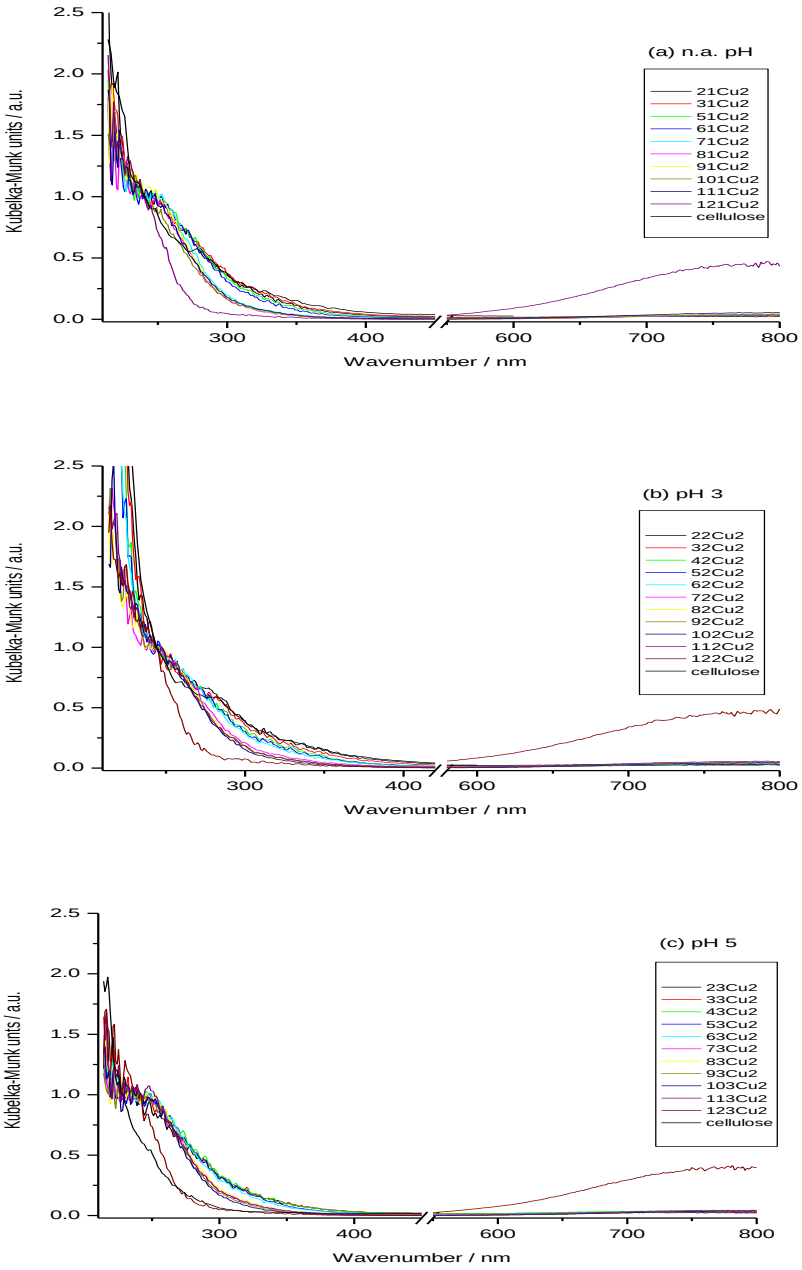

Figure 3.28. The DRUV spectra for samples with non-adjusted pH (a), pH 3 (b) and pH 5 (c), normalized at 240, 244 and 242 nm respectively

In the spectra of all three sets of samples both characteristic bands, CT and d-d transitions, are present but only in the higher range of metal complex concentrations (1mM/g of cellulose and higher). Clearly, the d-d band at around 800 nm is present, although with very low intensity,

indicating the metal Cu(II) is coordinated in distorted octahedral symmetry. After normalization band at around 800 nm is more visible but only in the control sample. In aqueous solutions copper forms aqua complexes $[Cu(H_2O)_6]^{2+}$ with distorted octahedral structure.[19] The aqua copper complex can hydrolyze into copper hydroxide at relatively low pH, which does not absorb in the visible region. Hence the disappearance of the d-d bands at around 800 nm can indicate the hydrolysis of copper.

3.4.3.2. Zinc (II) samples:

$ZnSO_4$ shows weak absorptivity in UV-Vis region. It is found to be transparent in the UV region and shows low absorbance in the visible spectral region around 400 nm[133,138]. The spectra of Zn (II) adsorbed onto cellulose prepared at the different pH are in **Figure 3.29**, the spectra were normalized at 250 nm.

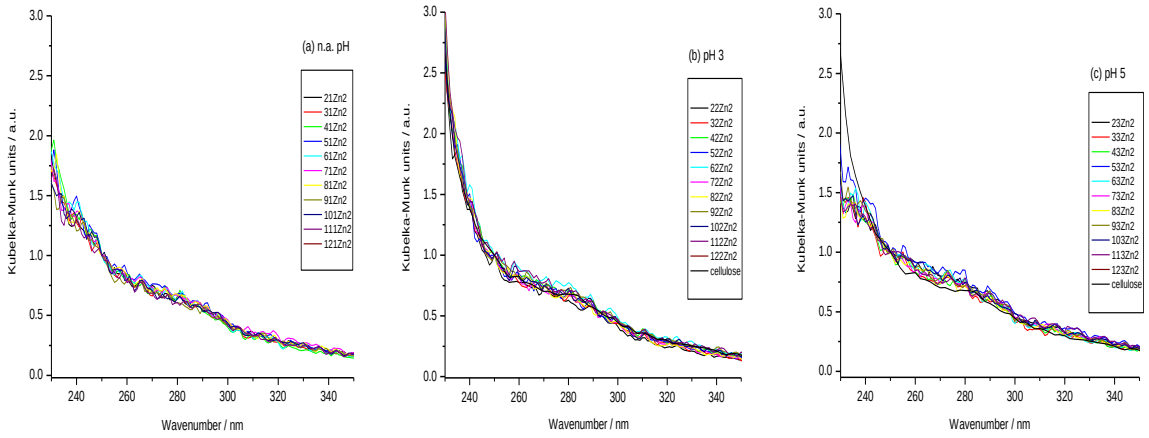

Figure 3.29 Normalized DRUV spectra of Zn (II) samples with non-adjusted pH (a), pH 3 (b) and pH 5 (c), normalized at 250 nm

In our samples there was no absorption in the UV or Vis part of the spectra, all samples with metal have a spectrum that is similar to that of cellulose. Since absorption in the Vis region is expected to be low it is possible that occurrence of no absorption bands in the case of our samples can be due to the low Zn concentration combined with a very high level of spectral noise. Even after normalization of all the spectra no bands are noticeable and in the case of Zn we can't get any information from the UV-Vis spectra.

3.5 Quantitative analysis

Quantitative analysis in UV-Vis diffuse reflectance spectroscopy is performed using Kubelka-Munk theory that relates concentration of the sample with the intensity of reflected radiation. Reflectance spectra obtained in the DRUVS measurements were transformed in Kubelka-Munk units in UVprobe software using the equation $F(R) = (1 - R)^2/2R$ and plotted against the wavenumbers. All fallowing calculations for the regression analysis were performed in Excel.

According to Kubelka Munk function we can perform quantitative determination of metal ions (M^{n+}) by plotting the KM intensity of the transition bands at selected wavelengths against the concentration of M^{n+} in the samples and in that way we can represent the correlation of the M^{n+} concentration and F(R). Since the concentrations of metals in our samples are known we can use F(R) values at selected wavenumbers to obtain calibration equation for each of the metals.

According to the equation F(R)=c/K, where K is assumed to be constant value at given wavelength, it is expected that F(R) will increase with the increase of concentration. In the case of Zn(II) samples all the values of F(R) are randomly distributed and there seems to be no relation between concentration of the metal in the samples and reflectance, therefore in this case we can't get any information for quantitative analysis. However in the graphs obtained for all the other samples increase of F(R) with increase of concentration is evident. This is especially expressed in the lower wavelengths for all the samples and also in the high wavelengths in some of the samples (V (IV) samples with pH 5).

Regression analysis calculations were performed in Excel. For each set of samples we chose several wavenumbers corresponding to maximum values of the band peaks (except for iron 2 which only had one peak therefore only one wavenumber was chosen). When the analysis was done covering the whole range of concentrations from 0.20 to 10.00 mM/ g of cellulose in most of the cases the residual plots showed non-randomly distributed residuals usually with reversed U shaped pattern. This type of residuals distribution suggests that regression model is not a good fit for the data and it needs to be improved. The only exceptions were V(V) set of samples with pH 5 and V(IV) set with pH 3 which showed random distribution of the residuals in full concentration range and also values of R between 0.9560 and 0.9933. However, in the lower range of the concentrations from 0.20 up to 1.00, 3.00 or 5.00 mM/g of cellulose (depending of the sample set) regression models showed better fit for the data. The residuals had random distribution and the values for R were satisfactory. All obtained regression equations for given concentration range and wavenumber are presented in the **Table3.9.**

together with the calculated values for LD, LQ, DR and R. The best fit regression model for each of the metals is presented in Figure **3.30.**

Table 3.9. Regression equations with calculated values for LD, LQ, DR and R for each of the metals at chosen wavelengths and concentration range:

Copper:

Cu(II)	Conc. range (mM/g cell)	Wavenumber (nm)	LD (mM/g cell)	LQ (mM/g cell)	DR	Equation	R
na pH	**0.20 - 3.00**	240	0.94	3.14	0.96	y=(0.91 ± 0.32)x + (0.66 ± 0.43)	0.9695
	0.20 - 3.00	700	1.04	3.45	0.87	y=(0.0215 ± 0.0083)x + (0.019 ± 0.012)	0.9634
pH 3	**0.20 - 1.00**	244	0.10	0.33	3.06	y=(0.816 ± 0.089)x + (0.512 ± 0.050)	0.9970
	0.20 - 3.00	700	0.61	2.05	1.47	y=(0.0192 ± 0.0041)x + (0.0130 ± 0.0051)	0.9837
pH 5	**0.20 - 3.00**	242	0.67	2.22	1.35	y=(1.15 ± 0.27)x + (0.68 ± 0.33)	0.9809
	0.20 - 1.00	700	0.14	0.45	2.20	y=(0.0465 ± 0.0071)x + (0.0109 ± 0.0040)	0.9942

Iron 2:

Fe(II)	Conc. range (mM/g cell)	Wavenumber (nm)	LD (mM/g cell)	LQ (mM/g cell)	DR	Equation	R
na pH	**0.20 - 3.00**	290	0.34	1.14	2.63	y=(2.32 ± 0.28)x + (0.33 ± 0.35)	0.9948
pH 3	**0.20 - 3.00**	288	0.66	2.20	1.36	y=(1.06 ± 0.24)x + (0.09 ± 0.30)	0.9812
pH 5	**0.20 - 3.00**	288	0.35	1.15	2.60	y=(2.75 ± 0.33)x + (0.20 ± 0.41)	0.9947

Iron 3:

Fe(III)	Conc. range (mM/g cell)	Wavenumber (nm)	LD (mM/g cell)	LQ (mM/g cell)	DR	Equation	R
na pH	**0.20 - 3.00**	253	0.39	1.29	2.33	y=(3.68 ± 0.49)x + (0.19 ± 0.61)	0.9934
	0.20 - 5.00	340	0.57	1.91	2.61	y=(1.51 ± 0.16)x + (0.15 ± 0.33)	0.9949
pH 3	**0.20 - 5.00**	290	0.40	1.33	3.77	y=(1.41 ± 0.10)x + (0.31 ± 0.21)	0.9976
	0.20 - 5.00	500	0.62	2.06	2.43	y=(0.162 ± 0.018)x - (0.024 ± 0.038)	0.9942
pH 5	**0.20 - 1.00**	300	0.12	0.41	2.42	y=(2.81 ± 0.39)x + (0.37 ± 0.22)	0.9951
	0.20 - 3.00	500	0.15	0.51	5.84	y=(0.239 ± 0.013)x + (0.018 ± 0.016)	0.9989

Vanadium 4:

V(IV)	Conc. range (mM/g cell)	Wavenumber (nm)	LD (mM/g cell)	LQ (mM/g cell)	DR	Equation	R
na pH	**0.20 - 1.00**	222	0.39	1.29	0.78	y=(1.04 ± 0.45)x + (0.99 ± 0.26)	0.9558
	0.20 - 1.00	254	0.35	1.16	0.86	y=(0.76 ± 0.30)x + (0.40 ± 0.17)	0.9638
	0.20 - 1.00	400	0.42	1.38	0.72	y=(0.127 ± 0.059)x + (0.037 ± 0.033)	0.9493
	0.20 - 10.00	700	2.92	9.72	1.03	y=(0.0182 ± 0.0051)x + (0.031 ± 0.029)	0.9715
pH3	**0.20 - 10.00**	220	3.45	11.51	0.87	y=(0.57 ± 0.14)x + (3.21 ± 0.62)	0.9560
	0.20 - 10.00	248	1.31	4.35	2.30	y=(0.371 ± 0.033)x + (0.86 ± 0.16)	0.9933
	0.20 - 10.00	700	1.60	5.34	1.87	y=(0.0303 ± 0.0047)x + (0.031 ± 0.028)	0.9911
pH5	**0.20 - 3.00**	246	0.13	0.44	6.84	y=(1.30 ± 0.17)x - (0.06 ± 0.21)	0.9992
	0.20 - 1.00	400	0.12	0.38	2.60	y=(0.653 ± 0.084)x + (0.047 ± 0.048)	0.9958
	0.20 - 10.00	700	2.17	7.24	1.38	y=(0.392 ± 0.058)x + (0.21 ± 0.27)	0.9819

Vanadium 5:

V(V)	Conc. range (mM/g cell)	Wavenumber (nm)	LD (mM/g cell)	LQ (mM/g cell)	DR	Equation	R
na pH	**0.20 - 3.00**	244	0.50	1.65	1.82	y=(3.44 ± 0.59)x + (1.13 ± 0.73)	0.9893
	0.20 - 3.00	352	0.19	0.65	4.62	y=(1.219 ± 0.082)x + (0.13 ± 0.11)	0.9983
	0.20 - 3.00	400	0.19	0.62	4.84	y=(0.827 ± 0.053)x + (0.054 ± 0.066)	0.9985
pH3	**0.20 - 3.00**	256	0.28	0.93	3.23	y=(3.60 ± 0.35)x + (0.45 ± 0.43)	0.9966
	0.20 - 3.00	362	0.24	0.81	3.68	y=(1.63 ± 0.14)x + (0.12 ± 0.18)	0.9973
	0.20 - 3.00	400	0.31	1.02	2.95	y=(1.31 ± 0.14)x + (0.17 ± 0.18)	0.9959
pH5	**0.20 - 10.00**	258	2.94	9.80	1.02	y=(1.96 ± 0.39)x + (1.35 ± 1.80)	0.9916
	0.20 - 10.00	356	1.62	5.41	1.85	y=(1.12 ± 0.13)x + (0.01 ± 0.57)	0.9897
	0.20 - 10.00	400	1.47	4.90	2.04	y=(0.838 ± 0.083)x + (0.08 ± 0.39)	0.9916

However, despite the random distribution of the residuals and high values for regression coefficients, some of the other calculated parameters didn't have satisfactory values. LD should fulfill the following conditions: LD < c_{min} and 10 x LD > $c_{min.}$ As shown in the table in the most cases LD was higher than the lowest prepared concentration of our samples. If this problem occurs that can be a sign that used concentration range was too low for this method and that higher concentrations of analytes should be used in sample preparation.

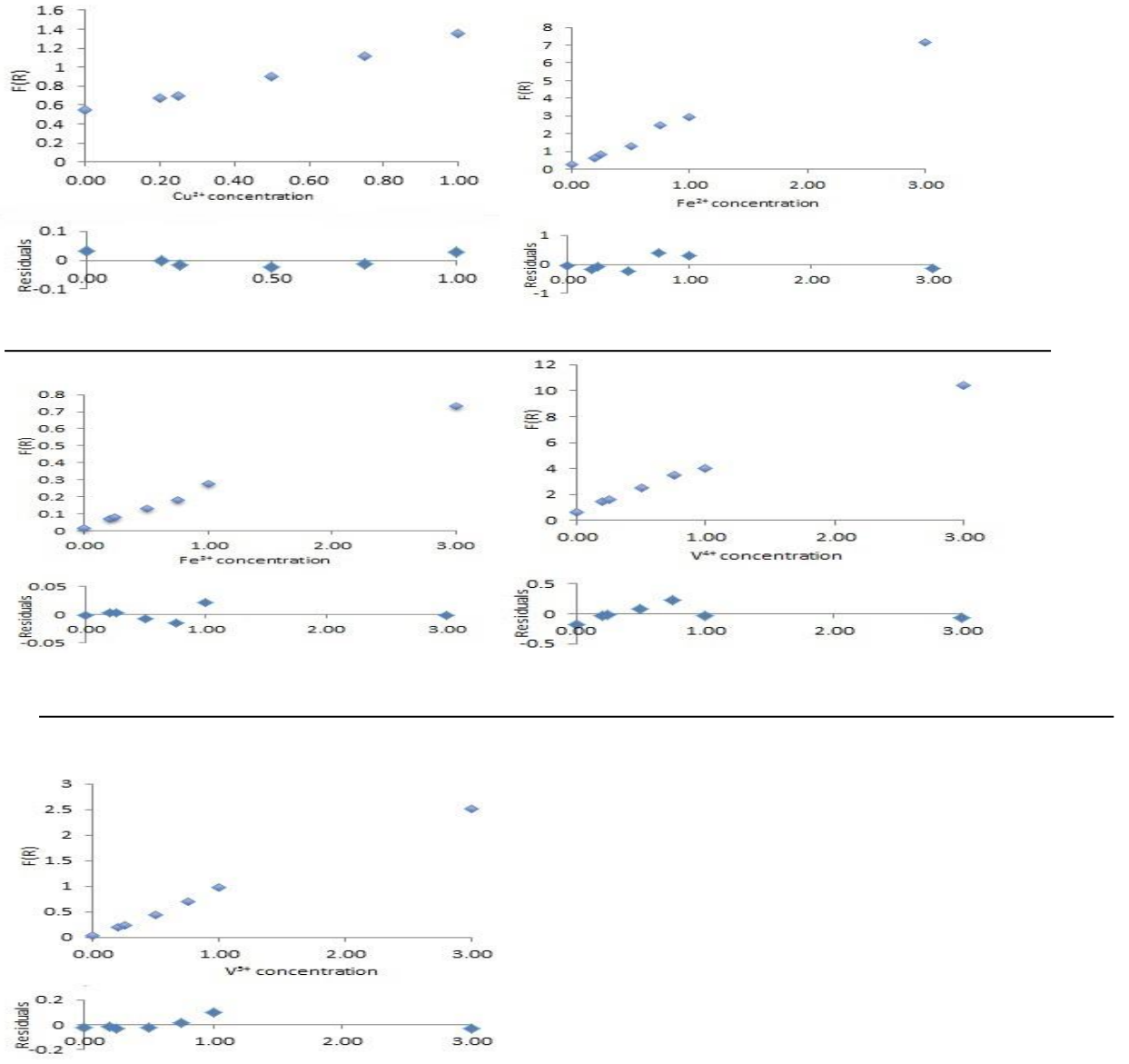

Figure 3.30. The best fitting models for each of the metals with the corresponding residual plots; Cu (II) at pH 3, ʎ=244nm; Fe (II) non-adjusted pH, ʎ=290nm; Fe (III) pH 5, ʎ=500nm; V (IV) pH 5, ʎ=246nm and V (V) non-adjusted pH ʎ=400nm.

The graphic representation of the relationship between the selected wavenumbers and the obtained corresponding slope was also made (**Figure 3.31**). The values for the slope were the highest in the low wavenumbers as expected since the maxima are in that spectral region and, therefore, in that ranges the sensibility of the method is the highest.

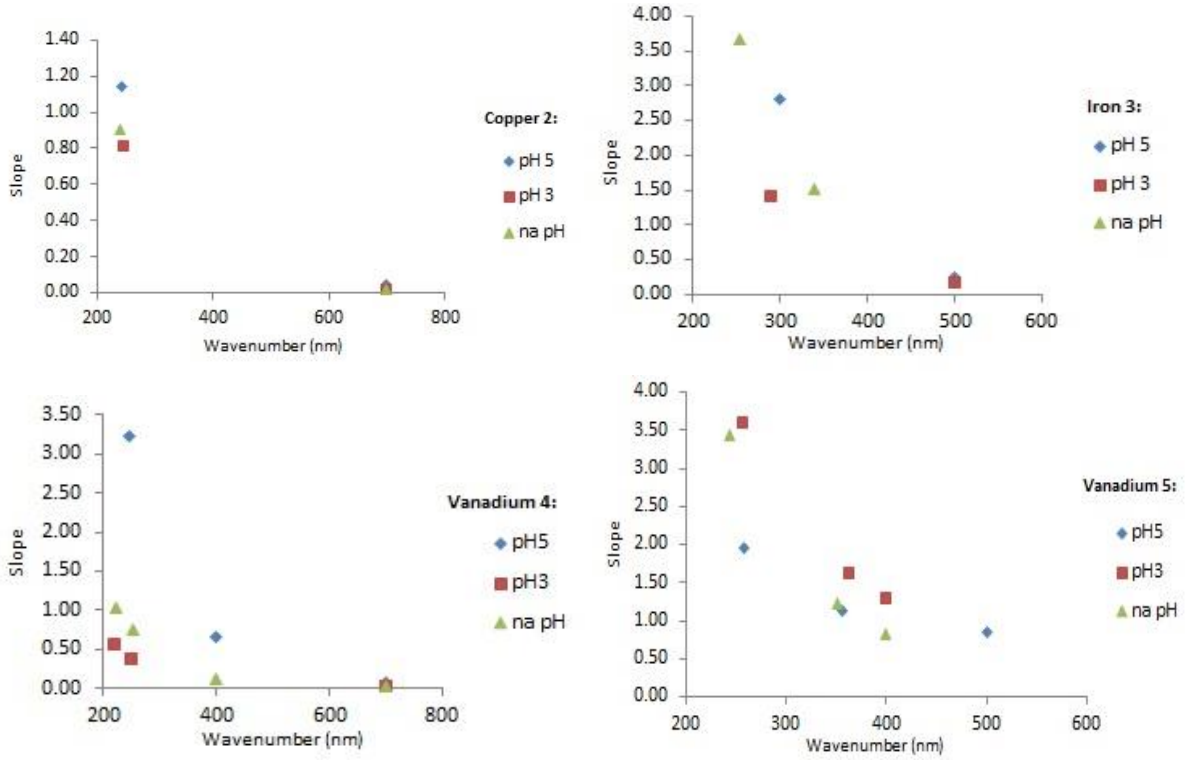

Figure 3.31. Graphs showing the correlation between wavelength and the slope

Besides the fact that the samples can need a high concentration for a more acceptable quantitative analysis, there are more possible reasons for unsatisfying results and they can be connected to the process of sample preparation or the analytical technique. In sample preparation there were more reasons such as contamination, temperature variations that could cause changes in the evaporation rate, loss of the analyte due to the absorption of metals on the walls of plastic beakers or due to the treatment of the samples during the preparation. A more important issue was the pH control of the samples, this parameter was measured daily using portable pH meter and it is possible that the results were affected by the loss of small amount of samples that remained on the electrode during each measurement. Loss of the sample was also possible during the homogenization step which was performed by stirring the samples 2-3 times every day using plastic spatula.

The sensibility of the equipment could also be one of the reasons that we did not get good results. In every measurement there was a lot of noise in both high and low wavelength regions. This problem can be reduced by dilution of the samples with $BaSO_4$ before measurements. However in this case we would have to consider the dilution ratio and it would be very difficult to perform quantitative analysis.

4. Conclusions

The objective of this work was to study the interaction of cellulose fibers with four different metal complexes using two spectroscopic techniques: DRIFTS was used to evaluate structural changes of native cellulose and of the metal complexes, while DRUV/VIS was used to analyze the metal compounds that are and of the metal complexes deposited over the cellulose surface.

It was found that the crystallinity of the cellulose was affected by the metal complexes only in the case of vanadium (V) and zinc (II) while for the other metals there was no noticeable influence. Analysis of the region between 1300 and 1180 cm^{-1} in DRIFT spectra of V(V) samples showed increase of the degree of crystallinity, in low pH values, from approximately 44 to 76% with the increase of vanadium complex concentration from 1 to 10 mM / g cellulose. Quantification of the change in the crystallinity degree was not possible in the case of zinc samples but the ratio between the intensity of the bands at 1430 and 898 cm^{-1} clearly showed increase with the increase of the zinc concentration. The increase of cellulose crystallinity can be explained by the hydrolysis of the amorphous regions of cellulose, catalyzed by the metal ions in acid medium.

Analysis of DRIFT and DRUV spectra provided information about deposition of different metal species onto cellulose depending on the concentration and pH value of the samples. The presence of adsorbed or deposit metal species was observed only in the samples with higher range of concentrations, where some influence of the cellulose matrix was observed, while the samples in the low concentration range did not show any significant changes. Dependence of the deposit species with the sample preparation pH was also proposed some metal complexes.

For vanadium (V), as expected, different species deposited onto cellulose were observed in the sets of samples with different pH values. At low pH values such as pH 3 it is found that decavanadates are dominant species. At pH 5 dominant species seemed to be mixture of tri and decavanadates and at pH 6-7 we found the mixture of tri and tetravanadates deposited on cellulose.

Analysis of the DRIFT spectra of the V(IV) in all three sets of samples indicated entrapment of the SO_4^{2-} ion and also different vanadium species in the cellulose chains but also only in the high range of concentrations. It was also concluded that there has been a change in the crystal structure of the initial compound from α to β-$VOSO_4$.

Analysis of iron (III) samples showed the deposition of different species onto the cellulose exterior surface with low interaction but also an adsorption onto the cellulose chains with stronger interactions.

A very weak interaction or no interaction was observed in the case of zinc, copper and iron (II). The adsorption of zinc and copper metal complexes onto cellulose had no significant effect when comparing the spectra of the deposit complex with those to the pure reagents. If fact, the spectra are dominated by the bands of cellulose without clear presence of the complex bands, moreover no new bands or shifts of the bands are observed in any of the samples indicating poor interaction between the complex and the matrix and adsorption/deposition on the cellulose surface or on the amorphous phase.

For the purpose of quantitative analysis we graphically represented the correlation of the M^{n+} concentration and F(R). As expected, F(R) increased with the increase of concentration in the case of all of the metals except Zn(II) where it seems to be no relation between concentration of the metal in the samples and the amount of adsorbed radiation. However, for all the metal complexes, the performed quantitative analysis did not give satisfying values of regression parameters. The low repeatability of the sample preparation procedure can be one important cause for this. There are more possible reasons for unsatisfying results including too low concentration range used, the analytical technique and the sensibility of the equipment, which presents a high spectral noise level for the diffuse reflectance analysis.

Since the cellulose is used as a excipient in pharmaceutical formulations and some of this metal ions can be present, it is possible to conclude that Zn(II), Cu(II), Fe(II) and Fe (III) are very stable in cellulose but V(IV) and in larger extension V(V) can participate in several equilibria with the influenced by the matrix. The cellulose structure can also be altered, mainly its crystallinity, by Zn(II) and V(V) at low pH values, while the others are inert. The quantification of the adsorbed complex species in cellulose it is possible but the sample preparation procedure must be optimized.

5. Annexes

5.1. Tables for evaporated samples preparation

Table 5.1. Preparation of stock solutions (evaporated)

compound / stock solution	pH sample set	$m_{compound}$(g)	M (g/mol)	$V_{stock\ sol}$ (L)	$c_{stock\ sol}$ (mM/L)
$VOSO_4x5H_2O$	n.a. pH	2.5373	253.10	0.1	100.25
	pH 3	2.5313		0.1	100.01
	pH 5	2.5323		0.1	100.05
NH_4VO_3	n.a. pH	1.1699	116.98	0.2	50.00
	pH 3	1.1699		0.2	50.00
	pH 5	1.1699		0.2	50.00
$CuSO_4x5H_2O$	n.a. pH	2.497	249.68	0.1	100.01
	pH 3	2.4976		0.1	100.03
	pH 5	2.4994		0.1	100.10
$FeSO_4x7H_2O$	n.a. pH	2.7813	278.01	0.1	100.04
	pH 3	2.7852		0.1	100.18
	pH 5	2.7802		0.1	100.00
$FeN_3O_9x9H_2O$	n.a. pH	4.043	404.00	0.1	100.07
	pH 3	4.0416		0.1	100.04
	pH 5	4.0418		0.1	100.04
$ZnSO_4x7H_2O$	n.a. pH	2.8765	287.54	0.1	100.04
	pH 3	2.8755		0.1	100.00
	pH 5	2.8759		0.1	100.02

Table 5.2a. Table for V (IV) non-adjusted pH set of samples (evaporated)

sample	$V_{stock\ sol}$ (mL)	V_{H2O} (mL)	V_{total} (mL)	$m_{cellulose}$ (g)	c (mM / $g_{cellulose}$)
1.1.V4	0.00	40	40	1.0016	0.00
2.1.V4	0.20	40	40	1.0032	0.20
3.1.V4	0.25	40	40	1.0007	0.25
4.1.V4	0.50	40	40	1.0004	0.50
5.1.V4	0.75	40	40	0.9997	0.75
6.1.V4	1.00	40	40	1.0030	1.00
7.1.V4	3.00	37	40	1.0009	3.00
8.1.V4	5.00	35	40	1.0013	5.01
9.1.V4	6.00	34	40	1.0031	6.00
10.1.V4	8.00	32	40	0.9998	8.02
11.1.V4	10.00	30	40	0.9990	10.03
12.1.V4	10.00	30	40	0.0000	0.00

Table 5.2b. Table for V (IV) pH 3 set of samples (evaporated)

sample	$V_{stock\ sol}$ (mL)	V_{H2O} (mL)	V_{total} (mL)	$m_{cellulose}$ (g)	c (mM / $g_{cellulose}$)
1.2.V4	0.00	20	20	1.0019	0.00
2.2.V4	0.20	20	20	1.0010	0.20
3.2.V4	0.25	20	20	1.0009	0.25
4.2.V4	0.50	20	20	1.0033	0.50
5.2.V4	0.75	19	20	0.9999	0.75
6.2.V4	1.00	19	20	1.0008	1.00
7.2.V4	3.00	17	20	1.0005	3.00
8.2.V4	5.00	15	20	1.0006	5.00
9.2.V4	6.00	14	20	0.9999	6.00
10.2.V4	8.00	12	20	0.9996	8.00
11.2.V4	10.00	10	20	1.0005	10.00
12.2.V4	10.00	10	20	0.0000	0.00

Table 5.2c. Table for V (IV) pH 5 set of samples (evaporated)

sample	$V_{stock\ sol}$ (mL)	V_{H2O} (mL)	V_{total} (mL)	$m_{cellulose}$ (g)	c (mM / $g_{cellulose}$)
1.3.V4	0.00	20	20	1.0037	0.00
2.3.V4	0.20	20	20	1.0014	0.20
3.3.V4	0.25	20	20	0.9988	0.25
4.3.V4	0.50	20	20	1.0006	0.50
5.3.V4	0.75	19	20	1.0004	0.75
6.3.V4	1.00	19	20	0.9991	1.00
7.3.V4	3.00	17	20	1.0015	3.00
8.3.V4	5.00	15	20	0.9994	5.01
9.3.V4	6.00	14	20	1.0002	6.00
10.3.V4	8.00	12	20	0.9997	8.01
11.3.V4	10.00	10	20	1.0024	9.98
12.3.V4	10.00	10	20	0.0000	0.00

Table 5.3a. Table for V (V) non-adjusted pH set of samples (evaporated)

sample	$V_{stock\ sol}$ (mL)	V_{H2O} (mL)	V_{total} (mL)	$m_{cellulose}$ (g)	c (mM / $g_{cellulose}$)
1.1.V5	0.00	20	20	1.0018	0.00
2.1.V5	0.40	20	20	1.0014	0.20
3.1.V5	0.50	20	21	1.0011	0.25
4.1.V5	1.00	20	21	1.0008	0.50
5.1.V5	1.50	20	22	0.9987	0.75
6.1.V5	2.00	18	20	1.0012	1.00
7.1.V5	6.00	14	20	0.9990	3.00
8.1.V5	10.00	10	20	1.0019	4.99
9.1.V5	12.00	8	20	1.0000	6.00
10.1.V5	16.00	5	21	1.0014	7.99
11.1.V5	20.00	5	25	0.9990	10.01
12.1.V5	20.00	0	20	0.0000	0.00

Table 5.3b. Table for V (V) pH 3 set of samples (evaporated)

sample	$V_{stock\ sol}$ (mL)	V_{H2O} (mL)	V_{total} (mL)	$m_{cellulose}$ (g)	c (mM / $g_{cellulose}$)
1.2.V5	0.00	20	20	0.9993	0.00
2.2.V5	0.40	20	20	0.9996	0.20
3.2.V5	0.50	20	21	0.9997	0.25
4.2.V5	1.00	20	21	0.9995	0.50
5.2.V5	1.50	20	22	1.0003	0.75
6.2.V5	2.00	18	20	1.0018	1.00
7.2.V5	6.00	14	20	1.0013	3.00
8.2.V5	10.00	10	20	0.9995	5.00
9.2.V5	12.00	8	20	1.0028	5.98
10.2.V5	16.00	5	21	1.0008	7.99
11.2.V5	20.00	5	25	1.0004	10.00
12.2.V5	20.00	0	20	0.0000	0.00

Table 5.3c. Table for V (V) pH 5 set of samples (evaporated)

sample	$V_{stock\ sol}$ (mL)	V_{H2O} (mL)	V_{total} (mL)	$m_{cellulose}$ (g)	c (mM / $g_{cellulose}$)
1.3.V5	0.00	20	20	1.0013	0.00
2.3.V5	0.40	20	20	1.0007	0.20
3.3.V5	0.50	20	20	0.9990	0.25
4.3.V5	1.00	19	20	1.0017	0.50
5.3.V5	1.50	19	20	1.0011	0.75
6.3.V5	2.00	18	20	0.9999	1.00
7.3.V5	6.00	14	20	1.0036	2.99
8.3.V5	10.00	10	20	1.0025	4.99
9.3.V5	12.00	8	20	1.0017	5.99
10.3.V5	16.00	5	21	0.9989	8.01
11.3.V5	20.00	5	25	1.0012	9.99
12.3.V5	20.00	0	20	0.0000	0.00

Table 5.4a. Table for Cu (II) non-adjusted pH set of samples (evaporated)

sample	$V_{stock\ sol}$ (mL)	V_{H2O} (mL)	V_{total} (mL)	$m_{cellulose}$ (g)	c (mM / $g_{cellulose}$)
1.1.Cu2	0.00	20	20	1.0030	0.00
2.1.Cu2	0.20	20	20	1.0004	0.20
3.1.Cu2	0.25	20	20	1.0002	0.25
4.1.Cu2	0.50	20	20	1.0005	0.50
5.1.Cu2	0.75	20	20	1.0009	0.75
6.1.Cu2	1.00	20	20	1.0002	1.00
7.1.Cu2	3.00	17	20	1.0044	2.99
8.1.Cu2	5.00	15	20	0.9991	5.00
9.1.Cu2	6.00	14	20	0.9970	6.02
10.1.Cu2	8.00	12	20	1.0018	7.99
11.1.Cu2	10.00	10	20	0.9966	10.03
12.1.Cu2	10.00	10	20	0.0000	0.00

Table 5.4b. Table for Cu (II) pH 3 set of samples (evaporated)

sample	$V_{stock\ sol}$ (mL)	V_{H2O} (mL)	V_{total} (mL)	$m_{cellulose}$ (g)	c (mM / $g_{cellulose}$)
1.2.Cu2	0.00	20	20	0.9997	0.00
2.2.Cu2	0.20	20	20	0.9999	0.20
3.2.Cu2	0.25	20	20	1.0004	0.25
4.2.Cu2	0.50	20	20	0.9999	0.50
5.2.Cu2	0.75	20	20	1.0006	0.75
6.2.Cu2	1.00	20	20	1.0014	1.00
7.2.Cu2	3.00	17	20	1.0019	3.00
8.2.Cu2	5.00	15	20	1.0028	4.99
9.2.Cu2	6.00	14	20	1.0003	6.00
10.2.Cu2	8.00	12	20	1.0022	7.98
11.2.Cu2	10.00	10	20	1.0023	9.98
12.2.Cu2	10.00	10	20	0.0000	0.00

Table 5.4c. Table for Cu (II) pH 5 set of samples (evaporated)

sample	$V_{stock\ sol}$ (mL)	V_{H2O} (mL)	V_{total} (mL)	$m_{cellulose}$ (g)	c (mM / $g_{cellulose}$)
1.3.Cu2	0.00	20	20	1.0013	0.00
2.3.Cu2	0.20	20	20	0.9997	0.20
3.3.Cu2	0.25	20	20	0.9997	0.25
4.3.Cu2	0.50	20	20	1.0020	0.50
5.3.Cu2	0.75	20	20	0.9997	0.75
6.3.Cu2	1.00	20	20	0.9998	1.00
7.3.Cu2	3.00	17	20	1.0003	3.00
8.3.Cu2	5.00	15	20	0.9998	5.01
9.3.Cu2	6.00	14	20	1.0005	6.00
10.3.Cu2	8.00	12	20	1.0001	8.01
11.3.Cu2	10.00	10	20	1.0023	9.99
12.3.Cu2	10.00	10	20	0.0000	0.00

Table 5.5a. Table for Fe (II) non-adjusted pH set of samples (evaporated)

sample	$V_{stock\ sol}$ (mL)	V_{H2O} (mL)	V_{total} (mL)	$m_{cellulose}$ (g)	c (mM / $g_{cellulose}$)
1.1.Fe2	0.00	20	20	0.9995	0.00
2.1.Fe2	0.20	20	20	1.0066	0.20
3.1.Fe2	0.25	20	20	1.0012	0.25
4.1.Fe2	0.50	20	20	0.9994	0.50
5.1.Fe2	0.75	20	20	0.9993	0.75
6.1.Fe2	1.00	20	20	1.0019	1.00
7.1.Fe2	3.00	17	20	0.9992	3.00
8.1.Fe2	5.00	15	20	0.9998	5.00
9.1.Fe2	6.00	14	20	1.0011	6.00
10.1.Fe2	8.00	12	20	1.0002	8.00
11.1.Fe2	10.00	10	20	0.9996	10.01
12.1.Fe2	10.00	10	20	0.0000	0.00

Table 5.5b. Table for Fe (II) pH 3 set of samples (evaporated)

sample	$V_{stock\ sol}$ (mL)	V_{H2O} (mL)	V_{total} (mL)	$m_{cellulose}$ (g)	c (mM / $g_{cellulose}$)
1.2.Fe2	0.00	20	20	0.9986	0.00
2.2.Fe2	0.20	20	20	1.0029	0.20
3.2.Fe2	0.25	20	20	1.0014	0.25
4.2.Fe2	0.50	20	20	0.9995	0.50
5.2.Fe2	0.75	20	20	0.9992	0.75
6.2.Fe2	1.00	20	20	1.0001	1.00
7.2.Fe2	3.00	17	20	1.0018	3.00
8.2.Fe2	5.00	15	20	1.0005	5.01
9.2.Fe2	6.00	14	20	0.9933	6.05
10.2.Fe2	8.00	12	20	1.0001	8.01
11.2.Fe2	10.00	10	20	1.0007	10.01
12.2.Fe2	10.00	10	20	0.0000	0.00

Table 5.5c. Table for Fe (II) pH 5 set of samples (evaporated)

sample	$V_{stock\ sol}$ (mL)	V_{H2O} (mL)	V_{total} (mL)	$m_{cellulose}$ (g)	c (mM / $g_{cellulose}$)
1.3.Fe2	0.00	20	20	1.0020	0.00
2.3.Fe2	0.20	20	20	1.0002	0.20
3.3.Fe2	0.25	20	20	0.9997	0.25
4.3.Fe2	0.50	20	20	1.0010	0.50
5.3.Fe2	0.75	20	20	1.0014	0.75
6.3.Fe2	1.00	20	20	0.9997	1.00
7.3.Fe2	3.00	17	20	1.0015	3.00
8.3.Fe2	5.00	15	20	1.0004	5.00
9.3.Fe2	6.00	14	20	0.9994	6.00
10.3.Fe2	8.00	12	20	0.9984	8.01
11.3.Fe2	10.00	10	20	1.0046	9.95
12.3.Fe2	10.00	10	20	0.0000	0.00

Table 5.6a. Table for Fe (III) non-adjusted pH set of samples (evaporated)

sample	$V_{stock\ sol}$ (mL)	V_{H2O} (mL)	V_{total} (mL)	$m_{cellulose}$ (g)	c (mM / $g_{cellulose}$)
1.1.Fe3	0.00	20	20	1.0012	0.00
2.1.Fe3	0.20	20	20	1.0000	0.20
3.1.Fe3	0.25	20	20	1.0016	0.25
4.1.Fe3	0.50	20	20	1.0010	0.50
5.1.Fe3	0.75	20	20	1.0019	0.75
6.1.Fe3	1.00	20	20	0.9992	1.00
7.1.Fe3	3.00	17	20	1.0040	2.99
8.1.Fe3	5.00	15	20	0.9992	5.01
9.1.Fe3	6.00	14	20	1.0002	6.00
10.1.Fe3	8.00	12	20	0.9999	8.01
11.1.Fe3	10.00	10	20	0.9999	10.01
12.1.Fe3	10.00	10	20	0.0000	0.00

Table 5.6b. Table for Fe (III) pH 3 set of samples (evaporated)

sample	$V_{stock\ sol}$ (mL)	V_{H2O} (mL)	V_{total} (mL)	$m_{cellulose}$ (g)	c (mM / $g_{cellulose}$)
1.2.Fe3	0.00	20	20	1.0009	0.00
2.2.Fe3	0.20	20	20	0.9991	0.20
3.2.Fe3	0.25	20	20	1.0018	0.25
4.2.Fe3	0.50	20	20	1.0026	0.50
5.2.Fe3	0.75	20	20	1.0021	0.75
6.2.Fe3	1.00	20	20	1.0003	1.00
7.2.Fe3	3.00	17	20	1.0000	3.00
8.2.Fe3	5.00	15	20	0.9999	5.00
9.2.Fe3	6.00	14	20	1.0010	6.00
10.2.Fe3	8.00	12	20	1.0006	8.00
11.2.Fe3	10.00	10	20	1.0005	10.00
12.2.Fe3	10.00	10	20	0.0000	0.00

Table 5.6c. Table for Fe (III) pH 5 set of samples (evaporated)

sample	$V_{stock\ sol}$ (mL)	V_{H2O} (mL)	V_{total} (mL)	$m_{cellulose}$ (g)	c (mM / $g_{cellulose}$)
1.3.Fe3	0.00	20	20	1.0002	0.00
2.3.Fe3	0.20	20	20	1.0010	0.20
3.3.Fe3	0.25	20	20	0.9990	0.25
4.3.Fe3	0.50	20	20	1.0002	0.50
5.3.Fe3	0.75	20	20	0.9995	0.75
6.3.Fe3	1.00	20	20	1.0007	1.00
7.3.Fe3	3.00	17	20	0.9996	3.00
8.3.Fe3	5.00	15	20	1.0018	4.99
9.3.Fe3	6.00	14	20	0.9996	6.01
10.3.Fe3	8.00	12	20	1.0013	7.99
11.3.Fe3	10.00	10	20	1.0002	10.00
12.3.Fe3	10.00	10	20	0.0000	0.00

Table 5.7a. Table for Zn (II) non-adjusted pH set of samples (evaporated)

sample	$V_{stock\ sol}$ (mL)	V_{H2O} (mL)	V_{total} (mL)	$m_{cellulose}$ (g)	c (mM / $g_{cellulose}$)
1.1.Zn2	0.00	20	20	0.9999	0.00
2.1.Zn2	0.20	20	20	1.0021	0.20
3.1.Zn2	0.25	20	20	0.9999	0.25
4.1.Zn2	0.50	20	20	1.0003	0.50
5.1.Zn2	0.75	20	20	1.0012	0.75
6.1.Zn2	1.00	20	20	1.0025	1.00
7.1.Zn2	3.00	17	20	1.0009	3.00
8.1.Zn2	5.00	15	20	1.0003	5.00
9.1.Zn2	6.00	14	20	1.0010	6.00
10.1.Zn2	8.00	12	20	1.0008	8.00
11.1.Zn2	10.00	10	20	1.0013	9.99
12.1.Zn2	10.00	10	20	0.0000	0.00

Table 5.7b. Table for Zn (II) pH 3 set of samples (evaporated)

sample	$V_{stock\ sol}$ (mL)	V_{H2O} (mL)	V_{total} (mL)	$m_{cellulose}$ (g)	c (mM / $g_{cellulose}$)
1.2.Zn2	0.00	20	20	1.0044	0.00
2.2.Zn2	0.20	20	20	0.9997	0.20
3.2.Zn2	0.25	20	20	1.0032	0.25
4.2.Zn2	0.50	20	20	1.0002	0.50
5.2.Zn2	0.75	20	20	1.0009	0.75
6.2.Zn2	1.00	20	20	1.0012	1.00
7.2.Zn2	3.00	17	20	1.0007	3.00
8.2.Zn2	5.00	15	20	1.0008	5.00
9.2.Zn2	6.00	14	20	1.0003	6.00
10.2.Zn2	8.00	12	20	1.0025	7.98
11.2.Zn2	10.00	10	20	1.0019	9.98
12.2.Zn2	10.00	10	20	0.0000	0.00

Table 5.7c. Table for Zn (II) pH 5 set of samples (evaporated)

sample	$V_{stock\ sol}$ (mL)	V_{H2O} (mL)	V_{total} (mL)	$m_{cellulose}$ (g)	c (mM / $g_{cellulose}$)
1.3.Zn2	0.00	20	20	1.0015	0.00
2.3.Zn2	0.20	20	20	1.0006	0.20
3.3.Zn2	0.25	20	20	0.9997	0.25
4.3.Zn2	0.50	20	20	0.9999	0.50
5.3.Zn2	0.75	20	20	1.0010	0.75
6.3.Zn2	1.00	20	20	1.0014	1.00
7.3.Zn2	3.00	17	20	0.9997	3.00
8.3.Zn2	5.00	15	20	1.0004	5.00
9.3.Zn2	6.00	14	20	1.0001	6.00
10.3.Zn2	8.00	12	20	0.9992	8.01
11.3.Zn2	10.00	10	20	0.9997	10.00
12.3.Zn2	10.00	10	20	0.0000	0.00

5.2. Tables for filtrated samples preparation

Table 5.8. Preparation of stock solutions (filtrated)

compound / stock solution	pH	$m_{compound}$(g)	M (g/mol)	$V_{stock\ sol}$ (L)	$c_{stock\ sol}$ (mM/L)
$VOSO_4x5H_2O$	n.a. pH	2.5317	253.10	0.1	100.03
	pH 3				
	pH 5				
$FeN_3O_9x9H_2O$	n.a. pH	4.0431	404.00	0.1	100.08
	pH 3				
	pH 5				

Table 5.10a. Table for V (IV) non-adjusted pH set of samples (filtrated)

sample	$V_{stock\ solution}$ (mL)	V_{H2O} (mL)	V_{total} (mL)	$m_{cellulose}$ (g)	c (mM/ g $_{cellulose}$)
1.1.V4.1	0.0	1.0016	10	20.0	0.00
2.1.V4.1	10.0	1.0015	10	20.0	10.00
3.1.V4.1	5.0	1.0000	10	20.0	5.00
4.1V4.1	2.0	0.9982	10	20.0	2.00
5.1.V4.1	1.0	0.9996	10	21.0	1.00
6.1.V4.1	1.0	0.0000	10	21.0	1.00

Table 5.10b. Table for V (IV) pH 3 set of samples (filtrated)

sample	$V_{stock\ solution}$ (mL)	V_{H2O} (mL)	V_{total} (mL)	$m_{cellulose}$ (g)	c (mM/ g $_{cellulose}$)
1.2.V4.1	0.0	0.9983	10	20.0	0.00
2.2.V4.1	10.0	0.9992	10	20.0	10.00
3.2.V4.1	5.0	1.0001	10	20.0	5.00
4.2V4.1	2.0	1.0020	10	20.0	2.00
5.2.V4.1	1.0	0.9971	10	21.0	1.00
6.2.V4.1	1.0	0.0000	10	21.0	1.00

Table 5.10c. Table for V (IV) pH 5 set of samples (filtrated)

sample	$V_{stock\ solution}$ (mL)	V_{H2O} (mL)	V_{total} (mL)	$m_{cellulose}$ (g)	c (mM/ g $_{cellulose}$)
1.3.V4.1	0.0	0.9986	10	20.0	0.00
2.3.V4.1	10.0	0.9973	10	20.0	10.00
3.3.V4.1	5.0	1.0018	10	20.0	5.00
4.3.V4.1	2.0	1.0011	10	20.0	2.00
5.3.V4.1	1.0	0.9979	10	21.0	1.00
6.3.V4.1	1.0	0.0000	10	21.0	1.00

Table 5.9a. Table for Fe (III) non-adjusted pH set of samples (filtrated)

sample	$V_{stock\ solution}$ (mL)	V_{H2O} (mL)	V_{total} (mL)	$m_{cellulose}$ (g)	c (mM/ $g_{cellulose}$)
1.1.Fe3.1	0.0	20.0	20.0	1.0002	0.00
2.1.Fe3.1	10.0	10.0	20.0	1.0017	9.99
3.1.Fe3.1	5.0	15.0	20.0	0.9983	5.01
4.1Fe3.1	2.0	18.0	20.0	1.0032	2.00
5.1.Fe3.1	1.0	20.0	21.0	1.0045	1.00
6.1.Fe3.1	1.0	20.0	21.0	0.0000	0.00

Table 5.9b. Table for Fe (III) pH 3 set of samples (filtrated)

sample	$V_{stock\ solution}$ (mL)	V_{H2O} (mL)	V_{total} (mL)	$m_{cellulose}$ (g)	c (mM/ $g_{cellulose}$)
1.2.Fe3.1	0.0	20.0	20.0	1.0010	0.00
2.2.Fe3.1	10.0	10.0	20.0	0.9999	10.01
3.2.Fe3.1	5.0	15.0	20.0	0.9995	5.01
4.2Fe3.1	2.0	18.0	20.0	0.9996	2.00
5.2.Fe3.1	1.0	20.0	21.0	0.9981	1.00
6.2.Fe3.1	1.0	20.0	21.0	0.0000	0.00

Table 5.9c. Table for Fe (III) pH 5 set of samples (filtrated)

sample	$V_{stock\ solution}$ (mL)	V_{H2O} (mL)	V_{total} (mL)	$m_{cellulose}$ (g)	c (mM/ $g_{cellulose}$)
1.3.Fe3.1	0.0	20.0	20.0	1.0039	0.00
2.3.Fe3.1	10.0	10.0	20.0	0.9991	10.02
3.3.Fe3.1	5.0	15.0	20.0	1.0013	5.00
4.3.Fe3.1	2.0	18.0	20.0	1.0009	2.00
5.3.Fe3.1	1.0	20.0	21.0	1.0024	1.00
6.3.Fe3.1	1.0	20.0	21.0	0.0000	0.00

6. Bibliography:

[1] Kumar V. and Kothari S.H. International Journal of Pharmaceutics (1999) 177, 173–182

[2] Ragnar E.K., Wormald P., Ostelius J., Ivesen T and Nystrom C. International journal of Pharmaceutics (1995) 125, 257-264

[3] Kumar V., de la Luz Reus-Medina M., and Yang D. International Journal of Pharmaceutics (2002) 235, 129–140

[4] Zografi G, Kontny M.J. Pharmaceutical Research (1986), Vol 3, No4, 187-194

[5] Lin S.Y., Lin K.H. and Li M.J. Journal Of Pharmaceutical Sciences (2002) Vol. 91, No.9, 2040-2046

[6] Suzuki T. and Nakagami H. European Journal of Pharmaceutics and Biopharmaceutics (1999) 47, 225–230

[7] Shinzawa H., Awab K. and Ozaki Y. Analytical methods (2011) DOI: 10.1039/c1ay05392b

[8] Zhong Q. Q. Yue Q.Y., Li Q., Gao B.Y. and Xu X. Carbohydrate Polymers (2014) 111, 788–796

[9] Karatepe A.U., Soylak M. and Elci L. Analytical Letters (2002) Vol.3 5, No.9, 1561 –1574

[10]. Chen S., Zou Y., Yan Y., Shen W., Shi S., Zhang X. and Wang H. Journal of Hazardous Materials (2009) 161, 1355–1359

[11] Emam H.E, Manian A.P., Široká B., Duelli H., Merschak P., Redl B. and Bechtold T. Surface & Coatings Technology (2014) 254, 344–351

[12] Rehder D. Bioinorganic Vanadium Chemistry. John Wiley & Sons Ltd., Universitat Hamburg, Germany 2008.

[13] Sakurai H., Fujisawa Y., Fujimoto S., Yasui H., and Takino T. The Journal of Trace Elements in Experimental Medicine (1999) 12, 393–401

[14] Weckhuysen B. M., Keller D. E. Catalysis Today (2003) 78, 25–46.

[15] Evangelou A. M. Critical Reviews in Oncology/Hematology (2002) 42, 249–265

[16] Novotny L. and Kombian S.B. Journal of Cancer Research Updates (2014) 3, 97-102

[17] Pyrzyñska K., Chem. Anal. (Warsaw), (2006) 51, 339

[18] Crans D.C. Pure Appl. Chem. (2005) 77(9) 1497–1527

[19] Chambers C. and Holliday A.K. Modern inorganic chemistry. Butterworth & Co Ltd, 1975

[20] Stoltzfus R.J and Dreyfuss M.L. Guidelines for the Use of Iron Supplements to Prevent and Treat Iron Deficiency Anemia. International Nutritional Anemia Consultative Group (INACG), International Life Sciences Institute, Washington D.C. 1998.

[21] Auerbach M. and Ballard H. ASH Education Book, (2010) 2010 (1) 338-347

[22] Lee S.C., Park S.W., Kim D.K, Lee S.H. and Hong K.P. Hypertension. (2001) 38 (2) 166-170

[23] Parisi P., Villa M.P., Donfrancesco R., Miano S., Paolino M.C. and Cortese S. Medical Hypotheses (2012) 79, 246–249

[24] Sever Y., Askhenazi A., Tyano S. and Abraham Weizman A. Neuropsychobiology (1997) 35, 178-180

[25] Capek L., Kreibich V., Dedecek J., Grygar T., Wichterlova B., Sobalık Z., Martens J.A., Brosius R., Tokarova V.. Microporous and Mesoporous Materials (2005) 80, 279–289

[26] Georgopoulos P. G., Roy A., Yonone-Lioy M. J, Opiekun R. E. and Lioy P. J. J.Toxicol. Environmental Health B, Crit. Review. (2001) 4(4) 341-94.

[27] Emam H.E., Manian A.P., Široká B., Duelli H., Merschak P., Redl B. and Bechtold T. Surface & Coatings Technology (2014) 254, 344–351

[28] Albrecht T. W. J., Addai-Mensah J., Fornasiero D. Chemeca 2011 – Engineering a Better World Sydney, NSW 18-21 September 2011. Engineers Australia 2011, pp. 2100 - 2110

[29] Shankar A.H. and Prasad A.S. The American Journal of Clinical Nutrition (1998) 68, 447S – 463S

[30] Galvao T.F., de Silva Thees M.F.R., Pontes R.F., Silva M.S. and Pereira M.G. Rev Panam Salud Publica. (2013) 33(5) 370–377.

[31] Brewer G.J. The Journal of Trace Elements in Experimental Medicine (2000) 13, 51–61
[32] Klemm D., Schmauder, H.P., Heinze, T. Cellulose, in Biopolymers Online. Wiley online library (2005) 6.
[33] Carina Olsson and Gunnar Westman (2013). Direct Dissolution of Cellulose: Background, Means and Applications, Cellulose - Fundamental Aspects, Dr. Theo G.M. Van De Ven (Ed.), ISBN: 978-953-51-1183-2, InTech, DOI: 10.5772/52144
[34] Ciolacu D, Ciolacu F. and Popa V.I. Cellulose Chemistry and Technology. (2011) 45 (1-2) 13-21
[35] Zugenmaier P. Crystalline cellulose and cellulose derivatives; Characterization and structures. Springer-Verlag Berlin Heidelberg, 2008
[36] Saalwachter K., Burchard W., Klufers P., Kettenbach G., Mayer P., Klemm D. and Dugarma S. Macromolecules (2000) 33, 4094-4107
[37] Feng L., Chen Z.I. Journal of Molecular Liquids (2008) 142, 1–5
[38] M. Reichenbeacher and J. Popp, Theory of Infrared Absorption and Raman Spectroscopy, in Challenges in Molecular Structure Determination, DOI 10.1007/978-3-642-24390-5-2, Springer-Verlag Berlin Heidelberg 2012
[39] Siebert, F. and Hildebrandt, P. (2007) Theory of Infrared Absorption and Raman Spectroscopy , in Vibrational Spectroscopy in Life Science, Wiley-VCH Verlag GmbH & Co. KGaA, Weinheim, Germany. doi: 10.1002/9783527621347.ch2
[40] Fundamentals of modern UV-visible spectroscopy. Tony Owen. Agilent Technologies 2000
[41] The Royal Society of Chemistry, Ultraviolet/visible spectroscopy, in Modern Chemical Techniques Unilever. 1991-92
[42] https://en.wikipedia.org/wiki/Transition_metal consulted on July 2015
[43] Infrared Spectroscopy: Fundamentals and Applications. Barbara Stuart. 2004 John Wiley & Sons, Ltd ISBNs: 0-470-85427-8 (HB); 0-470-85428-6 (PB)
[44] Zahra Monsef Khoshhesab (2012). Reflectance IR Spectroscopy, Infrared Spectroscopy - Materials Science, Engineering and Technology, Prof. Theophanides Theophile (Ed.), ISBN: 978-953-51-0537-4, InTech, DOI: 10.5772/37180.
[45] Åmand L.E. and Tullin C.J. The Theory Behind FTIR Analysis. Application Examples From Measurement at the
12 MW Circulating Fluidized Bed Boiler at Chalmers. Chalmers University of Technology, Göteborg, Sweden.
[46] McKelvy M.L., Brit T.R., Davis B.L., Gillie K., Graves F.B., and Lentz L.A. Anal. Chem. (1998) 70, 119-177
[47] Coates J. Interpretation of Infrared Spectra, A Practical Approach, in Encyclopedia of Analytical Chemistry. R.A. Meyers (Ed.) John Wiley & Sons Ltd, Chichester England 2000. 10815–10837
[48] Hollas J.M. Modern spectroscopy 4th ed. John Wiley & Sons Ltd, Chichester, England 2004.
[49] Basic UV Vis Theory. Concepts and applications. Thermo Spectronic 2012
[50] Norkus E., Vaiciuniene J., Vuorinen T. and Macalady D.L. Carbohydrate Polymers (2004) 55, 47–55
[51]. Öztürk H.B., Vu-Manh H. and Bechtold T. Lenzinger Berichte (2009) 87,142-150
[52] Gurgel L.V.A. , Karnitz Junior O, Miriam R., de Freitas P.G., Frederic G.L.. Bioresource Technology (2008) 99, 3077–3083
[53] Ogawa Y., Hidaka H., Kimura S., Kim U.J., Kuga S. and Wada M. Cellulose (2014) 21, 999–1006
[54]. Li S.X., Lin X., Zheng F.Y., Liang W., Zhong Y. and Cai J. Anal. Chem. (2014) 86, 7079−7083
[55] Chen S., Shen W., Yu F., Hu W. and Wang H. Journal of Applied Polymer Science (2010) 117, 8–15
[56] Franco A.P. and Ramalho Merce A.L. Reactive & Functional Polymers (2006) 66, 667–681
[57] Houssni E.S., Basta A.H., Adly A.H. and El-Sayed A.M. Polym.-plast. technol. (1999) 38(5), 1095-1105

[58] Sen S., Martin J.D. and Argyropoulos D.S. Sustainable Chem. Eng. (2013) 1, 858−870
[59]. Myamoto I.,Inamoto M., Matsui T., Saito M. and Okajima K. Polymer Journal, (1995) 27(11), 1113-1122
[60] Kongdee A. and Bechtold T. Dyes and Pigments (2004) 60, 137–142
[61]. Kongdee A. and Bechtold T. Carbohydrate Polymers (2004) 56, 47–53
[62] Sundar S. Chemical modification of cellulose fibers and their orientation in magnetic field. M.S. Thesis. University of Toronto, Faculty of Forestry, 2011
[63]. Hosny W.M., Altaf H. Basta A.H. and El-Saied H. Polymer International (1997) 42, 157-162
[64]. Sundar S.T., Mohini M. Sain M.M. and Oksman K. Carbohydrate Polymers (2010) 80, 35–43
[65] Xu Q. and Chen L.F. Journal of Applied Polymer Science (1999) 71, 1441–1446
[66] Wang H., Zakirov A., Yuldashev S.U., Lee J., Fu D. and Kang T. Materials Letters (2011) 65, 1316–1318
[67] Cao N.J., Xu Q., Chen C.S., Gong C.S. and Chen L.F. Applied Blochemistry and Biotechnology (1994) 45/46, 521-530
[68] Zhanga J., Sunb M., Liuc X. and Han Y. Catalysis Today (2014)233, 77–82
[69]. Amadio E., Rosalia Di Lorenzoa D.R., Zonta C. and Licini G. Coordination Chemistry Reviews (2015) (article in press)
[70] Popova N. R,. Tortseva T. V, and Bogolitsyn K. G.. Russian Journal of Applied Chemistry (2013) 86 (8) 1275−1279.
[71]. Albert J., Lüders D., Andreas Bösmann A., Guldi D.M. and Wasserscheid P. Green Chem. (2014) 16, 226
[72] Tang Z., Deng W., Wang Y., Zhu E., Wan X., Zhang O. and Wang Y. ChemSusChem (2014) 7, 1557 – 1567
[73] Khalil M.I., El-Rafie M.H., and Hebeish A.. Journal of Applied Polymer Science (1981) 26, 149-157
[74] Kremer L.E., McLeod A.I., Aitken J.B., Levina A. and Lay P.A. Journal of Inorganic Biochemistry (2015) 147, 227–234
[75] Mizi Fan, Dasong Dai and Biao Huang (2012). Fourier Transform Infrared Spectroscopy for Natural Fibres, Fourier Transform - Materials Analysis, Dr Salih Salih (Ed.), ISBN: 978-953-51-0594-7, InTech, DOI: 10.5772/35482.
[76] Szymańska-Chargot M., Cybulska J. and Zdunek A. Sensors (2011) 11, 5543-5560
[77] Boghosian S., Eriksen K.M., Fehrmann R. and Nielsen K. Acta Chemica Skandinavica (1995) 49, 703-708
[78] Ballhausen C. J.,. Djurinskij B. F. and Watson K. J. J. Am. Chem. Soc., (1968) 90 (13), 3305–3309
[79] Longo J.M. and Arnott R.J. Journal of Solid State Chemsitry 1. (1970) 394-398
[80] De Waal N.D., Heyns A. M., Range K.J. and Eglmeier C. Spacrrmhimica Am. (1990) Vol. 46A. No. 2, 1639-1648
[81] Onodera S. and Ikegami Y. Inorg. Chem. (1980) 19 (3), 615–618
[82] Chine M.K., Sediri F., Gharbi N. Materials Sciences and Application (2011) 2, 964-970
[83] L. D. Frederickson, Jr. and D. M. Hausen, Anal. Chem. (1963) 35, 818
[84] Botto I.L., Vassallo M.B., Baran E.J. and Minelli G. Materials Chemistry and Physics (1997) 50, 267–270
[85] Holtz R.D., Souza Filho A.G., Brocchi M., Martins D., Duran N. and Alves O.L. Nanotechnology 21 (2010) 185102 (8pp)
[86] Dimitrova V., Zhetcheva K. and Pavlova L.P. Tubitak (2011) 35, 215 – 223
[87] Huang C.M., Pan G.T., Li Y.C.M, Li M.H., Yang T.C.K. Applied Catalysis A: General (2009) 358, 164–172

[88] Frost, R.L., Erickson K.L., Weier M.L. and Carmody O. Spectrochimica Acta, Part A: Molecular and Biomolecular Spectroscopy (2005) 61A(5), 829-834
[89] Griffith W. P., Wickins T. D. J. Chem. SOC A. 1966, 1087. Griffith, W. P. Ibid. (1967) 905
[90] Suchfi V. and Sivfik M. Monatshefte ftir Chemie (1996) 127, 1-6
[91] Melissa D. Lane M.D. American Mineralogist (2007) 92, 1-18
[92] Majzlan J., Charles N. Alpers C. N., Koch C. B., McCleskey R. B., Myneni S.C.B., Neil M. J. Chemical Geology (2011) 284, 296–305
[93] Lei L.,Jing S., Walton R.I., Xin X and O'Hare **D.** J. Chem. Soc., Dalton Trans.**,**(2002) 3477-3481
[94] Miller F.A. and Wilkins C.H.. Analyt. Chem 24 (1952) 24 (8), 1253-1294
[95] Krehula S., Popovic S., Music S. Materials Letters (2002) 54, 108–11
[96] Gamo I. Bulletin of the Chemical Society of Japan (1961) 34 (6) 764-766
[97] Ursescu M., Măluţan T. and Ciovic S. European Journal of Science and Theology, September 2009, Vol.5, No.3, 71-84
[98] Albrecht T. W. J., Addai-Mensah J., Fornasiero D. Chemeca 2011 – Engineering a Better World Sydney, NSW 18-21 September2011. Engineers Austrelia 2011, pp. 2100 - 2110
[99] Xin Zhang Y. X., Huang M., Li F. and Quan Z.Wen. Electrochem. Sci. (2013) 8, 8645 – 8661
[100] Korzhavyi P.A., and Johansson B. Thermodynamic properties of copper compounds with oxygen and hydrogen from first principles, TR-10-30. Royal Institute of Technology, Stockholm, 2010.
[101] Srivastavaan O. K. and Secco E. A. Canadian Journal of Chemistry. (1967) Vol 45, 585
[102] Saha J. K. and J. Podder J. Journal of Bangladesh Academy of Sciences, (2011) Vol. 35, No. 2, 203-210
[103] Rudolph W.W., Brooker M.H. and TremaineP.R. Journal of Solution Chemistry (1999) 28 (5), 621-630
[104] Selvarajan E. and Mohanasrinivasan V. Material letters. (2013) 112(1) 180-182
[105] Valentina I. Sumin de Portilla. American Mineralogist (1976) 6l, 95-99
[106] Kloprogge, J.T., Frost, R.L. and Hickey, L. Journal of Raman Spectroscopy (2004) 35, 967-974
[107] L.Segal, J. J. Creely, A. E. Maretin, Jr. and C. M. Conrad. Textile Research Journal (1959) 786-794
[108] Leppanen K., Andersson S., Torkkeli M., Knaapila M., Kotelnikova N., Serima R. Cellulose (2009) 16, 999–1015
[109] W. Ruland. Acta Cryst. (1961) 14, 1180
[110] B. H. Stuart. Vibrational Spectroscopy (1996) 10, 79-87
[111] Larson P. T., Wickholm K., Iversen T. Carbohydrate research (1997) 302, 19-25
[112] R,H, Ncwman, A. Hcmmingson. Holzforschung (1990) Vol. 44, No 5
[113] Poletto M., Ornaghi Júnior H. L. and Zattera A. J. Materials (2014) 7, 6105-6119
[114] Baldinger T., Moosbauer J. and Sixta H. Lenzinger Berichte (2000) 79, 15-17
[115] Hulleman S. H. D., van Hazendonk J. M., van Dam J. E. G. Carbohydr. Res. (1994) 261, 163
[116] Ilharco L. M., Garcia A. R., da Silva L. and Vieira Ferreira L. F. Langmuir (1997) 13, 4126-4132
[117] Bulanek R., Capek L., Setnicka M. and Cicmanec P. J. Phys. Chem. C (2011) 115, 12430–12438
[118] Morey M., Davidson A., Eckert H., and Stucky G. Chem. Mater. (1996) 8, 486-492
[119] Gao X. and Wachs I. E. J. Phys. Chem. B (2000) 104, 1261-1268
[120] Burcham L. J., Deo G., Gao X. a and Wachs I. E. Topics in Catalysis (2000) 11/12, 85–100
[121] Bulanek R., Cimanec P., Setnicka M. Physics Procedia (2013) 44, 195 – 205
[122] Dutoit D. C. M., Schneider M., Fabrizioli P. and Baiker A.. J. Mater. Chem. (1997) 7(2), 271–278
[123] Catana G., Ramachandra R. R., Weckhuysen B. M, Van Der Voort P., Vansant E., and Schoonheydt R. A. J. Phys. Chem. B (1998) 102, 8005-8012
[124] Kumar S. M., Schwidder M., Grünert W., Brückner A. Journal of Catalysis (2004) 227, 384–397

[125] Gurgul J., Łatka K., Hnat I, Rynkowski J., Dzwigaj S. Microporous and Mesoporous Materials (2013) 168, 1–6
[126] Dzwigaja S., Stievanoa L., Wagnerb F. E., Che M. Journal of Physics and Chemistry of Solids (2007) 68, 1885–1891
[127] Turner R. C. and Miles K.E. Canadian Journal of Chemistry (1957) 35, 1002-1009
[128] Stefansson A. Environ. Sci. Technol. (2007) 41, 6117-6123
[129] Dzwigaja S., Stievanoa L., Wagnerb F. E., Che M. Journal of Physics and Chemistry of Solids (2007) 68, 1885–1891
[130] Basaran A. H. and Tuovinen O. H. Appl Microbiol Biotechnol (1986) 24, 338-34
[131] Steiner M. And Lazaroff N.. Applied Microbiology, Nov. (1974) p. 872-880
[132] Pautieniene V. and Survila A. Chemija (2004) 15(3), 1-4
[133] Reddy B. J., Frost R. L. and Locke A. Transition Metal Chemistry 33(3):pp. 331-339
[134] Mesu J. G., van der Eerden M. J., de Groot F. M. F., and Weckhuysen B. M. J. Phys. Chem. B (2005) 109, 4042-4047
[135] Imrie F.E., Skakle J.M.S. and Gibson I.R. Bioceram Dev Appl (2013) S:1
[136] Kazin P. E., Zykin M. A., Tretyakov Y. D., and Jansen M.. Russian Journal of Inorganic Chemistry (2008) Vol. 53, No. 3, 362–366
[137] Velu S., Suzuki K., Okazaki M., Kapoor M. P., Osaki T., and Ohashi F. Journal of Catalysis (2000)194, 373–384
[138] Saha J.K. and Podder J. Journal of Bangladesh Academy of Sciences (2011) Vol. 35, No. 2, 203-210